

A quantum chemical description of proton transfer in zeolites

Citation for published version (APA):

Teunissen, E. H. (1994). *A quantum chemical description of proton transfer in zeolites*. [Phd Thesis 1 (Research TU/e / Graduation TU/e), Chemical Engineering and Chemistry]. Technische Universiteit Eindhoven.
<https://doi.org/10.6100/IR422200>

DOI:

[10.6100/IR422200](https://doi.org/10.6100/IR422200)

Document status and date:

Published: 01/01/1994

Document Version:

Publisher's PDF, also known as Version of Record (includes final page, issue and volume numbers)

Please check the document version of this publication:

- A submitted manuscript is the version of the article upon submission and before peer-review. There can be important differences between the submitted version and the official published version of record. People interested in the research are advised to contact the author for the final version of the publication, or visit the DOI to the publisher's website.
- The final author version and the galley proof are versions of the publication after peer review.
- The final published version features the final layout of the paper including the volume, issue and page numbers.

[Link to publication](#)

General rights

Copyright and moral rights for the publications made accessible in the public portal are retained by the authors and/or other copyright owners and it is a condition of accessing publications that users recognise and abide by the legal requirements associated with these rights.

- Users may download and print one copy of any publication from the public portal for the purpose of private study or research.
- You may not further distribute the material or use it for any profit-making activity or commercial gain
- You may freely distribute the URL identifying the publication in the public portal.

If the publication is distributed under the terms of Article 25fa of the Dutch Copyright Act, indicated by the "Taverne" license above, please follow below link for the End User Agreement:

www.tue.nl/taverne

Take down policy

If you believe that this document breaches copyright please contact us at:

openaccess@tue.nl

providing details and we will investigate your claim.

**A QUANTUM CHEMICAL DESCRIPTION
OF
PROTON TRANSFER IN ZEOLITES**

PROEFSCHRIFT

ter verkrijging van de graad van doctor aan de
Technische Universiteit Eindhoven, op gezag van
de Rector Magnificus, prof.dr. J.H. van Lint, voor
een commissie aangewezen door het College van
Dekanen in het openbaar te verdedigen op dinsdag
1 november 1994 om 16.00 uur

door

EVERT HENDRIK TEUNISSEN

geboren te Ermelo

Dit proefschrift is goedgekeurd door de promotoren:

prof.dr. R.A. van Santen

en

prof.dott. R. Dovesi

copromotor: dr. A.P.J. Jansen

CIP-DATA KONINKLIJKE BIBLIOTHEEK, DEN HAAG

Teunissen, Evert Hendrik

A quantum chemical description of proton transfer in
in zeolites / Evert Hendrik Teunissen. - Eindhoven :

Thesis Eindhoven. - With ref. - With summary in Dutch and
Italian.

ISBN 90-386-0054-2

Subject headings: zeolites / quantum chemistry /
adsorption.

Acknowledgement

We acknowledge support from the EC (contractnr. SC 1000199). The computer time on the Cray Y-MP4/464 was subsidized by the Foundation for the use of supercomputers, National Computing Facilities (NCF) (contractnr. SC-183).

*“ Considerate la vostra semenza:
fatti non foste per vivere come bruti ma per
seguire virtute e canoscenza ”*

DANTE ALIGHIERI,
La commedia,
(Inferno canto XXVI ; 118-120)

*“ Meglio far sciocchezze che star tutto il giorno
a guardare la caccia dei cavalli ! ”*

GUISEPPE TOMASO DI LAMPEDUSA,
Il gattopardo

Contents

1	Introduction	1
	General objectives	1
	Outline of this thesis	2
	Zeolites	2
	Quantum Chemical Methods	6
2	Basis set, electron correlation and geometry effects	22
	Introduction	22
	Computational Details	23
	Results and Discussion	26
	Conclusions	30
3	Coordination and Solvation effects	33
	Introduction	33
	Computational Details	34
	Results and Discussion	35
	Conclusions	43
4	A comparison between cluster and crystal calculations	46
	Introduction	46
	Computational Details	47
	Results and Discussion	50
	Conclusions	55
5	The embedded cluster model	58
	Introduction	58
	Methods and Computational Details	59
	Results and Discussion	63
	Conclusions	70
	Appendix	72
6	Large basis sets and geometry optimizations in the embedded cluster scheme	74
	Introduction	74
	Methods and Computational Details	75
	Results and Discussion	77
	Conclusions	82
7	The adsorption energy of NH_3 and NH_4^+ in chabazite	85
	Introduction	85
	Methods and Computational Details	86
	Results and Discussion	88
	Conclusions	95
	Summary and General Remarks	98
	Samenvatting en Algemene Opmerkingen	101
	Riassunto e Osservazioni Generale	104
	Dankwoord	107
	Curriculum Vitae	108
	List of Publications	109

1

Introduction

General objectives

The subject of this thesis is the quantum chemical description of adsorption and proton transfer processes in acidic zeolites. More specifically, the subject is the adsorption of NH_3 , the proton transfer forming NH_4^+ , and the interaction of the latter with the zeolite lattice. The aim of the thesis is twofold.

One aim is to obtain detailed information on the adsorption and proton transfer processes taking place in zeolites. As an example, we used the widely studied, and relatively simple case, of NH_3 and NH_4^+ . We studied the adsorption and proton transfer processes with quantum chemical methods to obtain information that cannot be obtained by experiment. We have studied the adsorption energy of the adsorbate, the geometry of the adsorbate and the zeolite and the changes therein upon adsorption, as well as the alignment of NH_4^+ with the zeolite.

The second aim is to develop a generally usable quantum chemical method enabling us to describe the adsorption and proton transfer processes of small molecules in zeolites satisfactorily. By satisfactory we mean that the method must provide reliable adsorption energies and a good representation of the zeolite. It is not necessarily a method that, through a coincidental cancellation of errors, reproduces experimental findings.

In order to find a satisfactory method we tried to clarify some of the important 'parameters' controlling the quality of the results: the size of the cluster and, linked to it, the importance of the boundary effects and the long-range electrostatic forces of the crystal; the importance of the geometry optimization and the coordination of the adsorbate; the quality of the basis set and the use of the counterpoise correction to correct for the basis set superposition error [1,2], and finally the importance of electron correlation.

Outline of this thesis

In this thesis we will study the adsorption of NH_3 and NH_4^+ in acidic zeolites. In order to give a proper description of the adsorption and proton transfer processes, we tested the accuracy of various quantum chemical methods and the validity of some zeolite models. Doing so, we obtained information on the adsorption of NH_3 and NH_4^+ and the proton transfer from the zeolite to NH_3 . The outline of the thesis is the following:

- In Chapter 2 we used a simple cluster model to study the effects of the basis set, electron correlation and the Basis Set Superposition Error, as well as the effect of the geometry optimization of the acidic site on the adsorption energy. In this chapter we chose a basis set for future use and we concluded that electron correlation and the counterpoise correction should be included to give a satisfactory description of the adsorption and proton transfer processes.
- In Chapter 3 the importance of the coordination between the NH_4^+ ion and the lattice is discussed. NH_4^+ becomes stable if it has a high coordination to the zeolite lattice. Optimum interaction requires a relatively large deformation of the lattice.
- In Chapter 4 we made a comparison between the results obtained on various clusters and the crystal were they were taken from. It appears that the minimal size clusters, as used in the previous chapters, do not give a satisfactory description of the zeolite and that the long range electrostatic effects are not negligible. Although the crystal calculations provide a good model for the zeolite, they cannot be used for the calculation of adsorption energies as only a minimal basis set can be used and geometry optimization is too elaborate.
- In Chapter 5 we described the development of a method enabling us to reproduce the results of the crystal calculations by means of embedded cluster calculations.
- In Chapter 6 we used large basis sets and optimized geometries within the embedded cluster method. By comparing some basis sets we found that a mixed basis set is a good compromise between required computer time and the required accuracy of the adsorption energy. The optimized geometries in the crystal, the cluster and the embedded cluster are very similar and the potential energy surfaces are parallel.
- In Chapter 7 we calculated the adsorption energies of NH_3 and NH_4^+ with the embedded cluster method. We used a mixed basis set, applied the counterpoise correction and included electron correlation. Also, we partially optimized the geometry and studied different orientations of NH_4^+ to the zeolite lattice. After correction for the deficiencies of the calculations, the adsorption energy of NH_3 was estimated to be -70 ± 10 kJ/mol and the adsorption energy of NH_4^+ was estimated to be -125 ± 15 kJ/mol. The latter compares well with the experimental heat of adsorption.

Zeolites

Zeolites are microporous aluminosilicates with a wide range of applications as a result of their specific and modifiable properties. The largest amount of zeolites is used as an ion exchanger, for example, as a substitute for phosphates in detergents. They are also used in adsorption and separation processes, *i.e.* as a drying agent and in gas purification. Perhaps the most interesting applications lie in catalysis. As a catalyst, the main application is as a

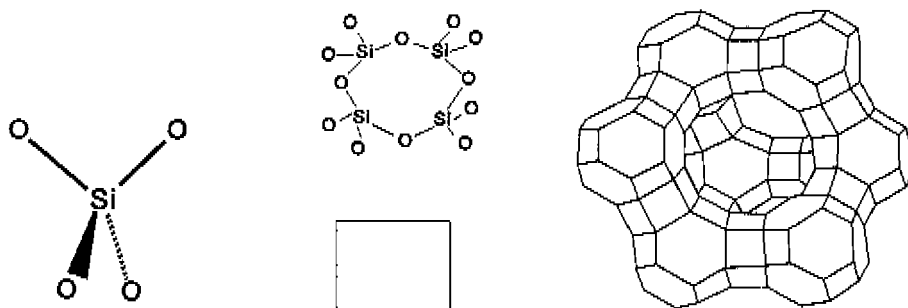


Figure 1.1. The structure of zeolites. On the left, the fundamental building unit, the SiO_4 -tetrahedron. In the middle, a ring of four tetrahedrons linked together, in two notations. Top, the notation in which all the atoms and bonds are shown and bottom, the short-hand notation in which only the silicon atoms are shown. In the latter notation the oxygen atoms are omitted. On the right, in short-hand notation, a faujasite unit cell [4]. A cage formed at the intersection of three channels is shown.

solid acid catalyst. Other applications of zeolites are in the fields of waste water treatment, nuclear effluent treatment, animal feed supplements and soil improvement [3].

Zeolite crystals are built from SiO_4 -tetrahedrons, linked together at the vertices to form rings. Such rings can contain three, or more, tetrahedrons. They can be linked together to form cages. By connecting these cages in a regular way a lattice containing channels can be built (fig. 1.1). The way in which the cages are connected and the intersecting channels are formed is dependent on the crystal structure. As a consequence of the regular crystalline structure the channels are uniform in size for each type of zeolite. The various zeolite structures differ by the size of the cages and the way they are linked together.

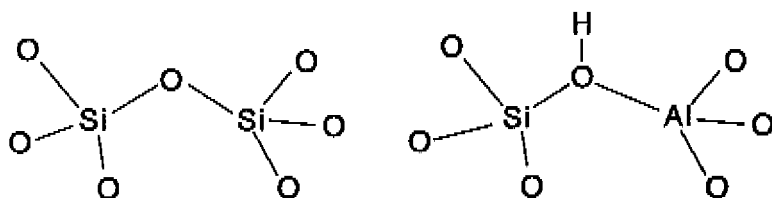


Figure 1.2. The creation of the acidic site in the zeolite. A silicon atom in the lattice is replaced by an aluminum atom. The proton, as a counterion, is bonded to the bridging oxygen atom.

In general, the crystal structure of zeolites is open and contains channels with diameters ranging from 2 to 13 Å. There are almost a hundred different zeolite structures [5]. Its structure gives the zeolite its specific properties. Depending on the zeolite structure and the diameter of the channels, some molecules are able to enter the zeolite channel, others

A quantum-chemical description of proton transfer in zeolites

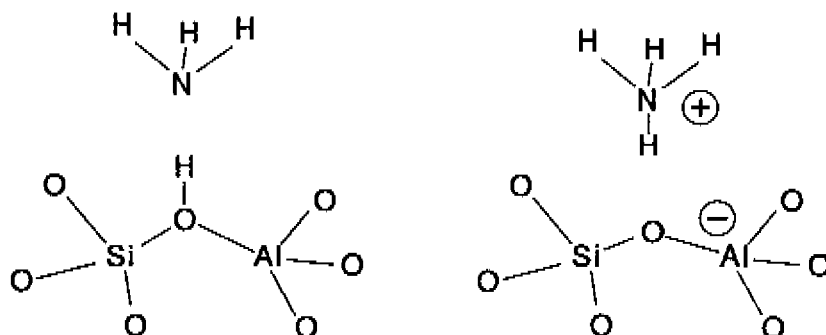


Figure 1.3. The adsorption of NH_3 and NH_4^+ . NH_3 is hydrogen bonded to the acidic site. If the proton is transferred, NH_4^+ bonded to the anionic zeolite is formed.

are excluded because of their size. Inside the channels and cages adsorption processes and chemical reactions can take place. Molecules entering the channels have a large interaction with the channel wall since all tetrahedrons are exposed to the internal surface of the zeolite.

In principle, the zeolite lattice is built from SiO_4 -tetrahedrons but silicon can be replaced relatively easily by other elements, the most common being aluminum. Since the formal charge of the aluminum atom is different from that of the silicon atom and the zeolite lattice should be kept charge neutral, a counter cation must be introduced in the zeolite lattice for each AlO_4^- -tetrahedron. Most of these cations are loosely bound and are easily exchanged. However, if the charge compensating cation is a proton, it forms a covalent bond with one of the oxygen atoms bonded to the aluminum atom and the characteristic zeolite acidic site is formed (fig. 1.2).

The subject of this thesis, the adsorption of NH_3 on the acidic site and the proton transfer are shown schematically in fig. 1.3. These processes have been studied experimentally quite extensively. Experimentally, information concerning the heat of adsorption, the geometry and the motion of NH_3 and NH_4^+ in zeolites has been obtained. However, none of the experiments, or a combination of them, gives a complete picture of the adsorption and proton transfer processes. Thus, the quantum-chemical calculations can provide missing information. Although not complete, the experimental findings are helpful in the choice of the models used in the quantum-chemical calculations and the verification of the results. We will give an overview of the various results obtained by experimentalists.

The experimental quantities giving the most direct comparison with the quantum chemical calculations are the heat of adsorption and the heat of desorption. Two methods are used to measure the heat of adsorption of NH_3 on the Brønsted acidic site: Temperature Programmed Desorption (TPD) and Micro-Calorimetry (MC). Although, in principle, TPD measures the activation barrier for the desorption, this quantity can often be interpreted as the heat of adsorption. We collected 31 heats of desorption, measured with TPD, on various acidic zeolites: Y, ZSM-5, Mordenite and Ferrierite, all of them with various Si/Al ratios [6-16]. The average heat of adsorption on the Brønsted acidic site was 129 kJ/mol with a standard deviation of 20 kJ/mol. We collected 131 heats of adsorption,

measured with MC, on various acidic zeolites, Y, ZSM-5, ZSM-11, Ferrierite and Mordenite, with various Si/Al ratios [13-34]. The average heat of adsorption was 150 kJ/mol with a standard deviation of 35 kJ/mol. The heat of adsorption seems relatively independent of the structure and the Si/Al ratio of the zeolite and seems largely determined by the acidic site itself. Thus, it can serve as a guide for the quality of the quantum chemical model.

Nuclear Magnetic Resonance (NMR) gives information about the local environment of atoms. With NMR, the zeolite acidic site, and NH_4^+ adsorbed on it, have been studied by several research groups. Although, in general, NMR gives only qualitative information about the local environment, some quantitative results have been obtained as well. For example, the Al-H distance in the acidic site of zeolite Y and ZSM-5 was measured to be 2.38 Å, and 2.43 and 2.48 Å respectively [35-37]. Some research groups concluded that, in acidic zeolites, at low loadings and at room temperature, NH_3 is present in the form of NH_4^+ [38,39]. At higher loadings, the excess NH_3 is hydrogen bonded to NH_4^+ ions. At these loadings there is a fast proton exchange between adsorbed NH_3 and NH_4^+ [40]. Also the position and the motion of the NH_4^+ ions have been investigated [41,42]. At 77 K the NH_4^+ cations, distorted from their T_d symmetry as a result of the interaction with the zeolite framework, are rotating around their axes in the vicinity of the Al-tetrahedrons. At higher temperatures they gain some translational velocity. Thus, in the quantum chemical model used to describe the interaction between NH_4^+ and the zeolite lattice, NH_4^+ should be relatively close to an Al-tetrahedron. A detailed study on the proton transfer equilibrium between 0°C to 300°C showed that the probability of NH_3 to capture a proton decreases from 1 at 0°C to 0.06 at 300°C; at higher temperatures the equilibrium shifts to NH_3 . Correspondingly, the average lifetime of a NH_4^+ ion in the zeolite decreased from 91 seconds to $7 \cdot 10^{-8}$ seconds [43].

X-Ray Diffraction (XRD) provides information about the structure and geometry of a crystal. It is very difficult to obtain information about the local geometry around the acidic site since XRD gives lattice constants and fractional coordinates averaged over the crystal. As the acidic sites are not ordered over the crystal no information about the local geometry of the acidic site is obtained. However, average changes in the lattice as a result of the adsorption of NH_3 can be monitored. Experiments on the D-form and the ND_4^+ -form of zeolite Rho showed that T-O distances (a T-atom is a silicon or aluminum atom), O-T-O and T-O-T angles change upon adsorption of NH_3 [44-46]. Apparently, the lattice adjusts itself to the adsorbate but no details can be obtained from the XRD data. The measurements of McCusker show that NH_4^+ is close to two oxygen atoms [44]. The XRD data do not provide a geometry of the acidic site or NH_4^+ that could be used in a quantum-chemical model but only show that after adsorption of NH_3 rearrangement of the lattice occurs.

Infrared spectroscopy is widely used to study zeolites and the zeolite-adsorbate interaction. Information on the zeolite-adsorbate interaction or, more specifically, the interaction between the zeolite and NH_4^+ and the change in the lattice vibrations thereupon can be obtained from several regions in the infrared spectra. Below 500 cm^{-1} there are the frequencies corresponding to the rotation of NH_4^+ and its vibrations against the zeolite lattice. The Si-O-Si bending region lies between 400 and 600 cm^{-1} . The symmetric and asymmetric Si-O stretching region are between 700 and 800 cm^{-1} and 1000 and 1200 cm^{-1} .

respectively. Between 1200 and 1500 cm^{-1} there are the bending modes of NH_3 and NH_4^+ . Finally, above 3000 cm^{-1} the N-H and O-H stretching modes appear. Infrared measurements do not give direct information about the internal geometries and the local environment of NH_3 and NH_4^+ but do show weakening or strengthening of bonds. We will discuss the relevant infrared measurements more extensively in Chapter 3 of this thesis. However, measurements of the lattice vibrations of zeolites seem to confirm the NMR measurements in the sense that NH_4^+ instead of NH_3 is the stable species. The lattice vibrations in the Na-form and the NH_4^+ -form of zeolite Y are almost equivalent whereas the H-form of zeolite Y is different [47–50].

Quantum Chemical Methods

Many electron wavefunctions

Methods for the calculation of the electronic structure of molecules based on quantum mechanics have, by now, become widespread and can be found in many textbooks [51–54]. The electronic structure and the total electronic energy of atoms, molecules and crystals can be obtained by solving the time-independent, non-relativistic Schrödinger equation. Usually, the electronic structure of molecules and crystals is solved within the Born–Oppenheimer approximation. In this approximation the motion of the electrons and the nuclei are separated by expanding the total molecular wavefunction as a product of the electronic and nuclear wavefunction. This approximation allows us to calculate the wavefunction for the electrons as moving in the potential field of the nuclei, treated as fixed point charges. The time independent Schrödinger equation for the electrons can be written as

$$\hat{H}\Psi = E\Psi, \quad (1.1)$$

in which \hat{H} is the Hamilton operator, or the Hamiltonian, and Ψ is a many electron wavefunction. E is the electronic energy of the system. The Hamiltonian is given by

$$\hat{H} = \sum_{i=1}^N \hat{h}(i) + \sum_{i=1}^N \sum_{j>i}^N \hat{g}(i, j), \quad (1.2)$$

and consists of two parts. The first is the one-electron part of the Hamiltonian $\hat{h}(i)$, consisting of the kinetic energy operator of electron i , in atomic units, and its potential of the field of the nuclei,

$$\hat{h}(i) = -\frac{1}{2}\nabla^2(i) + V(i). \quad (1.3a)$$

The second part is the two electron part, describing the electrostatic interaction between the electrons;

$$\hat{g}(i, j) = \frac{1}{r_{i,j}}. \quad (1.3b)$$

The normalized many-electron wavefunction, Ψ describes the movement of the electrons and is a solution of Eq. (1.1).

As electrons are fermions, the wavefunction should be antisymmetric under the interchange of electrons. We start the construction of a wavefunction meeting the antisymmetry demand from Molecular Spin Orbitals (MSO's). A MSO is a product of a spatial function, the molecular orbital (MO), and a spin function, α or β . From the MSO's, $\psi_i(i)$, we construct a many-electron wavefunction, by making a product of orthogonal and normalized MSO's. This simple product does, however, not meet the antisymmetry demand. A wavefunction meeting it is constructed by giving it the form of a determinant,

$$\Psi = (N!)^{-\frac{1}{2}} \begin{vmatrix} \psi_1(1) & \psi_2(1) & \dots & \psi_N(1) \\ \psi_1(2) & \psi_2(2) & \dots & \psi_N(2) \\ \vdots & \vdots & \ddots & \vdots \\ \psi_1(N) & \psi_2(N) & \dots & \psi_N(N) \end{vmatrix}, \quad (1.4)$$

in which $(N!)^{-\frac{1}{2}}$ is a normalization factor. This determinant of MSO's is called the Slater determinant.

From the Slater determinant, wavefunctions meeting the antisymmetry demand can be constructed. The simplest wavefunction consists of a single determinant. The best single-determinant wavefunction is found by optimizing the MSO's such that the lowest electronic energy E is obtained. For a orthonormal basis set of MSO's the expression for E is given by

$$E = \langle \Psi | \hat{H} | \Psi \rangle = \sum_i \langle \psi_i | \hat{H} | \psi_i \rangle + \frac{1}{2} \sum_i \sum_j \left[\langle \psi_i \psi_j | \hat{g} | \psi_i \psi_j \rangle - \langle \psi_i \psi_j | \hat{g} | \psi_j \psi_i \rangle \right]. \quad (1.5)$$

The summations run over the occupied orbitals, i.e. the orbitals containing an electron.

The Hartree Fock equations

The orbitals and, with them, the energy in Eq. (1.5), can be optimized using the Hartree-Fock, or Self-Consistent Field, scheme. The Coulomb operator \hat{J}_i and the exchange operator \hat{K}_i are defined:

$$\hat{J}_i(1)\psi_j(1) = \left[\int \hat{g}(1,2)\psi_i(2)\psi_i^*(2)d\tau_2 \right] \psi_j(1) \quad (1.6)$$

and

$$\hat{K}_i(1)\psi_j(1) = \int \hat{g}(1,2)\psi_i(1)\psi_i^*(2)d\tau_2\psi_j(2). \quad (1.7)$$

The Coulomb operator working on a function $\psi_j(1)$ multiplies it by the potential energy of the charge distribution $|\psi_i(2)|^2$. The integration runs over $d\tau_2$, the coordinates of ψ_i . The integral $\langle \psi_j | \hat{J}_i | \psi_j \rangle$ is equal to the potential energy between the charge distributions in ψ_i and ψ_j . With respect to the Coulomb operator the exchange operator \hat{K}_i has the two

variables, 1 and 2, interchanged. The exchange operator does not have a classical analogue and is purely quantum mechanical. The total Coulomb and exchange operators \hat{J} and \hat{K} are obtained by summing the Coulomb and exchange operators over the occupied orbitals,

$$\hat{J} = \sum_i^{occ} \hat{J}_i \quad (1.8)$$

and

$$\hat{K} = \sum_i^{occ} \hat{K}_i. \quad (1.9)$$

If we use Eqs. (1.8) and (1.9) we can simplify the two-electron part in Eq. (1.5) by

$$\sum_j \langle \psi_i \psi_j | \hat{g} | \psi_i \psi_j \rangle - \langle \psi_i \psi_j | \hat{g} | \psi_j \psi_i \rangle = \langle \psi_i | \hat{J} - \hat{K} | \psi_i \rangle. \quad (1.10)$$

The electronic energy is given by

$$E = \sum_i \langle \psi_i | \hat{h} + \frac{1}{2}(\hat{J} - \hat{K}) | \psi_i \rangle. \quad (1.11)$$

Now, we have reached a point in which there is only a summation over i ; by introducing the total Coulomb and exchange operators, we have written the two electron terms as a one-electron operator. However, as the operators \hat{J} and \hat{K} are still dependent on the position of the other electrons we call them pseudo one-electron operators.

In a single-determinant wavefunction the best orbitals, those giving the lowest energy, are obtained for MSO's that are eigenfunctions of the Fock operator,

$$\hat{F}\psi_i = \epsilon_i \psi_i, \quad (1.12)$$

in which \hat{F} is the Fock operator,

$$\hat{F} = \hat{h} + \hat{J} - \hat{K}, \quad (1.13)$$

and ϵ_i is the eigenvalue of the MSO,

$$\epsilon_i = \langle \psi_i | \hat{F} | \psi_i \rangle. \quad (1.14)$$

The Fock operator describes the motion of an electron in the potential of the nuclei and, as the operators \hat{J} and \hat{K} integrate over the positions of all the other electrons, in the averaged potential field of all the other electrons in the molecule.

For the calculation of the electronic structure of molecules it is very efficient to construct the MSO's as a Linear Combination of Atomic Orbitals (LCAO), the AO's being one-electron wavefunctions, usually centered on the nuclei,

$$\psi_i = \sum_{j=1}^N c_{ji} \phi_j. \quad (1.15)$$

In the LCAO-scheme the Fock equation in its canonical matrix form is given by:

$$\mathbf{FC} = \epsilon \mathbf{SC}. \quad (1.16)$$

This is a general eigenvalue problem. The columns of \mathbf{C} are the eigenvectors of \mathbf{F} , the eigenvalues ϵ_i are on the diagonal of ϵ . \mathbf{S} is the overlap matrix,

$$S_{\mu\nu} = \langle \phi_\mu | \phi_\nu \rangle. \quad (1.17)$$

The Fock matrix is square and has the dimension of the number of AO's in the basis set. As the number of electrons is smaller than the number of MSO's, there is a number of virtual, or empty, orbitals. Which orbitals are occupied depends on the orbital energies ϵ_i ; the orbitals having the lowest energy are occupied, the rest is empty.

As the Fock operator, through the Coulomb and exchange operator, depends on the occupied orbitals, we need an iterative method to calculate the wavefunction. The iterative process starts with a guess for the occupied orbitals. With this set of occupied orbitals the Fock operator and the elements of the Fock matrix, $\langle \psi_i | \hat{F} | \psi_j \rangle$, can be calculated. In the next step, the eigenvectors of \mathbf{F} are calculated by solving the eigenvalue problem of Eq. (1.16). With the new wavefunction a new Fock matrix can be constructed, etc.. This cycle is repeated until convergence, either in energy or in the wavefunction, is reached. If convergence has been reached, the Fock equations and the orbitals are consistent with each other. Therefore, this wavefunction is called the Self-Consistent Field (SCF) wavefunction.

Restricted Hartree Fock

In the Restricted Hartree Fock (RHF) method the spatial parts of the MSO's are equal for the α and β spin. For an even number of N electrons there are $N/2$ occupied orbitals. The total Coulomb and exchange operator, as well as the expressions for the Fock operator and the electronic energy, are modified as the summations run over doubly occupied orbitals containing one electron with α and one electron with β spin.

Before giving the expression for the Fock matrix and electronic energy in the RHF-scheme it is useful to introduce the density matrix \mathbf{P} . This matrix is also helpful for the analysis of the wavefunction and the calculation of some properties. The density matrix is defined by

$$P_{\mu\nu} = 2 \sum_{i=1}^{occ} c_{\mu i}^* c_{\nu i}. \quad (1.18)$$

The elements $P_{\mu\nu}$ are found by summing the product of the coefficients $c_{\mu i}^*$ and $c_{\nu i}$ belonging to the MO Ψ_i over the occupied MO's, each containing two electrons. The value of the elements $P_{\mu\nu}$ times the overlap $S_{\mu\nu}$ equals the charge in an product function of two atomic orbitals μ and ν .

With the use of the density matrix \mathbf{P} , we can write the Fock matrix in the AO-basis instead of the MO-basis. For the Coulomb and exchange integrals the following notation is used (compare Eqs. (1.6) and (1.7)):

$$(\mu\nu|\lambda\sigma) = \int \int \phi_\mu^*(1)\phi_\nu(1)\hat{g}(1,2)\phi_\lambda^*(2)\phi_\sigma(2)d\tau_1 d\tau_2. \quad (1.19)$$

The expression for the Fock operator becomes

$$F_{\mu\nu} = H_{\mu\nu}^{core} + \sum_{\lambda=1}^N \sum_{\sigma=1}^N P_{\lambda\sigma} [(\mu\nu|\lambda\sigma) - \frac{1}{2}(\mu\lambda|\nu\sigma)]. \quad (1.20)$$

H^{core} is the one electron Hamiltonian containing the kinetic energy and the potential energy of the electron in the field of the nuclei

$$H_{\mu\nu}^{core} = \langle \mu | -\frac{1}{2}\nabla^2 | \nu \rangle - \sum_{A=1}^M \langle \mu | \frac{Z_A}{r_A} | \nu \rangle. \quad (1.21)$$

The corresponding electronic energy is given by

$$E^{elec} = \frac{1}{2} \sum_{\mu=1}^N \sum_{\nu=1}^N P_{\mu\nu} (H_{\mu\nu}^{core} + F_{\mu\nu}). \quad (1.22)$$

The total energy of a molecule is the sum of the electronic energy and the nuclear repulsion energy between M nuclei;

$$E^{total} = \frac{1}{2} \sum_{\mu=1}^N \sum_{\nu=1}^N P_{\mu\nu} (F_{\mu\nu} + H_{\mu\nu}^{core}) + \sum_A^M \sum_{B>A}^M \frac{Z_A Z_B}{R_{AB}}, \quad (1.23)$$

where Z_A is the nuclear charge and R_{AB} the distance between the nuclei A and B .

Basis sets

Although there are different choices for its functional form, in Hartree-Fock calculations the AO's, characterized by the quantum numbers n , l and m , are usually chosen as linear combinations of real and normalized spherical gaussians with fixed exponents and coefficients, [54-56]:

$$\mu_\omega^{n,l,m} = \sum_{j=1}^d d_{\omega j}^{n,l} G_l^m(\alpha_{n,l,j}, \mathbf{r}) \quad (1.24)$$

in which

$$G_l^m(\alpha_{n,l,j}, \mathbf{r}) = N_l^m(\alpha) X_l^m(\mathbf{r}) \exp(-\alpha \mathbf{r}^2). \quad (1.25)$$

$N_l^m(\alpha)$ are normalization factors [55] and X_l^m are real solid harmonics (see Appendix A of Ref. [56]).

Chapter 1 : Introduction

For a proper description of the wavefunction the basis set should be saturated. In practice however, it is only feasible to work with a limited number of atomic orbitals. As the basis set is unsaturated the calculated wavefunction and corresponding energy will depend on the choice of the basis set. Thus, it is important to choose a basis set giving a proper description of the system studied. Therefore, a part of the thesis, Chapter 2, is dedicated to the choice of the basis set and the implications of the use of a limited basis set.

Molecular Hartree Fock programs

By now, programs able to calculate RHF-wavefunctions and energies of molecules and atoms, and optimizing geometries with the use of analytical gradients, such as GAMESS, Gaussian and TURBOMOLE [57-59], have become widespread and generally accessible. The architecture and the algorithms in these programs are relatively standard and are described well in literature [54].

The reciprocal lattice and periodic boundary conditions

The RHF-scheme described thus far can be applied to atoms and molecules. The calculation of the electronic structure of a crystal, built from unit cells repeating in three dimensions, is more complicated. For this kind of problems the concepts of the periodic boundary conditions and the reciprocal lattice are very useful. They are introduced in several text books [60,61].

The main difference between a molecule and a crystal is the translational symmetry of the latter. If a crystal is translated by a translational vector \mathbf{g} , the charge density and other properties of the crystal remain unchanged. Such a translational vector \mathbf{g} can be written as a linear combination of the three lattice vectors \mathbf{a}_1 , \mathbf{a}_2 and \mathbf{a}_3 ,

$$\mathbf{g} = n_1 \mathbf{a}_1 + n_2 \mathbf{a}_2 + n_3 \mathbf{a}_3, \quad (1.26)$$

n_1 , n_2 and n_3 being integers. The properties of the crystal remain equal under translation by a vector \mathbf{g} if the single-particle wavefunction of the crystal, $u(\mathbf{r})$, obeys the Bloch theorem [62];

$$u_{\mathbf{k}}(\mathbf{r} + \mathbf{g}) = e^{i\mathbf{k}\mathbf{g}} u_{\mathbf{k}}(\mathbf{r}). \quad (1.27)$$

The absolute value of $u(\mathbf{r})$ is equal to the absolute value of $u(\mathbf{r} + \mathbf{g})$. \mathbf{k} is a reciprocal lattice vector (to be defined below) and labels one of the irreducible representations of the translational group of the crystal.

Starting from an AO representation, a Bloch function can be defined as follows:

$$\phi_{\omega}(\mathbf{k}, \mathbf{r}) = \sum_{\varrho} \mu_{\omega}(\mathbf{r} - \mathbf{g}) e^{i\mathbf{k}\mathbf{g}}, \quad (1.28)$$

where μ_{ω} is an atomic orbital (Eq. (1.24)). It is relatively easy to prove that $\phi_{\omega}(\mathbf{k}, \mathbf{r})$ obeys the Bloch theorem;

$$\begin{aligned}\phi_{\omega}(\mathbf{k}, \mathbf{r} + \mathbf{l}) &= \sum_{\mathbf{g}} \mu(\mathbf{r} + \mathbf{l} - \mathbf{g}) e^{i\mathbf{k}\mathbf{g}}, \\ &= \sum_{\mathbf{g}'} \mu(\mathbf{r} - \mathbf{g}') e^{i\mathbf{k}(\mathbf{g}'+\mathbf{l})} = \phi_{\omega}(\mathbf{k}, \mathbf{r}) e^{i\mathbf{k}\mathbf{l}},\end{aligned}\quad (1.29)$$

where $\mathbf{g}-\mathbf{l}=\mathbf{g}'$, and $\sum_{\mathbf{g}}^{\infty} = \sum_{\mathbf{g}'}^{\infty}$.

The exponential factor in Eq. (1.27), and thus the translational properties of the Bloch functions, is the same for two vectors \mathbf{k} and \mathbf{k}' ($\mathbf{k}'=\mathbf{k}+\mathbf{K}$) if \mathbf{K} is such that $\mathbf{K}\cdot\mathbf{l}=2\pi$. It is useful, at this point, to define the reciprocal lattice. The vectors of the reciprocal lattice $\mathbf{b}_1, \mathbf{b}_2, \mathbf{b}_3$ satisfy

$$\mathbf{a}_i \cdot \mathbf{b}_j = \delta_{ij}.\quad (1.30)$$

As with the vectors \mathbf{a}_i , with the vectors \mathbf{b}_i we can make unit cells and with the help of the integers h_1, h_2 and h_3 we can set up a lattice called the reciprocal or the \mathbf{K} lattice. The vectors \mathbf{K} are defined as

$$\mathbf{K} = 2\pi(h_1\mathbf{b}_1 + h_2\mathbf{b}_2 + h_3\mathbf{b}_3).\quad (1.31)$$

We can now go back to Eq. (1.28). For a given $\mu_{\mathbf{k}}$ all the \mathbf{k} within the first cell of the reciprocal lattice, the first Brillouin zone, define a different Bloch function. Bloch functions built with a \mathbf{k}' vector outside the first Brillouin zone coincide with those built with the \mathbf{k} vector in the zero or reference cell differing from \mathbf{k}' by a reciprocal space translation vector: $\mathbf{k}'=\mathbf{k}+\mathbf{K}$. Each \mathbf{k} vector in the first Brillouin zone labels one of the irreducible representations of the translation group.

Bloch functions are very a useful basis for representing totally symmetric operators, such as the Fock operator, that take a block diagonal structure, a block for each irreducible representation. In principle, one should consider the infinite number of \mathbf{k} points within the first Brillouin zone. In practice however, it is sufficient to consider a limited number of \mathbf{k} points, and to interpolate between them.

If the integrand $\phi(\mathbf{k})$ is a well behaving function in reciprocal space of \mathbf{k} the integration over the BZ can be approximated as a weighted sum of selected $\phi(\mathbf{k})$ values at the sampling points \mathbf{k}_j , V_{BZ} being the volume of the Brillouin zone;

$$\frac{1}{V_{BZ}} \int_{BZ} \phi(\mathbf{k}) d\mathbf{k} \simeq \sum_{j=1}^J w_j \phi(\mathbf{k}_j).\quad (1.32)$$

There are other, more efficient, integration schemes that are also more suitable for less well behaving functions [56], but we will not discuss them here.

The CRYSTAL program

CRYSTAL is a program able to calculate Hartree-Fock wavefunctions of systems with periodic boundary conditions [63]. The program has been applied successfully to molecules, polymer chains, slabs, and crystals of insulators, semi conductors and metals. The structure of the program and its concepts are described in Ref. [56]. We will give a short overview of the CRYSTAL program.

As a result of the infinite size of the crystal the direct space Fock matrix has an infinite dimension. Therefore, it is not possible to treat a crystal as a molecule of infinite size as infinite matrices should be multiplied and diagonalized. A solution is found by a transformation from direct space to reciprocal space. For different \mathbf{k} vectors Bloch functions corresponding to a different irreducible representation of the translational group are formed. As we keep in mind that matrix elements of the Fock matrix between functions belonging to different irreducible representations of a group are zero, we have now created a situation where we have matrices with dimensions equal to the number of AO's in the unit cell, one for each \mathbf{k} . By the transformation from direct space to reciprocal space we have reduced the size of the problem to one that can be handled.

In CRYSTAL, the AO's have the same functional form as in molecular calculations, *i.e.* a set of contracted gaussians. A limited number of AO's is defined in the reference cell, or zero cell. All other AO's are generated from these by translation with lattice vectors \mathbf{g} . Thus, $\mu_{\mathbf{g}}$ is an AO obtained by translation from the corresponding AO in the reference cell, μ_0 , by a translation with a vector \mathbf{g} . From the AO's Bloch functions are generated according to Eq. (1.28). From these, as an analogue to the MO's, the crystal orbitals (CO), $\psi_j(\mathbf{k}, \mathbf{r})$, are defined as linear combinations of Bloch functions,

$$\psi_j(\mathbf{k}, \mathbf{r}) = \sum_{\omega=1}^M a_{\omega j}(\mathbf{k}) \phi_{\omega}(\mathbf{k}, \mathbf{r}), \quad (1.33)$$

where M is equal to the number of AO's in the unit cell.

Each \mathbf{k} point has its own Fock matrix:

$$F_{\mu\nu}(\mathbf{k}) = \langle \phi_{\mu}(\mathbf{k}) | \hat{F} | \phi_{\nu}(\mathbf{k}) \rangle, \quad (1.34)$$

and its own Hartree-Fock equation

$$\mathbf{F}(\mathbf{k})\mathbf{A}(\mathbf{k}) = \mathbf{S}(\mathbf{k})\mathbf{A}(\mathbf{k})\mathbf{E}(\mathbf{k}). \quad (1.35)$$

$\mathbf{E}(\mathbf{k})$ is a diagonal matrix containing the eigenvalues ϵ_j and $\mathbf{A}(\mathbf{k})$ is the matrix with the eigenvectors $a_j(\mathbf{k})$. As the eigenvalues and eigenvectors of $\mathbf{F}(\mathbf{k})$ are continuous functions of \mathbf{k} , it is sufficient to diagonalize $\mathbf{F}(\mathbf{k})$ in a relatively small set of \mathbf{k} points and then to interpolate or to use appropriate weights in the integration, Eq. (1.32).

The Fock matrix is diagonalized in reciprocal space. This reciprocal-space Fock matrix is built from direct-space Fock matrices, $\mathbf{F}_{\mu\nu}^g$ by Fourier transforms. A direct-space Fock matrix is a sum of the kinetic energy matrix (\mathbf{T}^g), the matrix containing the interaction with the nuclei (\mathbf{Z}^g), the Coulomb matrix (\mathbf{C}^g) and the exchange matrix (\mathbf{X}^g),

$$F_{\mu\nu}^g = T_{\mu\nu}^g + Z_{\mu\nu}^g + C_{\mu\nu}^g + X_{\mu\nu}^g, \quad (1.36a)$$

$$T_{\mu\nu}^g = \langle \mu_0 | \frac{1}{2} \nabla^2 | \nu_{\mathbf{g}} \rangle, \quad (1.36b)$$

$$Z_{\mu\nu}^g = \sum_{\mathbf{h}} \sum_A^M \langle \mu_0 | \frac{Z_A}{|\mathbf{r} - \mathbf{h} - \mathbf{s}_z|} | \nu_{\mathbf{g}} \rangle, \quad (1.36c)$$

$$X_{\mu\nu}^g = -\frac{1}{2} \sum_{\mathbf{h}} \sum_{\mathbf{n}} \sum_{\lambda=1}^N \sum_{\sigma=1}^N P_{\lambda\sigma}^n (\mu_0 \lambda_{\mathbf{h}} | \nu_{\mathbf{g}} \sigma_{\mathbf{n}+\mathbf{h}}), \quad (1.36d)$$

$$C_{\mu\nu}^g = \sum_{\mathbf{h}} \sum_{\mathbf{n}} \sum_{\lambda=1}^N \sum_{\sigma=1}^N P_{\lambda\sigma}^n (\mu_0 \nu_{\mathbf{g}} | \lambda_{\mathbf{h}} \sigma_{\mathbf{n}+\mathbf{h}}). \quad (1.36e)$$

The AO's in the various unit cells are denoted as μ_0 , $\nu_{\mathbf{g}}$, $\lambda_{\mathbf{h}}$ and $\sigma_{\mathbf{n}+\mathbf{h}}$, the positions of the nuclei in the reference cell are given by \mathbf{s}_z . In building the Fock matrix, problems are caused by the fact that, in principle, an infinite number of integrals should be evaluated and by the fact that Z^g and C^g are individually divergent. However, both problems can be circumvented.

The exchange term in the Fock matrix of the crystal is more complicated than in a molecule since there is the summation over all lattice vectors \mathbf{h} and \mathbf{n} . However, the exchange term converges relatively rapidly as the magnitude of the density matrix elements falls to zero exponentially with the distance for insulators and ionic systems; this permits the truncation of the \mathbf{n} summation. As regards \mathbf{h} , it can be truncated if the overlaps $\langle \mu_0 | \lambda_{\mathbf{h}} \rangle$ and $\langle \lambda_{\mathbf{h}} | \sigma_{\mathbf{n}+\mathbf{h}} \rangle$ fall below a certain threshold.

The Coulomb and the nuclear attraction terms in the Fock matrix do, as a result of their long range character, not converge. To circumvent the individual divergence of the terms they are grouped together and, in order to avoid the evaluation of an infinite number of integrals, a part of them is calculated through multipolar expansions. For the evaluation of the integrals a division is made into a 'monoelectronic' zone $M\epsilon_{\lambda}$ and a 'bielectronic' zone $B\epsilon_{\lambda}$. If the value of the overlap between the interacting charge distributions are above a certain threshold, the integrals fall in the bielectronic zone and are evaluated exactly. If they are below a certain threshold they fall into the monoelectronic zone and they are approximated.

A first step towards the approximation of integrals in the monoelectronic zone by multipolar expansions is the definition of the Mulliken net charge distributions. The charge distribution of the crystal is partitioned over the atoms Λ through a Mulliken partitioning scheme [64] and the nuclear charge is added to it, thus creating net atomic charge distributions $\rho_{\Lambda\mathbf{h}}$,

$$\rho_{\Lambda}(\mathbf{r} - \mathbf{h}) \equiv \sum_{\lambda \in \Lambda} \sum_{\sigma} \sum_{\mathbf{n}} \left[P_{\lambda\sigma}^n (\lambda_{\mathbf{h}} | \sigma_{\mathbf{n}+\mathbf{h}}) - Z_{\Lambda} \right], \quad (1.37)$$

By combining the electronic and nuclear charge contribution of cell \mathbf{h} , a neutral charge distribution has been obtained and the combined mono-electronic Coulomb term has become convergent. In the next step an approximation is made; the charge distributions $\rho_{\Lambda\mathbf{h}}$ are expanded in multipoles. Integrals like

$$(C_{\mu\nu}^g + Z_{\mu\nu}^g)^{mono} = \sum_{\Lambda}^M \sum_{\mathbf{h}}^{Mc} \langle \mu_0 \nu_{\mathbf{g}} | \rho_{\Lambda\mathbf{h}} \rangle, \quad (1.38)$$

describing the interaction between the charge distributions ($\mu_0 \nu_{\mathbf{g}}$) and $\rho_{\Lambda\mathbf{h}}$, are calculated through multipole expansions of $\rho_{\Lambda\mathbf{h}}$ [56]. The infinite summation over the multipoles of $\rho_{\Lambda\mathbf{h}}$ in all unit cells \mathbf{h} in Eq. (1.38) is evaluated using Ewald techniques and recursion formula's [65,66]. By the expansion of charge distribution and the use of Ewald techniques the evaluation of an infinite number of integrals is avoided. The combined Coulomb and nuclear attraction term now takes the following form:

$$\begin{aligned} C_{\mu\nu}^g + Z_{\mu\nu}^g &= \sum_{\Lambda}^{Mc} \sum_{\mathbf{h}}^{Bc} \sum_{\mathbf{n}} \sum_{\lambda} \sum_{\sigma} P_{\lambda\sigma}^n(\mu_0 \nu_{\mathbf{g}} | \lambda_{\mathbf{h}} \sigma_{\mathbf{h}+\mathbf{n}}) \\ &\quad - \sum_{\Lambda}^{Mc} \sum_{\mathbf{h}}^{Bc} \langle \mu_0 \nu_{\mathbf{g}} | \rho_{\Lambda\mathbf{h}} \rangle \\ &\quad + \sum_{\Lambda}^{Mc} \sum_{\mathbf{h}}^{\infty} \langle \mu_0 \nu_{\mathbf{g}} | \rho_{\Lambda\mathbf{h}} \rangle \end{aligned} \quad (1.39)$$

The first term contains the electron-electron integrals in the bielectronic zone that are evaluated exactly. The third term, describes the interaction between ($\mu_0 \nu_{\mathbf{g}}$) and the charge distributions ρ_{Λ} over the infinite number of unit cells \mathbf{h} of the CRYSTAL. It is calculated with multipolar expansions and Ewald techniques. The second term subtracts the integrals, calculated at the same level of approximation as the third term, already included in the bielectronic zone. As the summation in third term runs over all charge distributions in all unit cells, the second term avoids double counting of those already calculated exactly by the first term. It appears that the approximation of the charge distribution by the multipoles is very good as the combined Coulomb term converges quite rapidly with the order of the multipole, if a reasonable threshold is selected for the separation between the bielectronic and mono-electronic zone [56].

Now that the AO's have been defined and the construction of the Fock matrix has been explained, we can discuss the calculation of the SCF wavefunction. A scheme of the Self-Consistent process in CRYSTAL is given in fig. 1.4. The first step in the SCF process is the construction of the \mathbf{F}^g 's from the given input. The geometry and the basis set, as well as the symmetry of the crystal are read in (CRYSTAL uses all space-group symmetry). Then, the integrals are sorted into the mono-electronic and the bielectronic zone, according to their overlaps. In the next step, they are calculated and the Fock matrices in direct space are constructed. The direct space Fock matrices \mathbf{F}^g , Eq. (1.36),

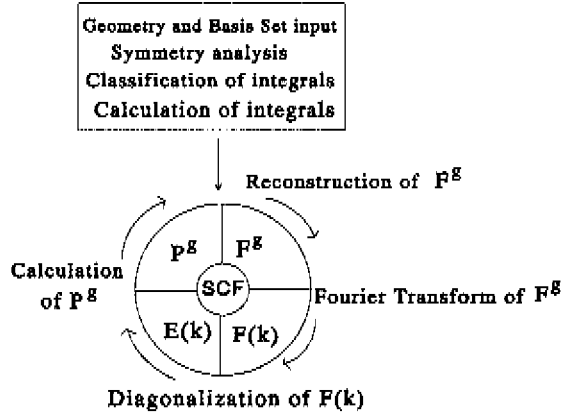


Figure 1.4. The SCF-process in CRYSTAL. From the geometry and the basis set of the crystal the Fock matrixes in direct space are built for a limited number of \mathbf{g} vectors. From these, the Fock matrixes in reciprocal space are constructed and diagonalized. From the new set of CO's and energies the new direct space Fock matrixes are calculated. This process is repeated until convergence is reached.

are built for a limited number of \mathbf{g} vectors, these are then converted to reciprocal space Fock matrixes through Fourier transforms. In the next step these are diagonalized.

Before calculating the density matrix, necessary to build the new Fock matrix, one should calculate the Fermi energy. It is calculated in the following way; if there are $N=Nq$ electrons in the crystal, i.e. q electrons per unit cell, the Fermi energy ϵ_F must be such that there are $\frac{N}{2}$ CO's with an eigenvalue $\epsilon_j(\mathbf{k})$ smaller than ϵ_F . The Fermi-energy is defined implicitly by

$$q = \frac{2}{N} \sum_j \sum_{\mathbf{k}} \theta[\epsilon_F - \epsilon_j(\mathbf{k})] \simeq \frac{2}{V_B} \sum_j \int_{BZ} \theta[\epsilon_F - \epsilon_j(\mathbf{k})] d\mathbf{k}. \quad (1.40)$$

With the Fermi energy the density matrix in \mathbf{k} space can be calculated as follows:

$$P_{\mu\nu}(\mathbf{k}) = 2 \sum_j a_{\mu j}^*(\mathbf{k}) a_{\nu j}(\mathbf{k}) \theta[\epsilon_F - \epsilon_j(\mathbf{k})]. \quad (1.41)$$

in which θ is the Heavyside stepfunction [67]. With the density matrix in reciprocal space, $P(\mathbf{k})$, the direct space density matrix can be calculated and the total energy is evaluated. The new direct space density matrix is used to calculate the new Fock matrix. The SCF-cycle is repeated until convergence is reached.

From the wavefunction the total energy per unit cell can be calculated. It is a sum of the kinetic (E^k), exchange (E^{ex}) and combined Coulomb (E^C) energy,

$$E = E^k + E^{ex} + E^C, \quad (1.42)$$

$$E^k = \frac{1}{2} \sum_{\mu}^N \sum_{\nu}^N \sum_{\mathbf{g}} P_{\mu\nu}^g \langle \mu_0 | -\frac{1}{2} \nabla^2 | \nu_{\mathbf{g}} \rangle, \quad (1.43)$$

$$E^{\epsilon\epsilon} = -\frac{1}{4} \sum_{\mu}^N \sum_{\nu}^N \sum_{\mathbf{g}} P_{\mu\nu}^g \sum_{\mathbf{h}} \sum_{\mathbf{n}} \sum_{\lambda=1}^N \sum_{\sigma=1}^N P_{\lambda\sigma}^h (\mu_0 \lambda_{\mathbf{h}} | \nu_{\mathbf{g}} \sigma_{\mathbf{n}+\mathbf{h}}). \quad (1.44)$$

The Coulomb energy is the sum of the electron–electron, electron–nuclear, nuclear–electron and nuclear–nuclear interaction energy,

$$E^C = E_{ee}^C + E_{en}^C + E_{ne}^C + E_{nn}^C \quad (1.45)$$

E_{en}^C and E_{ne}^C only differ by a constant C . This constant has its origin in the difference between the exact charge distribution and the charge distribution described by the multipolar expansions [56,66], it is evaluated easily in the expression of the total energy. The Coulomb energy can be written as

$$\begin{aligned} E^C &= \frac{1}{2} \sum_{\mu}^N \sum_{\nu}^N \sum_{\mathbf{g}} P_{\mu\nu}^g \sum_{\mathbf{h}} \sum_{\mathbf{n}} \sum_{\lambda=1}^N \sum_{\sigma=1}^N P_{\lambda\sigma}^h (\mu_0 \nu_{\mathbf{g}} | \lambda_{\mathbf{h}} \sigma_{\mathbf{n}+\mathbf{h}}) \\ &+ \sum_{\mu}^N \sum_{\nu}^N \sum_{\mathbf{g}} P_{\mu\nu}^g \sum_{\mathbf{h}} \sum_M \langle \mu_0 | \frac{Z_M}{|\mathbf{r} - \mathbf{h} - \mathbf{s}_z|} | \nu_{\mathbf{g}} \rangle \\ &+ \frac{1}{2} \sum_A^M \sum_B^M \sum_{\mathbf{g}} \left(\frac{Z_A Z_{B\mathbf{g}}}{(\mathbf{r} + \mathbf{g})} - \delta_{AB\mathbf{g}} \frac{Z_{A_0} Z_{B\mathbf{g}}}{\mathbf{r}} \right) \\ &+ C. \end{aligned} \quad (1.46)$$

As in the calculation of the Fock matrix F^g , the summations over \mathbf{g} in Eqs. (1.43), (1.44) and (1.46) are truncated if the value of the overlap between the functions μ_0 and $\nu_{\mathbf{g}}$ are below a certain threshold.

Electron correlation

The Hartree–Fock wavefunction is obtained with a model in which the electrons move in the averaged potential of the other electrons. In correlated wavefunctions the chance that an electron is at a certain position is explicitly dependent on the position of other electrons. Thus, the Hartree–Fock wavefunction contains an error. If this error is almost constant for the various states of a system that are compared the Hartree–Fock approach is working well. For some cases however it is not, for example if there is a relatively large change in electron density. Also, the Hartree–Fock wavefunction is not sufficient if Van de Waals forces must be included. For these cases, we have to construct a wavefunction containing more determinants. The multiple-determinant wavefunction is constructed as a sum of determinant functions, Ψ_k , created from Ψ_0 , the Hartree–Fock wavefunction, by exciting electrons to the virtual orbitals. To calculate the fully correlated wavefunction

the coefficients of the determinants in the multiple-determinant wavefunction should be optimized. As this is a time consuming process, we will use Møller-Plesset perturbation theory to calculate the correlation energy.

The contribution of the determinants is calculated by means of Raleigh-Schrödinger perturbation theory. In the Møller-Plesset approach the Hamiltonian is partitioned as:

$$\hat{H} = \hat{H}_0 + \hat{V}. \quad (1.47)$$

\hat{H}_0 is the Hartree-Fock Hamiltonian, Eq. (1.13), and \hat{V} is replacing the pseudo one-electron Coulomb and exchange operators in the Fock matrix by the many electron operator, where the summation i runs over the MSO's, and

$$\hat{V} = \sum_{i < j} \frac{1}{r_{ij}} - \sum_i \left[J_i - K_i \right]. \quad (1.48)$$

The Hartree-Fock wavefunction Ψ_0 is an eigenfunction of \hat{H}_0 . In the Møller-Plesset partitioning of the Hamiltonian the sum of the zero-order and first-order perturbation energy is equal to the Hartree-Fock energy,

$$E^0 + E^1 = \langle \Psi_0 | \hat{H}_0 | \Psi_0 \rangle + \langle \Psi_0 | \hat{V} | \Psi_0 \rangle \quad (1.49.a)$$

$$= \sum_i c_i - \frac{1}{2} \sum_i (J_i - K_i). \quad (1.49.b)$$

The full correlation energy is the sum of the second order term up to the infinite order. The second order perturbation is given by

$$E^2 = - \sum_{k \neq 0} \frac{|\langle \Psi_k | \hat{V} | \Psi_0 \rangle|^2}{\langle \Psi_0 | \hat{H}_0 | \Psi_0 \rangle - \langle \Psi_k | \hat{H}_0 | \Psi_k \rangle}, \quad (1.50)$$

and only double excitations contribute to it. If Ψ_k is a determinant resulting from an excitation of electrons from the MSO's a and b to the MSO's r and s the denominator is equal to the difference in the molecular orbital energies of r,s and a,b ,

$$\langle \Psi_0 | \hat{H}_0 | \Psi_0 \rangle - \langle \Psi_k | \hat{H}_0 | \Psi_k \rangle = \Delta\epsilon = \epsilon_a + \epsilon_b - \epsilon_r - \epsilon_s \quad (1.51)$$

The second order correlation energy can be calculated relatively easy with

$$E^2 = - \sum_a^{\text{occ}} \sum_{a < b}^{\text{occ}} \sum_r^{\text{virt}} \sum_{r < s}^{\text{virt}} \frac{|(ar|bs) - (as|br)|^2}{\Delta\epsilon}. \quad (1.52)$$

In this thesis we only calculate the second order perturbation energy. For systems not having low lying excited states or a near degeneracy this is a reasonable approach [54].

References

- [1] S. F. Boys and F. B. Bernardi, *Mol. Phys.* **19**, 553 (1970).
- [2] J. H. van Lenthe, J. G. C. M. van Duijneveldt-van de Rijdt and F. B. van Duijneveldt, *Adv. in Chem. Phys.* **79**, 521 (1987).
- [3] L. Moscou in *Introduction to Zeolite Science and Practice* edited by H. van Bekkum, E. M. Flanigen and J. C. Jansen, (Elsevier, Amsterdam, 1991).
- [4] *Reproduced by kind permission from* A. J. M. de Man, PhD-thesis, Eindhoven (1993).
- [5] W. M. Meier and D. H. Olson *Atlas of Zeolite Structure Types* 2nd ed. (Butterworths, London, 1987).
- [6] N.-Y. Topsøe, K. Pedersen and E. G. Derouane, *J. Catal.* **70**, 41 (1981).
- [7] E. Dima and L. V. C. Rees, *Zeolites* **10**, 8 (1987).
- [8] C. V. Hidalgo, H. Itoh, T. Hattori, M. Niwa and Y. Murakumi, *J. Catal.* **85**, 362 (1984).
- [9] H. G. Karge and V. Dondur, *J. Phys. Chem.* **94**, 765 (1990).
- [10] H. G. Karge, V. Dondur and J. Weitkamp, *J. Phys. Chem.* **95**, 283 (1991).
- [11] J. G. Post and J. H. C. van Hooff, *Zeolites* **4**, 9 (1984).
- [12] I. Bankós, J. Valyon, G. I. Kapustin, D. Kalló, A. L. Klyachko and T. R. Brueva, *Zeolites*, **8**, 189 (1988).
- [13] H. G. Karge, *Stud. Surf. Sci. and Catal.* **65**, 133 (1991).
- [14] M. Sawa, M. Niwa and Y. Murakumi, *Zeolites* **10**, 307 (1990).
- [15] G. I. Kapustin, T. R. Brueva, A. L. Klyachko, S. Beran and B. Wichterlová, *Appl. Catal.* **42**, 239 (1988).
- [16] A. Auroux, Y. S. Jin, J. C. Vedrine and L. Benoit, *Appl. Catal.* **36**, 323 (1988).
- [17] A. Auroux and J. C. Vedrine, in *Catalysis by acids and bases*, edited by B. Imelek (Elsevier, Amsterdam, 1985).
- [18] A. Auroux, V. Bolis, P. Wierzchowski, P. C. Gravelle and J. C. Vedrine, *J. C. S. Farad. Trans. I* **75**, 2544 (1979).
- [19] Z. C. Shi, A. Auroux and Y. B. Taarit, *Can. J. Chem.* **66**, 1013 (1988).
- [20] K. Tsutsumi, Y. Mitani and H. Takahashi, *Bull. Chem. Soc. Jpn.* **56**, 1912 (1983).
- [21] Y. Mitani, K. Tsutsumi and H. Takahashi, *Bull. Chem. Soc. Jpn.* **56**, 1917 (1983).
- [22] Y. Mitani, K. Tsutsumi and H. Takahashi, *Bull. Chem. Soc. Jpn.* **56**, 1921 (1983).
- [23] J. C. Vedrine, A. Auroux, V. Bolis, P. Dejaifve, C. Nacchane, P. Wierzchowski, E. G. Derouane, J. B. Nagy, J.-P. Gilson, J. H. C. van Hoof, J. P. van den Berg and J. Wolthuizen, *J. Catal.* **59**, 248 (1979).
- [24] A. L. Klyachko, G. I. Kapustin, T. R. Brueva and A. M. Rubinstein, *Zeolites* **7**, 119 (1987).
- [25] U. Lohse, B. Parlitz, V. Patzelova, *J. Phys. Chem.* **93**, 3677 (1989).
- [26] D. J. Parillo and R. J. Gorte, *J. Phys. Chem.* **97**, 8786 (1993).
- [27] H. Stach, J. Jänchen, H.-G. Jersckewitz, U. Lohse, B. Parlitz, M. Hunger *J. Phys. Chem.* **96**, 8480 (1992).
- [28] R. D. Shannon, K. H. Gardner, R. H. Staley, G. Bergeret, P. Gallezot and A. Auroux, *J. Phys. Chem.* **89**, 4778 (1985).
- [29] M. B. Sayed, A. Aline, J. C. Vedrine, *Appl. Catal.* **23**, 49 (1986).

- [30] B. E. Spiewak, B. E. Handy, S. B. Sharma and J. A. Dumesic, *Catal. Lett.* **23**, 207 (1994).
- [31] N. Cardona-Martinez and J. A. Dumesic, *Adv. in Catal.* **38**, 149 (1992), and references therein.
- [32] G. Vorbeck, J. Jänchen, B. Parlitz, M. Schneider and R. Fricke, *J. C. S. Chem. Comm.* **1994**, 123 (1994).
- [33] D. J. Parillo and R. J. Gorte, *J. Phys. Chem.* **97**, 8786 (1993).
- [34] D. J. Parillo, C. Lee and R. J. Gorte, *Appl. Catal.* **110**, 67 (1994).
- [35] R. L. Stevenson, *J. Catal.* **21**, 113 (1971).
- [36] N. P. Kenastan, A. T. Bell and J. A. Reimer, *J. Phys. Chem.* **98**, 894 (1993).
- [37] D. Freude, J. Klinowski, H. Hamdan, *Chem. Phys. Lett.* **149**, 355 (1988).
- [38] W. L. Earl, P. D. Fritz, A. A. V. Gibson and J. H. Lunsford, *J. Phys. Chem.* **91**, 2091 (1987).
- [39] D. Michel, A. Germanus and H. Pfeifer, *J. C. S. Farad. Trans. I*, **78**, 237 (1982).
- [40] W. P. J. H. Jacobs, J. W. de Haan, L. J. M. van de Ven and R. A. van Santen, *J. Phys. Chem.* **97**, 10394 (1993).
- [41] A. J. Vega and Z. Luz, *J. Phys. Chem.* **91**, 365 (1987).
- [42] D. Deininger and B. Reiman, *Z. phys. Chem. (Leipzig)* **251**, 351 (1972).
- [43] M. M. Mestdagh, W. E. E. Stone and J. J. Fripiat, *J. Catal.* **38**, 358 (1975).
- [44] L. B. McCusker, *Zeolites* **4**, 51 (1984).
- [45] D. R. Corbin, L. Abrams, G. A. Jones, M. M. Eddy, W. T. A. Harrison, G. D. Stucky and D. E. Cox, *J. Am. Chem. Soc.* **112**, 4821 (1990).
- [46] R. X. Fischer, W. H. Bauer, R. D. Shannon, J. B. Parise, J. Faber and E. Prince, *Acta Cryst.* **C45**, 983 (1989).
- [47] R. A. van Santen, A. J. M. de Man, W. P. J. H. Jacobs, E. H. Teunissen and G. J. Kramer, *Catal. Lett.* **9**, 273 (1991).
- [48] T. Stock, D. Dombrowski and J. Fruwert, *Z. phys. Chemie (Leipzig)*, **265**, 738 (1984).
- [49] W. P. J. H. Jacobs, J. H. M. C. van Wolput and R. A. van Santen, *J. C. S. Farad. Trans.* **89**, 1271 (1993).
- [50] W. P. J. H. Jacobs, J. H. M. C. van Wolput and R. A. van Santen, *Zeolites* **13**, 170 (1993).
- [51] R. McWeeny, *Methods of Molecular Quantum Mechanics*, 2nd ed. (Academic Press, London, 1992).
- [52] J. C. Slater, *Quantum Theory of Molecules and Solids* Vol. 1 (McGraw Hill, New York, 1964).
- [53] A. Szabo and N. S. Ostlund, *Modern Quantum Chemistry*, 1st. rev. ed. (McGraw-Hill, New York, 1989).
- [54] W. J. Hehre, L. Radom, P. v. R. Schleyer and J. A. Pople, *Ab-initio Molecular Orbital theory* (Wiley, New York, 1986).
- [55] V. R. Saunders, in *Computational Techniques in Quantum Chemistry and Molecular Physics* edited by G. H. F. Diercksen, B. T. Sutcliffe and A. Veillard, NATO ASI series C **15** (Reidel, Dordrecht, 1975).
- [56] C. Pisani, R. Dovesi and C. Roetti, *Hartree Fock Ab Initio Treatment of Crystalline systems*, (Springer, Berlin, 1988).

Chapter 1 : Introduction

- [57] M. F. Guest and J. Kendrick, *GAMESS Users Manual*, (SERC Daresbury Laboratory, CCP1/86/1, 1986), M. Dupuis, D. Spangler and J. Wendoloski, *GAMESS (NRCC Software Catalog, Vol. 1, Program No. QG01, 1980)*, M. F. Guest, R. J. Harrison, J. H. van Lenthe and L. C. H. van Corler, *Theor. Chim. Acta.* **71**, 117 (1987).
- [58] M. J. Frisch, G. W. Trucks, M. Head-Gordon, P. M. W. Gill, M. W. Wong, J. B. Foresman, B. G. Johnson, H. B. Schlegel, M. A. Robb, E. S. Replogle, R. Gomperts, J. L. Andres, K. Raghavachari, J. S. Binkley, C. Gonzalez, R. L. Martin, D. J. Fox, D. J. DeFrees, J. Baker, J. J. P. Stewart, and J. A. Pople, *Gaussian 92 Revision D.3*, (Gaussian Inc., Pittsburgh PA, 1992).
- [59] M. Häser and R. Ahlrichs, *J. Comput. Chem.* **10**, 104 (1989), R. Ahlrichs, M. Bär, M. Häser, H. Horn and C. M. Kölmel, Program TURBOMOLE (1989).
- [60] J. C. Slater, *Quantum Theory of Molecules and Solids* Vol. 2, (McGraw-Hill, New York, 1965).
- [61] C. Kittel, *Introduction to Solid state Physics* 6th ed. (Wiley, New York, 1986).
- [62] F. Bloch, *Z. Physik*, **52**, 555 (1928).
- [63] R. Dovesi, V. R. Saunders and C. Roetti *Crystal 92 Users's Manual*, Gruppo di Chimica Teorica, Università di Torino, and SERC Laboratory (1992).
- [64] R. S. Mulliken *J. Chem. Phys.* **23**, 1833 (1955).
- [65] R. Dovesi, C. Pisani, C. Roetti and V. R. Saunders, *Phys. Rev. B* **28**, 5781 (1983).
- [66] V. R. Saunders, C. Freyria-Fava, R. Dovesi, L. Salasco and C. Roetti, *Mol. Phys.* **77**, 629 (1992).
- [67] M. Abramowitz and I. A. Stegun, *Handbook of Mathematical functions* (Dover, New York, 1964).

2

Basis set, electron correlation and geometry effects

Introduction

For a quantum chemical description of adsorption and proton transfer processes in zeolites there is a large choice for the model representing the zeolite and for the quantum chemical method. Usually, the zeolite is represented by a cluster. In the cluster approach, a group of atoms is cut from the zeolite lattice and the dangling bonds are saturated, usually with hydrogen atoms. The choice of the cluster, i.e. the choice for its size, shape and geometry, is not trivial since it determines the model representing the zeolite, and thus the calculated adsorption energies. The geometry of the cluster has to be determined in some way; it can be taken from experimental data, from molecular mechanics, or it can be optimized quantum chemically. Apart from the choice of the cluster, the description of the adsorption process is also determined by the choice of the quantum chemical method.

In practice, the choice of the cluster and the quantum-chemical methods is a compromise between the aim of the research, the required accuracy and the available computer facilities. The computational costs increase rapidly with the size of the system and the requested accuracy. For example, for a standard SCF calculation the required computer time increases roughly with N^4 , in which N is the number of basis functions. Electron correlation, and the calculation of the counterpoise correction, increase the computational effort by a factor of ten or more [1,2]. A quantum chemical optimization of the geometry of the zeolite cluster increases the computational effort by a factor of ten to ninety.

The aim of this chapter is to choose a satisfactory method for future calculations. Therefore, we studied the effect on the calculated adsorption energy of the basis set, of the counterpoise correction, of electron correlation and the effect of the optimization of the geometry. We studied the adsorption of NH_3 on the acidic OH-group of the zeolite and the proton transfer from the zeolite to NH_3 , forming NH_4^+ . As a model for the zeolite acidic site we used a HOSiAlH_6 cluster. We compared two structures. In the first, NH_3 is hydrogen bonded to the zeolite OH-group; this is the $\text{NH}_3 \cdots \text{HOSiAlH}_6$ structure. In the second, the proton is transferred to the zeolite, resulting in the ionic $\text{NH}_4^+ \cdots \text{OSiAlH}_6^-$ structure.

For these two structures we calculated the adsorption energies of NH_3 and NH_4^+ , i.e. the energy of the complexes with respect to the separated NH_3 and HOSiAlH_6 fragments, as well as the proton transfer energy, the difference in adsorption energy between NH_3 and NH_4^+ .

The effect of electron correlation is studied by comparing the adsorption energies at the RHF-level and at the correlated level. Electron correlation is calculated using second-order Møller-Plesset perturbation theory (MP2) [3,4]. This method yields a good estimate for the correlation energy with a relatively small computational effort. The effect of the Basis Set Superposition Error (BSSE) is investigated by calculating the adsorption energies with and without the full counterpoise correction (CPC) [1,2]. We studied the effect of the basis set on the adsorption and proton transfer energies by comparing the results of three basis sets.

To study the effect of the geometry on the adsorption energy we have compared two extremes. In one set of calculations we optimized the geometry of the zeolite clusters and their complexes with the adsorbate quantum chemically without any constraint. In a second set of calculations the geometries were obtained partly from molecular modeling calculations and were kept fixed. The calculations in which the geometry is optimized have the disadvantage of requiring more computer time but have the advantage that much more complete infrared and Raman spectroscopic properties can be obtained from them. Also the cluster can adjust its geometry to the adsorbate. Later, we will answer the question if the optimized geometries are transferable to a zeolite crystal.

Computational Details

We calculated the adsorption energy of NH_3 on a HOSiAlH_6 cluster, and of NH_4^+ on a OSiAlH_6^- cluster using two different geometries. In one set of calculations we kept the geometry of the interacting species, i.e. $\text{NH}_3/\text{NH}_4^+$ and the zeolite cluster, fixed and in another set we optimized the geometry of the interacting species quantum chemically. For the fixed-geometry calculations the position of the silicon and aluminum atoms of the zeolite cluster were taken from a crystal structure obtained with a molecular mechanics optimization of a 1:1 Si/Al Na-Faujasite [5,6]. The hydrogen atoms saturating the dangling bonds are put in the direction of the corresponding T-O bond. The Si-H bond length is fixed at 1.615 Å and the Al-H bond length at 1.480 Å. The positions of the oxygen atom and the proton of the acidic OH-group were optimized at the SCF-level using a 6-21G basis set with d-functions on oxygen only [7,8]. In the HOSiAlH_6 cluster the positions of the atoms of the OH-group were optimized and in the OSiAlH_6^- cluster the position of the oxygen atom was optimized. The internal geometries of the zeolite cluster and the adsorbate were kept fixed during the adsorption process, only the intermolecular distances were optimized. Experimental geometries were used for NH_3 and NH_4^+ [9,10]. NH_3 and NH_4^+ were adsorbed such that their C_3 -axes coincided with the O-H axis. This seems reasonable, since for several hydrogen bonds formed between acidic XH molecules and NH_3 , little or no deviation from linearity has been reported for the X-H-N bond [11-13]. In Table I the geometrical parameters, for both the covalent, i.e. the hydrogen bonding structure, and the ionic structure, in which the proton has been transferred, are given.

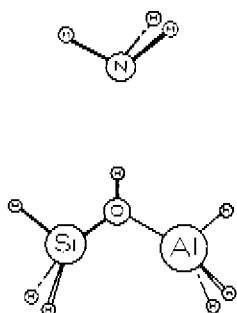


Figure 2.1. The zeolite cluster interacting with ammonia. The bond lengths and angles for the ionic and hydrogen bonding structure are given in Table I.

Table I The geometrical parameters of NH_3 and NH_4^+ interacting with the zeolite cluster. The bond lengths and angles are given in Å and degrees respectively. The $r_{\text{N-H}}$ corresponds to the distance between two atoms inside the adsorbate. The H-N-O angle corresponds to the angle the NH -bond makes with the C_3 -axis and the H-N-H angle to the angle between three atoms in the adsorbate.

parameter	covalent structure	ionic structure
$r_{\text{N-H}}$	1.01	1.03
$r_{\text{O-H}}$	0.96	-
$r_{\text{O-Si}}$	1.67	1.60
$r_{\text{O-Al}}$	1.85	1.82
$\angle_{\text{H-N-H}}$	107	109.471
$\angle_{\text{H-N-O}}$	112	109.471
$\angle_{\text{Si-O-Al}}$	129	137
$\angle_{\text{H-O-Si}}$	118	118

In the second set of calculations the geometries were optimized quantum chemically at the RHF level, using the ‘small’ basis set described below. HOSiAlH_6 , OSiAlH_6^- , NH_3 and NH_4^+ are fully geometry optimized. The former two are kept in a C_s -symmetry, the latter two in their C_{3v} and T_d symmetry respectively. The fixed geometry clusters and their complexes with the adsorbates were the starting geometries for the geometry optimizations. The geometry of the cluster adsorbate complexes were optimized with some restrictions. For the dangling bonds the T-H distance and the O-T-H -angle were kept fixed to the values obtained with the optimization of the HOSiAlH_6 and the OSiAlH_6^- cluster, respectively. Furthermore, the N-H-O angle is kept fixed at 180° and the cluster-adsorbate complex is kept in C_s -symmetry.

The interaction energy between two interacting molecules or ions called A and B , for example OSiAlH_6^- and NH_4^+ , is calculated from:

$$\Delta E^{\text{int}} = E^{AB} - E^A - E^B, \quad (2.1)$$

in which E^{AB} is the energy of the complex, for example the OSiAlH_6^- cluster bonded to NH_4^+ , in the equilibrium geometry. E^A and E^B are the energies of the fragments optimized in the absence of the other fragments, in this example the optimized ions NH_4^+ and OSiAlH_6^- . The interaction energy, Eq (2.1), may be biased by the BSSE. The incompleteness of the basis set of each molecule is partially compensated by using the basis set of the other fragment. In other words, the energy of the interacting fragments is lowered by using the orbitals of the other fragments to improve their own wavefunction. To avoid the BSSE, the CPC should be applied. It is calculated with Eq. (2.2) and is equal to, or larger than zero,

$$E^{BSSE} = (E^{A,comp}(\chi_A) + E^{B,comp}(\chi_B)) - (E^{A,comp}(\chi_A \oplus \chi_B) + E^{B,comp}(\chi_A \oplus \chi_B)). \quad (2.2)$$

Here *comp* denotes that the energy is evaluated at the geometry the molecules have in the complex, χ_A denotes the basis set of *A*, χ_B the basis set of *B* and $(\chi_A \oplus \chi_B)$ the sum of the basis sets of *A* and *B*. The counterpoise corrected interaction energy is labeled CPC:

$$\Delta E^{int/CPC} = E^{AB} - E^A - E^B + E^{BSSE}. \quad (2.3)$$

For NH_3 adsorbed on the HOSiAlH_6 cluster the adsorption energy is equal to the interaction energy, i.e. ΔE^{int} or $\Delta E^{int/CPC}$ Eq. (2.1) or Eq. (2.3). The adsorption energy of NH_4^+ , however, is calculated via a two-step process. The first step is the proton transfer, *PT*, at infinity. The second step is the adsorption of NH_4^+ onto the anionic zeolite fragment. The proton transfer energy at infinity is calculated as the difference in proton affinity (PA) between the zeolitic anionic fragment and NH_3 ,

$$\Delta E_{\infty}^{PT} = PA_{\text{NH}_3} - PA_{Z^-}. \quad (2.4)$$

The required proton affinities are the energies of the isolated and fully optimized NH_4^+ and HOSiAlH_6 minus the energies of the fully optimized and isolated NH_3 and OSiAlH_6^- ions respectively. The adsorption energy of NH_4^+ is the sum of the interaction energy and the proton transfer energy,

$$\Delta E^{ads} = \Delta E^{int} + \Delta E^{PT}. \quad (2.5)$$

The adsorption energy of NH_4^+ can also be found from Eq. (2.1) by taking the energy of the $\text{NH}_4^+ \cdots \text{OSiAlH}_6^-$ complex as E^{AB} and the energies of NH_3 and HOSiAlH_6 as E^A and E^B but the scheme described here allows us to study the interaction energy between NH_4^+ and the zeolite fragment and the ΔE^{PT} separately. Also, it enables us to calculate the CPC.

The energy of the complex, E^{AB} , and the intermolecular stretching frequency are calculated from the intermolecular potential curve. This curve is generated by calculating the interaction energy in a number of equidistant (0.1 Å) points around the assumed equilibrium O-N distance. For the fixed geometry calculation only the O-N distance is varied. For the optimized geometry calculations E^{AB} is obtained in a little more complicated way. At each O-N distance, all internal coordinates, except those determining the position of the dangling bond protons, are optimized. For both sets of geometries the interaction energy is calculated at the various quantum-chemical levels at each point of the potential energy curve. E^{int} corresponds to the minimum in the potential energy curves and from the curvature in the minimum the intermolecular stretching frequency can be calculated. The intermolecular frequency calculated in this way allows us to study this vibration at other levels than the SCF-level and to study it decoupled from other modes. In a normal mode analysis the vibrational frequencies are calculated for a gas-phase complex of the zeolite and the adsorbate. The intermolecular frequency calculated from the potential energy curve pictures NH_3 or NH_4^+ vibrating against a lattice with infinite mass. Coupling of the intermolecular vibration with other low frequency modes is omitted.

The effect of electron correlation is studied by applying the MP2 method. On comparing the difference in proton affinity between OH^- and NH_3 it is seen that electron correlation calculated at the MP2-level gives a proper value of the correlation energy contribution to the proton transfer energy [13-15]. MP2 also gives a reasonable estimate for the Van der Waals interaction energy [16]. In the small basis set the MP2-calculations are carried out with frozen cores.

For the calculation of adsorption energies we used two different basis sets which are called 'small' and 'large'. Both basis sets have a minimal STO-3G basis set [17] on the dangling bond hydrogens. The small basis set has a 6-31G(d) [7,18] basis set on all atoms except the dangling bond hydrogens. In the large basis set the non-saturating hydrogen atoms, the aluminium and silicon atom have a 6-31G(d,p) basis [18]. The nitrogen atom has a 6-311G(d,p) basis set and the oxygen atom a 6-311+G(d,p) basis set [19]. On the oxygen atom diffuse functions were included because the calculated proton affinity of oxygen anions is sensitive to these functions [14]. For smaller systems the large basis set may be expected to yield the proton affinity within 7 kJ/mol at the MP2-level [14] and to give the interaction energy of NH_3 with the cluster with a precision of 3 kJ/mol [16]. By comparing the results obtained with the small and the large basis set the validity of the use of this smaller and computationally less demanding basis set can be tested. The adsorption energies with the fixed geometry clusters were repeated at the SCF-level with a 6-311++G(3df,2pd) basis set [19,20]. This basis set should give interaction and proton transfer energy within a few kJ/mol of the Hartree-Fock limit [16,14]. It is used to check the accuracy of the large basis set for the type of systems used in this thesis.

Results and Discussion

The results of the geometry optimizations of the zeolite clusters and the cluster-adsorbate complexes are given in fig. 2.2. In the protonated form of the zeolite cluster, HOSiAlH_6 , aluminum forms a weak complex with the bridging oxygen atom whereas in the anionic form, OSiAlH_6^- , this bond shortens to form a bond comparable to the Al-O bond in $\text{Al}(\text{OH})_4^-$. This means that, in absence of the proton, the cluster anion is stabilized by strengthening the Si-O and especially the Al-O bond. After adsorption of NH_3 , i.e. when the hydrogen bond is formed, the geometrical parameters of the HOSiAlH_6 cluster are slightly shifted towards the values in the OSiAlH_6^- cluster; the Si-O and Al-O bonds shorten and the Si-O-Al-angle gets smaller. Also NH_3 undergoes changes on the formation of the hydrogen bond: the N-H bonds lengthen and the H-N-H angle widens.

In the equilibrium structure of the zeolite cluster-adsorbate complex the acidic proton is attached to the zeolitic cluster. The minimum energy configuration was found by starting the optimization from the situation in which the HOSiAlH_6 cluster is hydrogen bonding to the NH_3 molecule. To check if there was a minimum in which the proton was transferred, the complex was also optimized starting from the ionic structure, i.e. from the complex consisting of the OSiAlH_6^- cluster in its equilibrium geometry interacting with NH_4^+ . The structure in which the proton is transferred appeared not to be even a local minimum: the result of the optimization was a structure with only minor differences from the optimization started at the neutral monomers. These small differences were the result of the internal parameters, determining the position of the dangling bond hydrogen atoms, which were

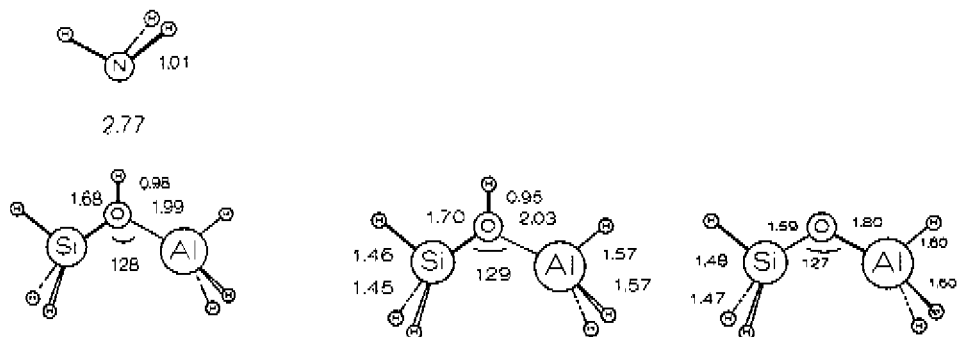


Figure 2.2. The results of the optimizations of the zeolite clusters and the cluster-adsorbate complex. The geometries were optimized with the small basis set.

Table II The harmonic frequencies (cm^{-1}) of the $\text{NH}_3 \cdots \text{HOSiAlH}_6$ complex, calculated with a normal mode analysis, the frequencies were scaled with a factor of 0.89.

description of mode	complex	neutral fragments	ionic monomers
OH bend in plane	1251	1001	-
OH stretch	3115	3666	-
NH deformation	1161/1599/1804	1407/1636	1106/1614
N-H stretch	3210/3325/3329	3095/3224	3199/3317

kept fixed to those of the HOSiAlH_6 and the OSiAlH_6^- cluster, respectively. Thus in this simple model, *i.e.* the zeolite is represented by a HOSiAlH_6 cluster and NH_4^+ interacting with one hydrogen bond with the bridging oxygen atom, no proton transfer takes place at the RHF-level.

The full set of harmonic frequencies was calculated at the RHF-level for the clusters and the complex of HOSiAlH_6 and NH_3 . They were not calculated for the $\text{NH}_4^+ \cdots \text{OSiAlH}_6^-$ complex since that structure was not a minimum. The frequencies and their shifts upon deprotonation and hydrogen bonding give additional information about the nature of the structures. A few selected frequencies are given in Table II. To make the comparison with experiment more convenient, the RHF normal-mode frequencies were scaled with a factor of 0.89, a generally used correction factor. The vibrational analyses confirm the weakening of the OH-bond on forming the hydrogen bond, already found with the geometry optimization. The bond lengthens by 0.03 Å and the frequency shifts down by 551 cm^{-1} . On the formation of the hydrogen bond, the frequencies of the N-H modes of NH_3 shift towards the values in the NH_4^+ cation. The frequencies of the N-H and O-H stretching modes shift into the region where the N-H stretching of NH_3 adsorbed in zeolites is found experimentally. A comparison between the calculated and experimental N-H stretching

frequencies will be made in Chapter 3.

The intermolecular vibrational modes between NH_3 and HOSiAlH_6 were mixed with the internal vibrations of NH_3 and HOSiAlH_6 . They appeared at 62, 91, 135, 217, 280 and 379 cm^{-1} . Because of the mixing with the intermolecular modes of the cluster, being different from the lattice vibrations of the lattice, they do not allow a comparison with the experimental values. From the intermolecular potential energy curve the intermolecular stretching frequency of NH_3 is calculated to be in the region $180\text{--}210\text{ cm}^{-1}$ (Tables III-VI). The frequency for NH_4^+ is much higher because of the large interaction between the NH_4^+ cation and the anionic zeolite cluster. Experimentally, modes at 169 cm^{-1} [21] at 204 and 174 [22] and in the region between 164 and 193 cm^{-1} [23] were assigned to be intermolecular modes between NH_4^+ and the crystal. The calculated intermolecular modes of NH_3 seems to be in the right region of the spectrum but it can be assumed that the cluster model is too simple to compare quantitatively the experimental and calculated frequencies.

The adsorption energies of NH_3 and NH_4^+ , in both basis sets and for both fixed and optimized geometry were calculated at the RHF-level as well as at the MP2-level and with and without the CPC. From the binding energies in Tables III to VI we can study the effect of the various strategies on the adsorption energy. For the structure in which NH_3 is hydrogen bonding to the HOSiAlH_6 cluster the effect of electron correlation and the CPC are relatively independent of the basis set and the geometry. The counterpoise correction is about 10 and 20 kJ/mol at the SCF-level and the MP2 level, respectively. Without the CPC, the strength of the hydrogen bond, especially at the correlated level is overestimated. If the CPC is applied, MP2 strenghtens the hydrogen bond by about 10 kJ/mol. Because of the opposing effects of the BSSE and the absence of correlation, the binding energies found at the RHF-level for the hydrogen bonded structure compare well with the values found at the SCF/MP2/CPC level: they are equal within 3 kJ/mol.

For the ionic structure, the structure in which the proton is transferred, the effect of the CPC and MP2 on the adsorption energy is more dependent on the basis set. Electron correlation affects the proton transfer energy; it stabilizes the ionic form by about 13 kJ/mol more than it does the covalent form. The effect of electron correlation is largely overestimated if the CPC is not applied. The comparison of the adsorption energies as calculated with the different methods shows that the adsorption energy of NH_4^+ and the proton transfer energy are not described well at the SCF-level. Electron correlation and the CPC are too important to be neglected, or to rely on cancellation. The adsorption energy of NH_4^+ is built from two energies; the interaction energy between the NH_4^+ ion and the zeolite ion, ΔE^{int} , and the difference in proton affinity, ΔE_{∞}^{PT} . Both are basis set dependent. However, since the dependency is similar, the adsorption energy is less dependent on the basis set and electron correlation than the ΔE_{∞}^{PT} and the ΔE^{int} individually. The interaction energy in the ionic system is much larger than in the hydrogen bonded system because of the electrostatic interaction between the anion and the cation. This stronger bond is expressed by the shorter equilibrium bond length and by the higher intermolecular stretching frequency.

Tables IV, V and VI show the effect of the basis set on the adsorption energy as the data in these tables were calculated with the same geometry and three different basis

Table III The adsorption energy and equilibrium O-N distances of NH_3 hydrogen bonding to the HOSiAlH_3 cluster. The geometry is optimized quantum chemically, for the calculation of the adsorption data and for the geometry optimization the small basis set was used. The binding energies are in kJ/mol bond lengths in Å and the frequencies in cm^{-1} .

method	R_{NO}	ΔE^{ads}	ν_{inter}
SCF/MP2/CP	2.74	-60	185
SCF/CP	2.82	-49	194
SCF/MP2	2.64	-78	227
SCF	2.77	-57	184

Table IV Adsorption data for NH_3 and NH_4^+ , calculated with the large basis set and the fixed geometry. Units as in Table III.

method	R_{NO}		ΔE^{ads}		ν_{inter}	
	NH_3	NH_4^+	NH_3	NH_4^+	NH_3	NH_4^+
SCF/MP2/CPC	2.73	2.53	-67	-15	193	275
SCF/CPC	2.79	2.55	-60	5	181	278
SCF/MP2	2.64	2.48	-88	-35	227	281
SCF	2.76	2.53	-69	-5	223	276

Table V Adsorption data for NH_3 and NH_4^+ , calculated with the small basis set and the fixed geometry. Units as in Table III.

method	R_{NO}		ΔE^{ads}		ν_{inter}	
	NH_3	NH_4^+	NH_3	NH_4^+	NH_3	NH_4^+
SCF/MP2/CPC	2.72	2.56	-68	24	211	508
SCF/CPC	2.77	2.54	-59	39	190	348
SCF/MP2	2.64	2.54	-89	-36	227	535
SCF	2.73	2.52	-68	6	204	364

Table VI Adsorption data for NH_3 and NH_4^+ , calculated with the 6-311++G(3df,2dp) basis set and the fixed geometry. Units as in Table III.

method	R_{NO}		ΔE^{ads}		ν_{inter}	
	NH_3	NH_4^+	NH_3	NH_4^+	NH_3	NH_4^+
SCF	2.75	2.65	-58	-15	216	247

Table VII The proton transfer energies (kJ/mol) at infinite distance calculated in the fixed geometry at the SCF and MP2-level

	$\Delta E_{\infty}^{\text{PT}} (\text{SCF})$	$\Delta E_{\infty}^{\text{PT}} (\text{MP2})$
small basis set	-495	-493
large basis set	-445	-436
6-311++G(3df,2pd)	-411	-406

sets. At the SCF/MP2/CPC-level the binding energy for the hydrogen-bonded cluster is described quite well by the small basis set: it is within 2 kJ/mol from the adsorption energies calculated in the larger basis set. The intermolecular stretching frequency shows a larger deviation. The ionic structure is poorly described by the small basis set. The adsorption energy calculated with the small basis set deviates 39 kJ/mol from the one obtained with the larger basis set at the SCF/MP2/CPC level and 11 kJ/mol at the SCF level. The 6-311++G(3df,2pd) basis set was used only at the SCF-level because of its computational demands. Since this basis set is very large the BSSE will be small at the SCF-level, therefore the adsorption energy calculated in this basis set should be compared with the SCF/CPC adsorption energies of the small and the large basis set. Again, the adsorption energy of NH_3 is found to be relatively independent of the basis set. NH_4^+ on the other hand is stabilized 20 kJ/mol more with respect to the large basis set. The difference between the large basis set and the 6-311++G(3df,2pd) basis set will be larger at the correlated level but the error made with the large basis set seems acceptable for the calculation of adsorption energies.

The effect of the geometry on the adsorption energy can be deduced from Tables III and IV as the data in the tables are calculated with the same basis set, in the Table III with optimized geometries and in Table IV with a fixed geometry. The binding energy, of the hydrogen bonded NH_3 , calculated in the optimized geometry is -60 kJ/mol, and -67 kJ/mol or -68 kJ/mol in the fixed geometry, depending on the basis set. The zeolite cluster, stabilized by the geometry optimization, is less reactive and the hydrogen bond is weaker.

Compared to other hydrogen bonds the zeolite cluster- NH_3 bond is very strong and short. For example, the $\text{H}_2\text{O} \cdots \text{NH}_3$ bond has a strength of 24 kJ/mol with a O-N distance of 3.01 Å [11]. CPC-uncorrected SCF/MP2 values for the $\text{H}_3\text{N} \cdots \text{HCl}$ and $\text{H}_3\text{N} \cdots \text{HF}$ are -46 and -63 kJ/mol respectively [24]. For the $\text{SiH}_3\text{OH} \cdots \text{NH}_3$ system Ugliengo *et al.* [25] found a hydrogen bond with a strength of -37 kJ/mol at the SCF/MP2 level. Geerlings *et al.* [26] found a interaction energy of -56 kJ/mol between the NH_3 and a HOSiAlH_6 cluster, with a 3-21G basis set at the SCF-level. At this level an O-N distance 2.69 Å was found. The comparison of the interaction energies of NH_3 with other acids shows that the zeolite OH-group has an acidity that is comparable to strong acids. The results of the calculations as described in this work are not in agreement with the results found by Allavena *et al.* [27,28]. They found that the ion-pair structure was 13 kJ/mol lower in energy than the covalent structure. They used a 6-21G basis set, a basis set smaller than the small basis set we used in this chapter. Most probably, the results of Allavena *et al.* were influenced by the deficiencies of the basis set, and the geometry, they used.

Conclusion

We studied the effect of the basis set, electron correlation and geometry optimization on the adsorption energy of NH_3 onto the zeolite and the proton transfer from the zeolite to NH_3 . The zeolite was modeled with a HOSiAlH_6 cluster.

In the chosen model, the zeolite cluster does not transfer its proton to NH_3 . NH_3 forms a strong hydrogen bond with the cluster, this bond has a strength of -60, -67 or 69 kJ/mol, depending on the basis set and the geometry of the cluster. Proton transfer is

unfavorable by 52 kJ/mol. The calculated adsorption energies are too small with respect to the experimental adsorption energy of about 130 kJ/mol [4].

Optimization of the geometry of the zeolite cluster makes it less reactive and NH_3 is adsorbed less strongly. The hydrogen bonded structure can be described satisfactorily at the SCF-level with a small basis set. The structure in which the proton is transferred needs a large basis set, electron correlation and the counterpoise correction for a proper description.

Electron correlation stabilizes the hydrogen bond by about 10 kJ/mol and the proton transferred complex by 15 to 20 kJ/mol, depending on the basis set. If the effect of the electron correlation is calculated the CPC should be used to avoid the BSSE, otherwise the effect of the electron correlation is overestimated.

The small basis set overestimates the proton transfer energy because of its inability to describe the proton transferred complex. The large basis set produces the adsorption energy of NH_4^+ with an error of about 10 kJ/mol at the SCF-level, at the correlated level this error will be larger.

References

- [1] S. F. Boys and F. B. Bernardi, *Mol. Phys.* **19**, 553 (1970).
- [2] J. H. van Lenthe, J. G. C. M. van Duijneveldt-van de Rijdt and F. B. van Duijneveldt, *Adv. in Chem. Phys.* **79**, 521 (1987).
- [3] C. Møller and M. S. Plesset, *Phys. Rev.* **46**, 618 (1934).
- [4] *Chapter 1 of this thesis.*
- [5] G. J. Kramer, N. P. Farragher, B. W. H. van Beest and R. A. Santen, *Phys. Rev. B* **43**, 5068 (1991).
- [6] W. M. Meier and D. H. Olson, *Atlas of Zeolite Structure Types* 2nd. ed. (Butterworths, London, 1987)
- [7] P. C. Hariharan and J. A. Pople, *Theor. Chim. Acta.* **28**, 213 (1973).
- [8] J. S. Binkley, J. A. Pople and J. W. Hehre, *J. Am. Chem. Soc.* **102**, 939 (1980).
- [9] G. Herzberg, *Molecular Spectra and Molecular Structure* Vol. 2, Van Nostrand, Princeton (1945).
- [10] J. A. Ibers and D. P. Stevenson, *J. Chem. Phys.* **28**, 929 (1958).
- [11] Z. Latajka and S. Scheiner, *J. Phys. Chem.* **94**, 217 (1990).
- [12] I. J. Kurnig, M. M. Szczęśniak and S. Scheiner, *J. Phys. Chem.* **90**, 4253 (1986).
- [13] J. E. DelBene, M. J. Frisch and J. A. Pople, *J. Phys. Chem.* **89**, 3669 (1985).
- [14] D. J. DeFrees and A. D. McLean, *J. Comp. Chem.* **7**, 321 (1986).
- [15] J. E. DelBene and I. Shavitt, *J. Phys. Chem.* **94**, 5514 (1990).
- [16] K. Szalewicz, S. J. Cole, W. Kołos; and R. J. Bartlett, *J. Chem. Phys.* **89**, 3662 (1988).
- [17] W. J. Hehre, R. F. Stewart and J. A. Pople, *J. Chem. Phys.* **51**, 2657 (1969).
- [18] M. S. Gordon, J. S. Binkley, J. A. Pople, W. J. Pietro and W. J. Hehre, *J. Am. Chem. Soc.* **104**, 2997 (1982), M. M. Franci, W. J. Pietro, W. J. Hehre, J. S. Binkley, M. S. Gordon, D. J. DeFrees and J. A. Pople, *J. Chem. Phys.* **77**, 3654 (1982), R. Ditchfield, W. J. Hehre and J. A. Pople, *J. Chem. Phys.* **54**, 724 (1971), W. J. Hehre, R. Ditchfield and J. A. Pople, *J. Chem. Phys.* **56**, 2257 (1972).

- [19] R. Krishnan, J. S. Binkley, R. Seeger and J. A. Pople, *J. Chem. Phys.* **72**, 650 (1980).
- [20] M. J. Frisch, J. A. Pople and J. S. Binkley, *J. Chem. Phys.* **80**, 3265 (1984).
- [21] G. A. Ozin, M. D. Baker, K. Helwig and J. Godber, *J. Phys. Chem.* **89**, 1846 (1985).
- [22] T. Stock, D. Dombrowski, J. Fruwert, and H. Ratajczak, *J.C.S. Farad. Trans. I* **79**, 2773 (1983).
- [23] G. A. Ozin, M. D. Baker, J. Godber and C. J. Gil, *J. Phys. Chem.* **93**, 2899 (1989).
- [24] Z. Latajka and S. Scheiner, *J. Chem. Phys.* **81**, 4014 (1984).
- [25] P. Ugliengo, V. R. Saunders and E. Garrone, *Surf. Sci.* **224**, 498 (1989).
- [26] P. Geerlings, N. Tariel, A. Botrel, R. Lissilour and J. W. Mortier, *J. Phys. Chem.* **88**, 5752 (1984).
- [27] E. Kassab, K. Seiti and M. Allavena, *J. Phys. Chem.* **92**, 6705 (1988).
- [28] M. Allavena, K. Seiti, E. Kassab, Gy. Ferenczy, and J. G. Ángyán, *Chem. Phys. Lett.* **168**, 461 (1990).

3

Coordination and solvation effects

Introduction

Experimentally, it is found that, in acidic zeolites, proton transfer takes place from the acidic HOSiAl-group to adsorbed NH_3 molecules. The heat of adsorption is approximately 130 kJ/mol [1]. So far, the results of the quantum-chemical calculations do not match the experimental results. With the model used in the previous chapter, i.e. NH_4^+ bonding to the zeolite cluster with a single hydrogen bond*, no proton transfer takes place. Also the heat of adsorption is too low with respect to the experimental one. Apparently, NH_4^+ is not stabilized to such an extent that it can overcome the difference in deprotonation energy between the zeolite cluster and NH_4^+ , the ΔE_{∞}^{PT} . In this chapter, we studied whether it is possible to stabilize NH_4^+ by multiple bonding such that proton transfer becomes favorable. We studied the stabilization of NH_4^+ by letting it form two or three hydrogen bonds with the zeolitic lattice and by coadsorption of a second NH_3 molecule. We studied the multiple bonding of NH_4^+ to the zeolite lattice in the cluster approach.

To describe NH_4^+ singly, doubly and triply bonding to the lattice we used HOSiAlH₆, Al(OH)₂H₂ and Al(OH)₃H clusters, respectively. Probably, they do not provide a good model for the zeolite but they allow us to use a relatively large basis set, to optimize geometries and to carry out vibrational analyses relatively easily at the SCF-level. Adsorption energies were calculated at the SCF/MP2/CPC level.

We studied the effect of the geometry optimization on the stabilization of NH_4^+ by comparing the adsorption energy of NH_4^+ on a Al(OH)₃H⁻ cluster whose geometry was taken from a crystal structure obtained with molecular mechanics and on the same cluster of which the geometry is optimized quantum chemically. The effect of the cluster size has been investigated by comparing the adsorption energy of NH_4^+ on a Al(OH)₃H⁻ and a Al(OH)₂(OSiH₃)H⁻ cluster. We also calculated the adsorption energies of NH_4^+ singly and doubly bonding on a Al(OH)₃H⁻ cluster, a Al(OH)₂H₂ cluster and a HOSiAlH₆ cluster,

* The term 'hydrogen bond', though perhaps not appropriate for a fully ionic system, is used to characterize the geometrical arrangements studied.

respectively. The results of the vibrational analysis of NH_4^+ adsorbed on the clusters were compared with experimental infrared spectra of NH_4^+ adsorbed in zeolites.

Computational Details

We treated the adsorption of NH_4^+ as a two step process: the proton transfer from the zeolite to NH_3 at infinity and the binding of NH_4^+ onto the zeolite. For the proton transfer step the zeolite is represented by a HOSiAlH_6 cluster. The clusters used to describe the interaction between NH_4^+ and the zeolite are the smallest clusters able to describe the specific coordination between NH_4^+ and the zeolite. To describe the structure in which NH_4^+ is adsorbed with two hydrogen bonds onto the zeolite lattice a $\text{Al}(\text{OH})_2\text{H}_2^-$ (fig. 3.2b) cluster was used, this is the double structure. NH_4^+ adsorbed with three hydrogen bonds on the zeolite wall is referred to as the triple structure, the zeolite wall is modeled by an $\text{Al}(\text{OH})_3\text{H}^-$ (fig. 3.2d) cluster. When dealing with the coadsorption of two NH_3 molecules on a single acidic site the HOSiAlH_6 cluster was adopted (fig. 3.3e). To study the dependence of the interaction energy on the choice of the cluster some additional calculations on NH_4^+ bonded singly or doubly on the $\text{Al}(\text{OH})_3\text{H}^-$ cluster have been performed as well. For the structures mentioned above, the geometry for the acidic cluster, the anionic cluster and the complexes of the cluster with NH_4^+ are optimized.

All the calculations were performed with the 6-311+G(d,p)/STO-3G basis set. This basis set is equal to the large basis set in Chapter 2 [2,3]. This notation means that the hydrogen atoms saturating the dangling bonds are described with a STO-3G basis set [4], the silicon and aluminum atoms with a 6-31G(d) basis set [5], the nitrogen with a 6-311G(d) [6] basis, the hydrogen atoms attached to the nitrogen atom with a 31G(p) basis set [7], and all oxygen atoms with a 6-311+G(d) basis set [6,8].

The adsorption energies for the geometry optimized clusters and the cluster-adsorbate complexes were calculated at the various levels, using Eqs. (2.1) to (2.5). The equilibrium geometries were found by geometry optimization of the clusters at the SCF level, using gradient techniques. No Counterpoise Correction (CPC) was applied in this step. Starting from the minimum found at the SCF-level the optimizations were repeated with the Al...N distance fixed at 0.1 and 0.2 Å shorter and longer, respectively. For each of the structures created in this way a calculation is performed in which electron correlation is included in the form of second-order Møller-Plesset theory [9], keeping the cores frozen. The CPC is applied in this step. The potential energy curves were used to obtain the equilibrium Al...N distances and interaction energies, ΔE^{int} .

In the two-step adsorption process the proton transfer at infinity is the same for all structures. The ΔE_{∞}^{PT} is the difference in proton affinity of NH_4^+ and the HOSiAlH_6 cluster. We used this cluster since it provides the best model for the zeolite acidic site. The cluster, from which the reference proton affinity is taken, was also optimized with the same basis set. Since the proton affinities are very similar, as can be seen from Table I, the choice to use a single proton affinity for all structures does not introduce erroneous artifacts.

To study the effect of the cluster choice and the role of the geometry optimization some rigid geometry calculations were performed on the cluster shown in fig. 3.1. We calculated the adsorption energy of NH_4^+ triply bonded on the $\text{OAl}(\text{OH})_2(\text{OSiH}_3)\text{H}^-$ cluster. The

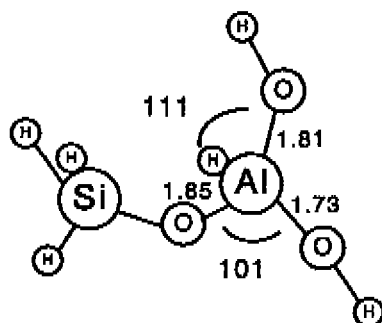


Figure 3.1. The anionic $\text{Al}(\text{OH})_2\text{HOSiH}_3$ cluster used to calculate the interaction energy between NH_4^+ and the zeolite wall in the rigid geometry calculations.

cluster is generated in the same way as the fixed geometry cluster in Chapter 2 [2,3]. The position of the atoms were taken from an optimization of Faujasite with a Si/Al ratio of 1. The position of the anionic oxygen was optimized using a 6-21G basis set. The ΔE_{∞}^{PT} at the SCF level was 444 kJ/mol. For NH_4^+ and NH_3 molecule experimental geometries were used [10,11]. The internal geometry of the fragments was kept fixed, only the $\text{Al} \cdots \text{N}$ distance was optimized. The aluminum atom is located along one of the C_3 -axes of the NH_4^+ ion. Because the aluminum tetrahedron is not regular, the angle of rotation of the NH_4^+ tetrahedron around the $\text{Al} \cdots \text{N}$ axis was optimized at the SCF-level, using a 3-21G basis set. The minimum energy was reached for a mean value of 6° for the Al-O-H-N dihedral angles.

To check the stability of the calculated adsorption date with respect to the cluster size the OSiH_3 group being replaced by a OH group, resulting in a $\text{Al}(\text{OH})_3^-$ cluster. We can study the effect of the geometry optimization on the adsorption energy of NH_4^+ on the $\text{Al}(\text{OH})_3^-$ cluster by comparing the heats of adsorption for the fixed geometry and the optimized geometry cluster.

Results and Discussion

The geometry optimized clusters

The results of the optimizations of the acidic and the anionic zeolite clusters are summarized in fig. 3.2. The optimized double and triple structures are shown in fig. 3.3. The zeolite clusters show large deviations from tetrahedral arrangement. The acidic $\text{Al}(\text{OH})_2\text{H}_2$ and $\text{Al}(\text{OH})_3\text{H}$ clusters show an almost planar aluminum cluster forming a complex with a deformed water molecule. The adsorption of NH_4^+ causes a distortion of the internal geometries of the cluster and the NH_4^+ -tetrahedron. The optimization of NH_4^+ adsorbed on the cluster shown in fig. 3.2f resulted in a hydrogen bonding $\text{NH}_3 \cdots \text{HOSiAlH}_6$ structure that will not be discussed in detail. The vibrational analysis of the double and triple structures show that both structures are minima as far as the coordination of the NH_4^+ is concerned. The triple structure showed one imaginary frequency. However, the vibrational

Table I. The deprotonation energies (deprotonation energy = $-PA$), in kJ/mol, at the SCF and at the MP2-level, of the clusters. The deprotonation energies are defined as the difference in energy between the optimized ZH and Z^- forms of the clusters or the difference in energy between the optimized NH_4^+ and NH_3 .

	$Al(OH)_2H_2$	$Al(OH)_3H_2$	$OSiAlH_6$	NH_4^+
SCF	1379	1364	1359	907
MP2	1377	1356	1358	905

amplitudes of this normal mode were completely located on the saturating hydrogen atoms bonded to the oxygen atoms and were considered not to be of influence on the adsorption process.

NH_4^+ becomes the stable species rather than NH_3 and proton transfer takes place when NH_4^+ is coordinating to the lattice with two or three hydrogen bonds. Apparently, proton transfer can take place, if after proton transfer, NH_4^+ has a high coordination towards the zeolite lattice. The adsorption energies of the double and triple structure are much higher than those of the hydrogen bonding NH_3 and are relatively close to the experimental heat of adsorption, especially if one notes that the basis set used here underestimates the stability of NH_4^+ by more than 10 kJ/mol [3]. Although the model representing the zeolite is too simple to draw definitive conclusions, the calculations presented here strongly suggest that in the zeolite proton transfer can take place, if after proton transfer NH_4^+ has a high coordination with the zeolite wall.

There remains the question whether the coordination and the stability of NH_4^+ is real, or caused by the choice and the symmetry of the cluster. As a check we adsorbed NH_4^+ doubly and singly bonding on the $Al(OH)_3H^-$ cluster and we compared the adsorption energies with those in which NH_4^+ is doubly and singly bonding on the $Al(OH)_2H_2^-$ and $OSiAlH_6^-$ cluster respectively. We performed a constraintless geometry optimization starting from NH_4^+ doubly bonding on the $Al(OH)_3H^-$ cluster. The result of this optimization was a doubly bonding structure. The vibrational analysis of this structure did not show imaginary frequencies. The binding energy of NH_4^+ doubly bonding on this cluster was -109 kJ/mol at the SCF-level. This is comparable to the adsorption energy of the doubly bonding NH_4^+ on the cluster shown in fig. 3.3b. NH_4^+ singly bonding on the $Al(OH)_3H^-$ cluster was optimized keeping the proton attached to the nitrogen atom and one Al-O-N angle fixed to keep the cation singly coordinated. The O-N distance was 2.51 Å, the adsorption energy at the SCF-level -9.0 kJ/mol. This is comparable to the adsorption of NH_4^+ singly bonded on the $OSiAlH_6^-$ cluster [2,3]. The adsorption energies of the singly and doubly bonding NH_4^+ are very similar on the $Al(OH)_3H^-$ and the $Al(OH)_2H_2^-$ and $OSiAlH_6^-$ clusters respectively. The heats of adsorption and the results of the geometry optimizations do not seem to be influenced strongly by the choice of the cluster.

NH_4^+ only seems stable when forming two or three hydrogen bonds with the zeolite lattice. From Eq. (2.5) we see that the stabilization of the doubly and triply bonded state relative to the singly bonded state can be caused by a change in proton affinity of the cluster or by a change in interaction energy. Since the proton affinity of the $OSiAlH_6^-$ cluster is used, the first possibility can be ruled out. Thus, the difference in stability between the

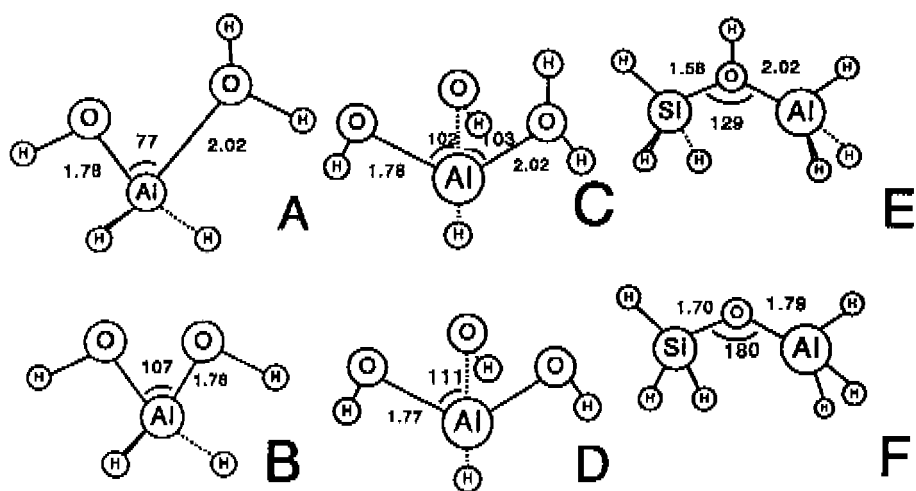


Figure 3.2. Optimized geometries of the clusters modeling the zeolite wall. Top, from left to right, the protonated forms (a,c,e) optimized in C_s symmetry. Bottom, from left to right, the anionic forms (b,d,f) optimized in C_{2v} , C_{3v} and C_s , respectively.

single the double and the triple structures is the result of the enhanced interaction energy. For the double and triple structure the E^{int} is lowered by about -100 kJ/mol relative to the singly coordinated NH_4^+ . From the small difference in binding or adsorption energy between the double and triple state it is clear that the binding energy is not proportional to the number of hydrogen bonds. In the case of an ion-ion interaction the exact alignment of the hydrogen bond does not seem to be very important. The factor determining the interaction energy, and thus the stability seems to be the short distance and the high coordination between the cation and the anion.

The fixed geometry calculations

The adsorption energy of NH_4^+ was calculated on the fixed geometry cluster shown in fig. 3.1, optimizing the O-N distance only. The adsorption energies were -18 kJ/mol and -11 kJ/mol at the SCF and SCF/CP level respectively, the Al-N distances 2.78 and 2.81 Å. The calculations were repeated with reduced cluster size. The $OSiH_3$ group was replaced by a OH group, resulting in a $Al(OH)_3H^-$ cluster. The adsorption energies did not differ much: -16 kJ/mol and -10 kJ/mol at the SCF and the SCF/CPC level respectively, the Al-N distances 2.77 and 2.79 Å. The difference in adsorption energy between the $Al(OH)_3H^-$ cluster and the $Al(OH)_2(OSiH_3)H^-$ cluster is small. From the calculations presented here, the adsorption energy seems relatively independent of the cluster size and seems to be determined to a large extent by the atoms directly interacting with the adsorbate.

Table II. The adsorption energy and Al...N bond length of the double and triple structures. Distances are in Å, adsorption energies in kJ/mol.

Method	$R_{Al...N}$		ΔE^{ads}	
	double	triple	double	triple
SCF/MP2/CPC	3.41	2.94	-114	-114
SCF/CPC	3.42	2.97	-98	-100
SCF/MP2	3.39	2.92	-141	-139
SCF	3.42	2.95	-110	-112

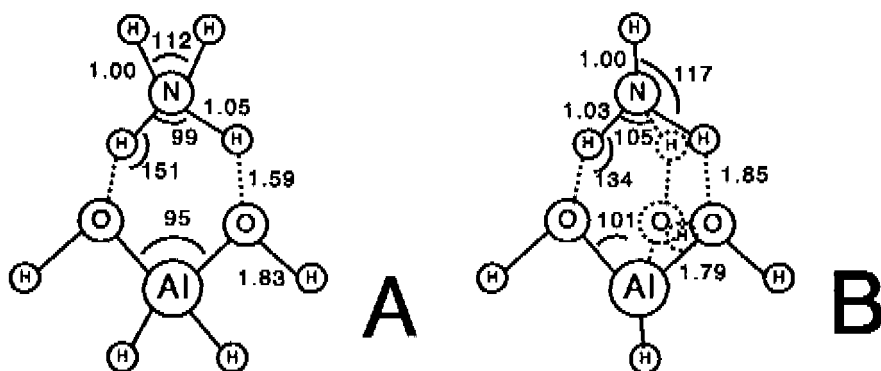


Figure 3.3. The result of the optimization of a) the double structure, and b) the triple structure.

The adsorption energies on the fixed geometry and the optimized geometry $Al(OH)_3H^-$ clusters differ considerably. The calculated heats of adsorption for the fixed geometry and optimized geometry $Al(OH)_3H_2$ (the optimized geometry cluster is described more correctly by $Al(OH)_2H(OH_2)$) clusters differ about 100 kJ/mol, the latter being more favorable. From Eq. (2.4) we see that this difference may be caused by a difference in ΔE_{∞}^{PT} or ΔE^{int} . There is only a small difference in ΔE_{∞}^{PT} : 444 kJ/mol for the fixed geometry cluster and 452 kJ/mol for the optimized geometry cluster. Thus, the difference in adsorption energy is caused by a difference in ΔE^{int} . The interaction energies for the fixed geometry cluster are -460 and -453 kJ/mol at the SCF and SCF/CPC level respectively. For the optimized geometry cluster they are -561 and -548 kJ/mol. This difference is caused by the difference in coordination of NH_4^+ with the cluster and the different alignment of the OH-groups. The fixed geometry cluster cannot coordinate to NH_4^+ optimally, because of its irregular shape; this decreases the interaction energy. Second, the fixed geometry cluster has a relatively flat shape. Because of this, a high NH_4^+ -zeolite anion coordination would imply NH_4^+ being close to the relatively large aluminum atom, leading to repulsion. Also in the fixed geometry the OH-groups cannot be positioned optimally.

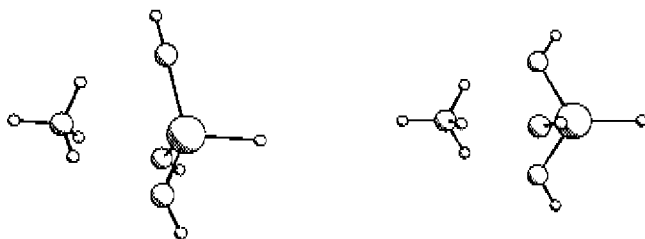


Figure 3.4. The difference in coordination between the fixed geometry and the optimized geometry structure. The fixed geometry structure on the left is relatively flat, its dipole moment is small and the aluminum atom is exposed to the NH_4^+ . In the optimized geometry, on the right, the O-Al-O-angle is decreased, hereby increasing the dipole moment and shielding the aluminum atom. The interaction energy between the cluster and the NH_4^+ is also increased by directing the dipole of the OH-bonds towards the cation.

The position of the OH-groups of the $\text{Al}(\text{OH})_3\text{H}^-$ cluster is important because of the relation between the geometry and the dipole moment of the $\text{Al}(\text{OH})_3\text{H}^-$ cluster. In the optimized geometry the O-Al-O angles are smaller. Since the negative charge is more or less located on the oxygen atoms a decrease in the angle increases the dipole moment. Also, in the optimized structure the OH-groups are pointing their dipoles in the direction of the NH_4^+ cation, fig. 3.4. Both features increase the dipole moment. In the fixed geometry cluster the dipole moment is 0.6 Debye. In the complex equilibrium geometry of the optimized geometry cluster the dipole is 3.5 Debye. For the calculation of the dipole moments, the origins were taken in the center of positive charge.

The $\text{Al}(\text{OH})_3\text{H}^-$ cluster can only obtain its high coordination with NH_4^+ and its large dipole moment by deformation. In the isolated state the O-Al-O-angle is 102° , in the optimized complex 111° , the Al-O bond length increases by 0.06 \AA . The deformation energy, the difference in energy between the fully optimized $\text{Al}(\text{OH})_3\text{H}^-$ cluster and the same cluster in the conformation of the equilibrium geometry of the triple structure, is 33 kJ/mol . In the complex, the extra binding energy compensates for the deformation energy. In the geometry optimization we gave the cluster complete freedom to deform. In a zeolite lattice the aluminum tetrahedron is constrained and the adsorption energy becomes dependent on the geometry of the AlO_4^- tetrahedron in the lattice. For example, if the AlO_4^- -tetrahedrons in the lattice would have the shape they have in the optimized triple structure the adsorption energy increases by -33 kJ/mol because the interaction energy is the same but the deformation energy is zero. If, on the other hand, the lattice would have the shape of the isolated $\text{Al}(\text{OH})_3\text{H}^-$ ion the adsorption energy will be less than the -112 found for this cluster. A rigid lattice with the shape of the cluster as shown in fig. 3.1 will give an adsorption energy of approximately -20 kJ/mol .

The completely geometry optimized clusters are able to reproduce the experimental

heat of adsorption, the fixed geometry cluster does not. This, together with the change in bond lengths as shown by XRD [1], indicates that a geometry optimized cluster seems a better model than a fixed geometry cluster. However, we should keep in mind that the freedom for deformation in the small cluster may give an overestimation for the deformation of the lattice. This means that, most probably, the geometry optimized clusters will give a higher coordination to NH_4^+ than a AlO_4^- -tetrahedron in a zeolite lattice [12].

The coadsorbed structure

In this section we studied the stabilization of NH_4^+ by a coadsorbed NH_3 molecule and we made an analysis of the various interactions in this system. The geometry of the zeolite cluster with two NH_3 molecules coadsorbed on the acid site was optimized at the SCF-level. The interaction energy calculations, at the SCF/MP2/CPC-level, were performed in the SCF-geometry only. One optimization started with a geometry in which the proton was transferred to the NH_3 molecule bonding to the zeolite cluster and another optimization started with a geometry in which the proton is attached to the zeolite. Both structures appeared to be minima. The results of the two geometry optimizations are given in fig. 3.5. In the proton transferred state, the N-O distance is very close to that in the $\text{NH}_4^+ \cdots \text{OSiAlH}_6$ complex [2,3]. The N-N distance however, is slightly longer than in the $\text{NH}_4^+-\text{NH}_3$ complex which is 2.85 Å [13], presumably because of repulsion between the anionic zeolite cluster and the dipole of the NH_3 molecule. Also in the covalent state, i.e. the state in which the proton is not transferred, the N-O and N-N distances do not deviate strongly from those in the NH_3 -dimer [14], and the $\text{NH}_3 \cdots \text{HOSiAlH}_6$ complex [2,3]. The adsorption energy of the proton transferred structure is 60 kJ/mol per two adsorbed NH_3 molecules; i.e. 30 kJ/mol per NH_3 -molecule. The structure in which the proton is attached to the zeolite, while hydrogen bonding to two NH_3 molecules is 15 kJ/mol more stable at the SCF-level. Since the anion is stabilized at the electron correlated level this difference will be smaller at the MP2-level.

In the coadsorbed structure, there appears to be a subtle balance between proton transfer energies and differences in binding energies. Energetically, this coadsorbed state is unfavorable compared to the double and triple structures, and also to the state where the proton is not transferred and a single NH_3 molecule is hydrogen bonded on a single site. However, it is interesting to see that NH_4^+ can be stabilized by a second adsorbed NH_3 molecule. This can be understood relatively easily. We saw that, for the singly bonding NH_4^+ the proton transfer was unfavorable by 52 kJ/mol [2,3]. The calculated binding energy between NH_3 and NH_4^+ is -99 kJ/mol [15], whereas for the NH_3 -dimer they were found to be 19, -14 and -18 kJ/mol [13,14,16]. From these differences in binding energy one could expect the proton transferred form of the structure to become favorable over the hydrogen bonded one when another NH_3 is coadsorbed. The required proton transfer energy is provided by the enhanced interaction energy. The fact that NH_4^+ is stabilized by a single extra NH_3 is an indication of the strong acidity of the zeolite acidic site. Experimentally, gas-phase α -Naphthol* ($\text{pK}_a \sim 0.5$) requires three additional NH_3 molecules to accomplish proton transfer to NH_3 [17]. This suggests that the acidic site of a zeolite is more acidic than strong mineral acids such as HI for which a pK_a of 0.77 has been reported [18].

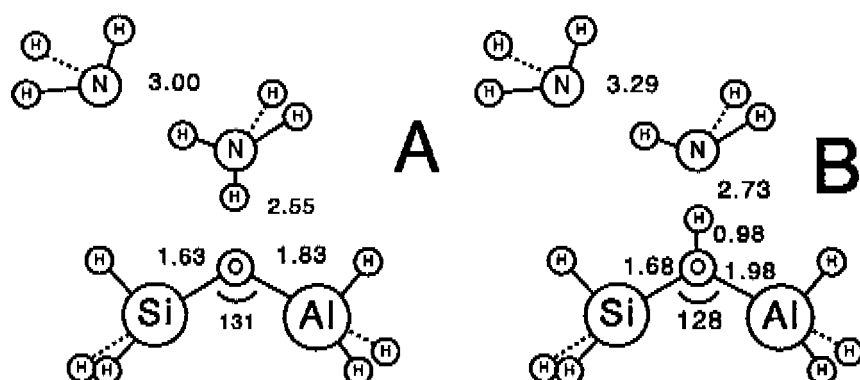


Figure 3.5. The coadsorbed structure, a) after proton transfer, b) before proton transfer. Indicated are the equilibrium distances between the nitrogen atoms of the adsorbates, the equilibrium distances between the nitrogen atom of the adsorbate and the oxygen atoms of the zeolite and some internal parameters of the zeolite cluster i.e. the Si-O, Al-O and the O-H distance as well as the Si-O-Al angle.

In Table III the overall adsorption energies and the interaction energies between all the individual pairs are tabulated. The latter are calculated in the absence of the third molecule. The binding energy for the complex involving NH_3 , NH_4^+ and OSiAlH_6^- is not equal to the sum of the binding energies of the separate pairs. The difference between this sum and the total binding energy, the three-body term is repulsive; 29 kJ/mol at the SCF/CPC-level. Electron correlation adds 2 kJ/mol to this three-body term. These numbers have an opposite sign and are somewhat larger than the values found for other hydrogen bonding systems. For example, at the SCF level it is -17 kJ/mol for the $\text{NH}_3 \cdots \text{HF} \cdots \text{HF}$ -system [19]. For the water trimer, this term is in between -3 to -5 kJ/mol, depending on the geometry. The contribution of the second order Møller-Plesset perturbation energy to the three-body term was almost negligible: 0.3 and 0.1 kJ/mol [20]. Since most of the SCF three-body energy is caused by polarization energy it can be expected that, in the coadsorbed structure with two ions the three-body term is repulsive and somewhat larger than in the other systems mentioned. Here, the three-body term becomes repulsive because the polarization of the NH_3 under influence of the NH_4^+ cation and the OSiAlH_6^- anion simultaneously, is less than under the influence of these ions separately.

Table III. An analysis of the binding energies in the coadsorbed structure (fig. 3.5a). The adsorption energies, the total of the interaction energies and the interaction energies between the pairs of molecules are tabulated. The interaction energies and the CPC are calculated with Eqs. (2.2) and (2.3). ΔE^{ads} is the ΔE^{ads} from Eqs. (2.4) for the complete system of the three interacting particles. ΔE^{int} , Eqs. (2.2) and (2.4), is the interaction energy for the three particles. AB, AC, and BC denote the pair interactions (explanation given below). $A=OSiAlH_6^-=Z^-$, $B=NH_4^+$, $C=NH_3$, $\Delta E^{ads}=E^{ABC}=E(Z^- \cdots NH_4^+ \cdots NH_3) - E(Z^-) - 2E(NH_3)$, $ABC=\Delta E^{int}=E(Z^- \cdots NH_4^+ \cdots NH_3) - E(Z^-) - E(NH_4^+) - E(NH_3)$, $AB=E(Z^- \cdots NH_4^+) - E(Z^-) - E(NH_4^+)$, $AC=E(Z^- \cdots NH_3) - E(Z^-) - E(NH_3)$, $BC=E(NH_4^+ \cdots NH_3) - E(NH_4^+) - E(NH_3)$, $\Delta E^{ABC}=ABC - AB - AC - BC$. ΔE^{ABC} is the three-body term.

Method	ΔE^{ads}	total	pair-energies			difference
		ABC	AB	AC	BC	ΔE^{ABC}
SCF	-60	-548	-495	14	97	30
SCF/CPC	-41	529	-481	16	-93	29
SCF/MP2	93	-577	-513	11	-107	33
SCF/MP2/CPC	-60	-543	-489	15	101	31

The calculated and experimental infrared spectra

For all geometry optimized cluster-adsorbate complexes normal mode analyses were carried out. From these analyses, the N-H and O-H stretching frequencies are tabulated in Table IV. The selection of these modes was simple as they were isolated from the other modes. We compared the N-H stretching region of the calculated infrared spectra with the experimental spectra of the NH_4^+ -forms of several zeolites: Mordenite (MOR) [21], Faujasite (FAU) [21], Beta (BET) [22], and Erionite (ERI) [23]. In interpreting the experimental spectra we must be aware that the model used here is very simple and lacks information concerning the influence of the structure of the zeolite on the spectra.

The spectrum of the hydrogen bonded structure, i.e. the structure in which the proton is still attached to the zeolite is dominated by one single peak; the OH-stretching frequency shifted into the N-H stretching region. The spectrum of the coadsorbed structure is also dominated by a single peak at 3142 (coming from the proton hydrogen bonding to the coadsorbed NH_3). These peaks, however, are not likely to appear in a experimental spectrum since the double and triple structures are more favorable energetically. At higher loadings peaks stemming from coadsorbed structures may appear [24].

Most likely, the experimental spectrum is dominated by the double and triple structures. From their almost equal adsorption energies it can be expected that the experimental spectra is a sum of the spectra of these two structures. Still, it is useful to compare the calculated and experimental frequencies. The spectrum of the double structure is dominated by two large peaks at 2623 and 2740 cm^{-1} . They might correspond to the two bands present in the experimental spectrum at 2780 and 2930 cm^{-1} (MOR), 2800 and 3040 cm^{-1} (FAU), 2970 (BET) and 2840 and 3068 cm^{-1} for the erionite. However, the values are too low by about 250 cm^{-1} .

Table IV. The N-H stretching frequencies of four zeolites and of the optimized cluster-adsorbate complexes. The frequencies are given in cm^{-1} . They are tabulated for four zeolites: Mordenite (MOR) [21], Faujasite (FAU) [21], zeolite Beta (BET), [22] and Erionite (ERI) [23]. The other spectra are calculated. 2H and 3H are the notation of the doubly and triply bonded NH_4^+ (fig. 3.3a and 3.3b respectively). H is the structure in which the proton is attached to the zeolite, the frequency given here thus comes from the OH-stretching. COAD is the structure as given in fig. 3.5a. The N-H stretching of the proton pointed towards the zeolite is shifted to 2123, but is not included in the Table because it is strongly mixed with a Si-H stretching. Modes belonging to frequencies typed slanted have a negligible intensity but are included for completeness. The calculated frequencies were scaled by 0.92, this value gave the best agreement between the calculated and experimentally measure N-H stretching frequencies of the NH_3 molecule [10].

MOR	FAU	BET	ERI	2H	3H	H	COAD
2780	2800	2970	2840	2623	3103	3142	3153
2930	3040		3068	2740	3141	3360	3363
3180	3270	3200	3260	3418	3478	3478	3401
3400	3360	3460	3384	3495		3483	3473
							3476
							3483

The spectrum of the triple structure has two large peaks relatively close together (3103 and 3141 cm^{-1}). In an experimental spectrum they may appear as one peak. It also has a less intense peak at 3478 cm^{-1} . The composite peak around 3120 may correspond to the band in the experimental spectrum at 3180 (MOR), 3270 (FAU), 3200 (BET) and 3260 (ERI). Again the band is calculated too low by 100 cm^{-1} . The less intense peak at 3478 may correspond to the less intense peak or shoulder appearing in the experimental spectra at 3400 , 3360 , 3460 , and 3384 cm^{-1} for the four zeolites respectively. The first peaks corresponds to the stretching frequency of hydrogen bonding protons, the numerical value may be wrong because the harmonic approach is not sufficient. The numerical value of the 3478 cm^{-1} peak seems to be right. This frequency corresponds to the stretch of the proton pointing away from the zeolitic cluster. Since it is not hydrogen bonding the harmonic approach might be sufficient. As seen from this interpretation, there is not a simple correspondence between the calculated harmonic frequencies and intensities and the experimental spectra. However, this interpretation supports the suggestion that the double and triple structures both appear at the same time.

Conclusions

We studied the stabilization of NH_4^+ by multiple bonding to the zeolite lattice or to a coadsorbed NH_3 molecule. The zeolite was modeled with small clusters. The geometries of the clusters and cluster-adsorbate complexes were optimized at the SCF level and the adsorption energies were calculated at the SCF/MP2/CPC level using the 6-311+G(d,p)/STO-3G basis set.

NH_4^+ can become stable, and the ΔE_∞^{PT} can be overcome, if NH_4^+ is stabilized by a large interaction energy. It is possible to stabilize NH_4^+ by solvation with a second

NH_3 molecule. Much more favorable however, is the situation in which NH_4^+ has a high coordination to the zeolite lattice, i.e. it is bonded to the zeolite lattice with two or three hydrogen bonds. The heats of adsorption calculated for the hydrogen bonded structure, the structures in which NH_4^+ is doubly and triply bonding to the zeolite lattice, and for the structure in which two NH_3 molecules are coadsorbed on one acidic site are -60, -110, -112 and -30 kJ/mol respectively. The heats of adsorption of the structures in which NH_4^+ is bonding with two or three hydrogen bonds to the lattice are close to the experimental heat of adsorption. Although the cluster calculations presented here have large deficiencies, the calculations suggest that in a zeolite proton transfer becomes favorable as a result of a high coordination between NH_4^+ and the zeolite lattice.

To stabilize NH_4^+ a high coordination between the zeolite cluster and NH_4^+ is necessary. For this high coordination it is necessary to optimize the geometry of the cluster. If the geometry of these structures is taken from a crystal structure and not optimized, a part of this high coordination is lost and the heat of adsorption is only -10 kJ/mol. For the clusters used here, the heat of adsorption seems relatively independent of the choice of the cluster. The heat of adsorption for a singly and doubly bonding NH_4^+ is similar on the $\text{Al}(\text{OH})_3\text{H}^-$ cluster and on the OSiAlH_6^- and the $\text{Al}(\text{OH})_2\text{H}_2^-$ cluster respectively. Enlargement of the the $\text{Al}(\text{OH})_3\text{H}$ cluster by replacing a OH-group by a OSiH_3 group also has relatively little effect on the adsorption energy.

The vibrational frequencies of the clusters were calculated at the SCF-level in the harmonic approach. They have been compared with experimental spectra of NH_4^+ forms of zeolites. The features of the experimental spectrum can be explained from the calculated spectra. This seems to confirm that NH_4^+ is present in the zeolite as a doubly or triply bonding structure.

References

- [1] Chapter 1 of this thesis.
- [2] E. H. Teunissen, F. B. van Duijneveldt and R. A. van Santen, *J. Phys. Chem.* **96**, 366 (1992).
- [3] Chapter 2 of this thesis.
- [4] W. J. Hehre, R. F. Stewart and J. A. Pople, *J. Chem. Phys.* **51**, 2657 (1969).
- [5] M. S. Gordon, J. S. Binkley, J. A. Pople, W. J. Pietro and W. J. Hehre, *J. Am. Chem. Soc.* **104**, 2797 (1982), M. M. Francl, W. J. Pietro, W. J. Hehre, J. S. Binkley, M. S. Gordon, D. J. DeFrees and J. A. Pople, *J. Chem. Phys.* **77**, 3654 (1982).
- [6] R. Krishnan, J. S. Binkley, R. Seeger and J. A. Pople, *J. Chem. Phys.* **72**, 650 (1980).
- [7] R. Ditchfield, W. J. Hehre and J. A. Pople, *J. Chem. Phys.* **54**, 724 (1971).
- [8] T. Clark, J. Chandrasekhar, G. W. Spitznagel and P. v. R. Schleyer, *J. Comp. Chem.* **4**, 294 (1983).
- [9] C. Møller and M. S. Plesset, *Phys. Rev.* **46**, 618 (1934).
- [10] G. Herzberg, *Molecular Spectra and Molecular Structure, II Infrared and Raman Spectra of Polyatomic Molecules* (van Nostrand, New York, 1960).
- [11] J. A. Ibers and D. P. Stevenson, *J. Chem. Phys.* **28**, 929 (1958).
- [12] Chapter 7 of this thesis.
- [13] J. E. DelBene, *J. Chem. Phys.* **86**, 2110 (1987).

Chapter 3 : Coordination and solvation effects

- [14] Z. Latajka and S. Scheiner, *J. Chem. Phys.* **84**, 341 (1986).
- [15] J. E. DelBene, M. J. Frisch and J. A. Pople, *J. Phys. Chem.* **89**, 3669 (1985).
- [16] M. J. Frisch, J. A. Pople and J. E. DelBene, *J. Phys. Chem.* **89**, 3664 (1985).
- [17] O. Cheshnovsky and S. Leutwyler, *J. Chem. Phys.* **88**, 4127 (1988).
- [18] *CRC Handbook of Chemistry and Physics*, 71st. ed., edited by D. R. Lide (CRC, Boston, 1990).
- [19] I. J. Kurnig, M. M. Szczeniński and S. Scheiner, *J. Phys. Chem.* **90**, 4253 (1986).
- [20] G. Chałasiński, M. M. Szczeniński, P. Cieplak and S. Scheiner, *J. Chem. Phys.* **94**, 2873 (1991).
- [21] E. H. Teunissen, R. A. van Santen, A. J. P. Jansen and F. B. van Duijneveldt, *J. Phys. Chem.* **97**, 203 (1993).
- [22] S. G. Hegde, R. Kumar, R. N. Bhat and P. Ratnasamy, *Zeolites* **9**, 231 (1989).
- [23] A. Kogelbauer, J. A. Lercher, K.-H. Steinberg, F. Roessner, A. Soellner, R. V. Dmitriev, *Zeolites* **9**, 224 (1989).
- [24] W. L. Earl and P. O. Fritz, A. A. V. Gibson and J. H. Lunsford, *J. Phys. Chem.* **91**, 2091 (1987).

4

A comparison between cluster and crystal calculations

Introduction

Quantum chemists have studied the adsorption of small molecules onto the acidic site in the cluster approach; a group of atoms, including the acidic site, is taken from the zeolite, the dangling bonds are saturated, usually with hydrogen atoms, and the adsorption process can be studied as a molecule-molecule interaction, with all its computational advantages. The cluster approach however, has three disadvantages. The first are the boundary effects due to the saturation of dangling bonds; atoms having saturated dangling bonds are in a different environment than in the crystal, which can lead to a different chemical behavior. The second disadvantage is that the cluster is, usually, relatively small. If, for example, the cluster describes the zeolite acidic site, the interaction of the adsorbate with the opposite wall of the zeolite channel is missing. The third disadvantage is that a finite cluster cannot describe the long-range electrostatic effects of the crystal, the Madelung potential. Some studies are reported in which the adsorption energy is calculated with clusters of different size. The adsorption energy depends quite strongly on the size of the cluster [1,2]. Other authors have embedded their cluster in an array of point charges to account in some way for the Madelung potential [3,4]. The main disadvantage of these studies however is that no comparison could be made with the reference, namely the crystal.

In this study, we would like to judge the value of the cluster approach by considering the adsorption of NH_3 and NH_4^+ on four clusters of different size cut from a chabazite crystal, and comparing the results with those obtained using a periodic model of the adsorption process. We used the CRYSTAL program [5-9] for calculating the electronic structure and the energy of the crystal. In this way we are able to estimate the boundary effects in the cluster calculations as well as the effect of the opposite side of the channel wall and of long-range electrostatic interactions on the adsorption energy. The choice of the adsorbates, NH_3 and NH_4^+ , enables us to study the effect of the cluster approach for a neutral and a charged adsorbate, as well as on the proton transfer from the zeolite to NH_3 [10,11]. Since the geometry is found to have a large influence on the calculated adsorption energy we have carried out all calculations with two different zeolite geometries.

Computational details

Zeolites are built from TO_4 tetrahedrons in which the T-atom can be silicon or aluminum. The tetrahedrons are linked together at the vertices such that a three-dimensional porous structure, with channels, is formed. In chabazite the channels are built from parallel eight-rings. Such an eight-ring has eight tetrahedrons linked together. The eight-ring channels are in three directions almost perpendicular to each other. Their diameter is about 4 Å. The structure of chabazite, with NH_3 adsorbed in it, is shown in fig. 4.1.

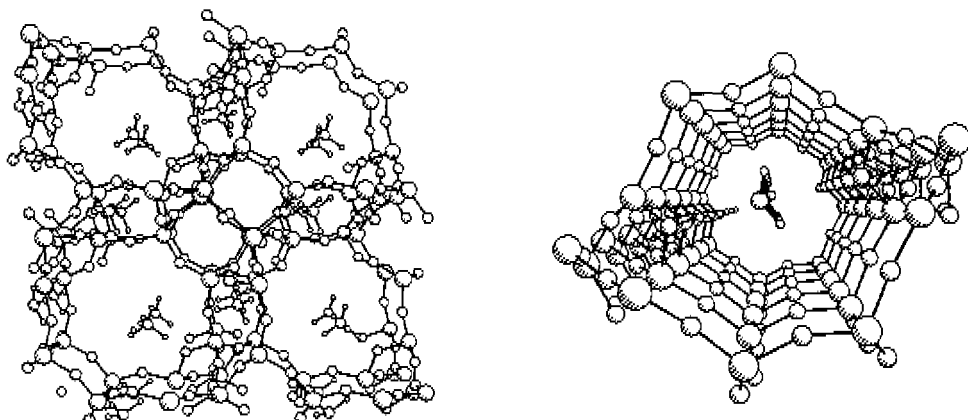


Figure 4.1. On the left, the structure of chabazite and NH_4^+ adsorbed into it, the view is perpendicular to the eight-ring channels. On the right, NH_4^+ adsorbed periodically in the eight-ring channel of the chabazite. Although NH_4^+ is adsorbed on one specific site there is also an interaction of NH_4^+ with the atoms of the opposite site of the channel.

Although for the purely silicious form of the chabazite it is possible to optimize the geometry quantum chemically [12], this is not feasible for an aluminum containing chabazite because, due to its lower symmetry, it has too many parameters to be optimized. We have used therefore two geometries, one derived from an experimental structure and one optimized with the shell model [13,14]. By comparing the two structures we can study the influence of the geometry on adsorption and proton transfer energies.

The first geometry we used is derived from an experimental structure of natural chabazite, as determined by X-ray diffraction by Wyckoff [15]. Its space group corresponds to $R\bar{3}m$ symmetry and contains twelve T-atoms per unit cell. In the asymmetric unit there is only one T-atom. From this atom the twelve T-atoms in the unit cell are generated by applying the symmetry operations. If we want to make a structure with different types of T-atoms we cannot use this symmetry, since all the T-atoms are symmetry related. We decided to remove some of the symmetry operations by reducing the symmetry to R3; the twelve T-atoms in the unit cell are generated from four T-atoms in the asymmetric unit. We assign one of these T-atoms to be aluminum. Thus, we generate a chabazite with a Si/Al ratio of three. The natural form of chabazite has a Si/Al ratio close to two. To obtain a structure with such a Si/Al ratio the symmetry should be lower than R3, leading to an increase in computer time that would make the calculations not feasible anymore.

To create the acidic HOSiAl group we put a proton on one of the oxygen atoms bonded to the aluminum atom. Although the proton can be bonded to four different oxygen atoms, we chose only one since we did not aim to compare different acidic sites. The hydroxyl group was positioned in such a manner that the structure of the acidic group resembled, as best as possible, the HOSiAl structure found by optimization of a HOSiAlH₆ cluster [10]. All other geometrical parameters were kept fixed at the experimental geometry. We will refer to this crystal structure as the Wyckoff structure. The disadvantage of X-ray diffraction is that it can not distinguish between silicon and aluminum atoms. Because of this, some Si-O bond lengths are too long and some Al-O bond lengths are too short in the Wyckoff crystal. The local structure around the acidic site of the Wyckoff crystal is shown in fig. 4.2.

For the second geometry we used the Wyckoff crystal as a start for the optimization of the geometry of the crystal with the shell model. The shell model describes the interaction between the atoms with pair potentials, containing a Coulombic and a covalent part. The oxygen is polarizable; it is described as a charged core and, bonded to it with a harmonic potential, a negatively charged shell. We used the parameter set as derived by Schröder *et al.* [16]. We tried to find the most stable structure by optimizing four geometries, each with the proton on a different oxygen atom. Their stabilities are given in Table I. We can see that three of them are close to each other in stability. We decided to use the shell model optimized geometry that has its proton on the same oxygen as the Wyckoff crystal structure, which is also the most stable structure according to the shell model optimization. We will call this structure the shell model crystal.

For NH₃ and NH₄⁺ we have used the experimental geometries [17,18]. We adsorbed NH₃ onto the acidic hydroxyl group in its equilibrium position i.e., the C₃ axis of the NH₃ coincides with the OH-axis. Although NH₄⁺ is more stable if it has a higher coordination than a single hydrogen bond we put NH₄⁺ in the same position as NH₃. We chose this coordination because the Small Cluster (defined below) is not able to describe the coordination of NH₄⁺ to more than one oxygen atom.

With the present choice, there are three NH₃ molecules or NH₄⁺ ions per chabazite unit cell. The distance between the adsorbates is about 6.5 Å. It is an important question to what extent the adsorption energies in the crystal are influenced by the adsorbate-adsorbate interaction. Therefore, we built lattices from NH₃ molecules in the same geometry they have in the chabazite. To study the NH₄⁺ ... NH₄⁺ interaction we put the cations in the position they have in the crystal. In order to make a neutral lattice we put the monovalent F⁻ as a counterion on the position of the anionic oxygen atom. In this way we built a lattice of NH₄⁺ ... F⁻ units. The formation energy, for one unit cell containing three adsorbates, of the NH₃ lattice is -3 kJ/mol for the Wyckoff crystal and -2 kJ/mol for the shell model crystal. For the NH₄⁺ ... F⁻ lattice the formation energies are -15 and 2 kJ/mol respectively. As another test to study the influence of the adsorbate concentration on the adsorption energy we calculated the adsorption of NH₄⁺ in the shell model crystal with a concentration of one ion per unit cell. In this case the symmetry of the unit cell was P1. The adsorption energy was 117 kJ/mol (compared to 122 kJ/mol with of three NH₄⁺ ions per unit cell). Thus, the concentration of adsorbate has a relatively small effect on the adsorption energy of about 5 kJ/mol. The comparison between cluster

Chapter 4 : A comparison between cluster and crystal calculations

Table I. Relative energies per unit cell (in kJ/mol) of the different chabazite structures. The energies are relative to the structure found most favorable with the shell model. The other shell model crystal structures refer to chabazites with the hydrogen atom attached to different oxygen positions (see text), Wyckoff crystal is an experimental structure. The energy per unit cell for the shell model crystal structure was calculated to be $-51.35951 H$ with the shell model (this is the energy relative to the separate ions) and $-5063.61286 H$ with the RHF calculations (the total energy of the crystal relative to separate electrons and nuclei) using a STO-3G basis set.

Structure	Method of calculation	
	Shell-Model	Quantum-chemical
shell model crystal	0	0
shell model crystal pos. 2	40.6	-2.6
shell model crystal pos. 3	29.6	2.1
shell model crystal pos. 4	41.0	59.2
Wyckoff crystal	3 000	767.8

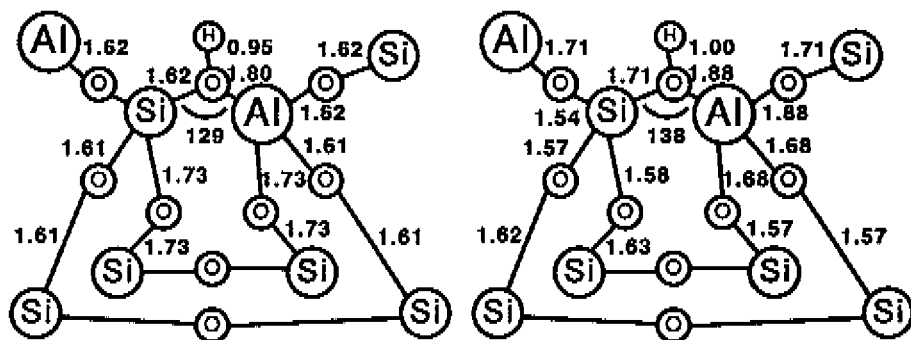


Figure 4.2. The geometry of the first and second shell of T-atoms around the acidic site for the experimental Wyckoff structure, on the left, and the shell model structure on the right. All distances are given in Ångstrom, the Si-O-Al angle is given in degrees.

and crystal calculations is not perturbed by adsorbate-adsorbate interactions.

We cut four clusters from the crystal: the Small Cluster, the Medium Cluster, the Large Cluster and the Giant Cluster. Each cluster is an extension of the previous one (see figs. 4.3-4.5). The coordinates of the atoms in the four clusters are taken either from the Wyckoff or from the shell model crystal. If we compare the clusters with each other and with the crystal we can distinguish three effects. The first effect is that the covalent description of the atoms of the cluster directly interacting with the adsorbate can be perturbed by boundary effects, because of the saturation with hydrogen atoms. Making the cluster larger should decrease this effect. The second effect is that the number of atoms directly interacting with the adsorbate can be different. In zeolites this effect relates to

a possible interaction of an adsorbate, not only with the acidic site, but also with other atoms forming the channels. The third effect is the Madelung potential, the long-range electrostatic effect. It is included in the crystal but is not present in any cluster.

The Small Cluster is the smallest possible cluster containing the acidic HOSiAl group. Only hydrogen atoms are added to saturate the dangling bonds, giving HOSiAlH_6 . In the Medium Cluster the oxygen atoms bonded to the acidic group as well as the second shell of T atoms around the acidic group are included. Two pairs of silicon atoms are connected with an oxygen atom to form two four-rings. In the Medium Cluster we have added atoms to improve the covalent description of the acidic site, the boundary effects due to hydrogen saturation will have less influence the acidic site. The Large Cluster has the T-atoms of the eight-ring and the oxygen atoms of the ring that can directly interact with the adsorbate. The extra atoms in the Large Cluster, with respect to the Medium Cluster, are able to describe the interaction between the oxygen atoms of the channel wall and the adsorbate. If NH_3 is adsorbed in its equilibrium position the distances between the hydrogen atoms of the NH_3 and the oxygen atoms of the eight-ring are in between 2.3 and 3.6 Å. In the Giant Cluster all the oxygen atoms bonded to the T-atoms in the eight-ring are included. The difference between the Giant and the Large Cluster is the covalent description of the T-atoms in the eight-ring. The Giant Cluster is able to describe all the covalent interactions between the zeolite and the adsorbate. The difference between the adsorption energy on the Giant Cluster and the crystal will be due to the effect of the Madelung potential. For all the clusters the saturating hydrogen atoms are put in tetrahedral positions with Si-H and Al-H bond lengths of 1.49 Å and with O-H bond lengths of 0.95 Å. The direction of the OH-bonds is along the corresponding O-T bonds.

All the calculations have been carried out at the Restricted Hartree Fock (RHF) level in a minimal STO-3G basis set [19]. Only at this level it is feasible to carry out calculations on the crystal. The deficiencies of this basis set will have their effect on the comparison between cluster and periodic calculations. The strength of the hydrogen bond with NH_3 will be overestimated and the stability of the ionic complex will be underestimated.

Results and Discussion

The adsorption energies, as well as the O-N equilibrium distances, of the adsorbates NH_3 and NH_4^+ on the four clusters and on the crystal are given in Table II and Table III, for both the shell model geometry and the Wyckoff geometry. The different models that have been used for the zeolite, differing in the quality of the covalent description, the number of the atoms interacting with the adsorbate, and the presence or absence of the long-range electrostatic effects, have produced a large spread in adsorption energies. For none of the geometries or adsorbates there seems to be a convergence with increasing cluster size for the adsorption energy.

We first compared the clusters that have more or less the same number of atoms directly interacting with the adsorbate but that differ in the covalent description. In the small Cluster as well as in the Medium Cluster the main interaction is the interaction between the adsorbate and the zeolite OH-group. The small Cluster is adsorbing the adsorbates stronger than the Medium Cluster. The difference in adsorption energy can be explained only as a difference of the nature of the atoms of the acidic site in the two

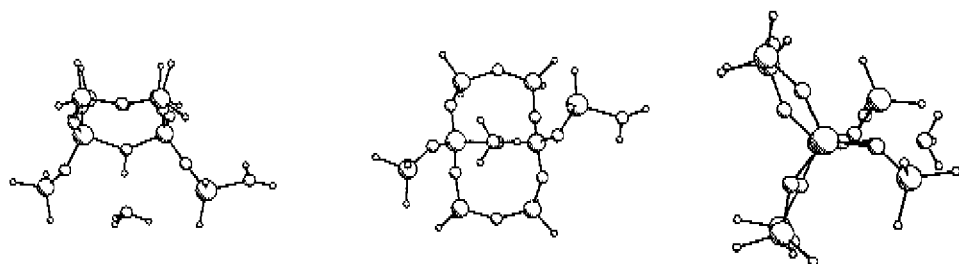


Figure 4.3. The Medium Cluster. The structure is shown as seen from three mutually perpendicular directions.

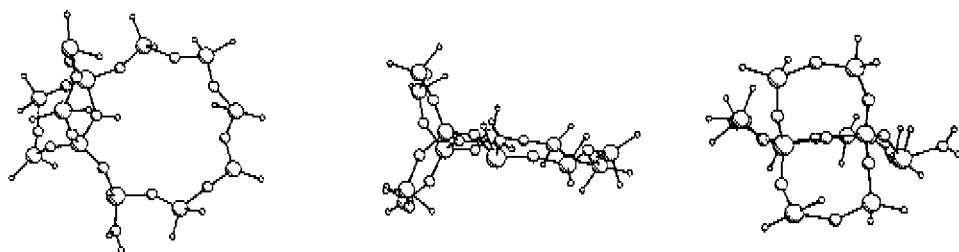


Figure 4.4. The Large Cluster. The structure is shown as seen from three mutually perpendicular directions.

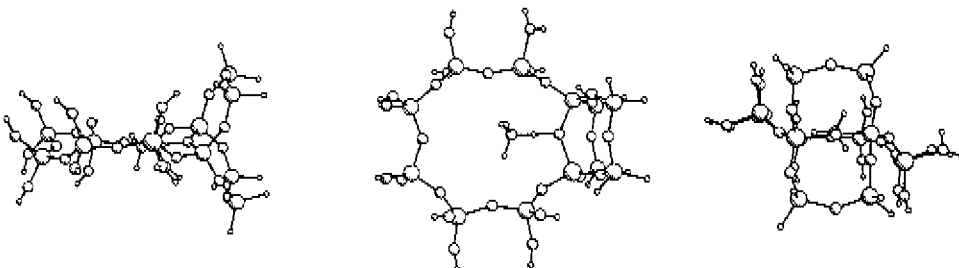


Figure 4.5. The Giant Cluster. The structure is shown as seen from three mutually perpendicular directions.

Table II. Adsorption energy, E^{ads} , and O-N equilibrium bond length, R_{N-O} , of NH_3 on the Small Cluster, Medium Cluster, Large Cluster, Giant Cluster and the crystal for the Wyckoff and shell model geometry. The geometries are denoted as WY and SH respectively. The equilibrium bond lengths are given in Å, the adsorption energies in kJ/mol. The adsorption energy is given with respect to the separated zeolite cluster and the NH_3 .

Structure	E^{ads}		R_{N-O}	
	WY	SH	WY	SH
Crystal	-101	-72	2.51	2.72
Giant Cluster	-95	-77	2.50	2.66
Large Cluster	-100	-82	2.50	2.63
Medium Cluster	-85	-53	2.57	2.65
Small Cluster	-94	-83	2.54	2.59

Table III. Adsorption energy, E^{ads} , and O-N equilibrium bond length, R_{N-O} , of NH_4^+ as well as the deprotonation energies of the clusters (E^{DP}), on the Small Cluster, Medium Cluster, Large Cluster, Giant Cluster and the crystal for the Wyckoff and shell model geometry. The geometries are denoted as WY and SH respectively. The equilibrium bond lengths are given in Å, the adsorption energies in kJ/mol. The adsorption energy is given with respect to the separated zeolite cluster and the NH_3 . A positive energy means that the energy of the complex is higher in energy than the separated zeolite cluster and NH_3 molecule. The deprotonation energy is defined as the difference in total energy between the ZH cluster and the Z^- cluster.

Structure	E^{ads}		R_{N-O}		Deprotonation Energy	
	WY	SH	WY	SH	WY	SH
Crystal	-15	122	2.28	2.25		
Giant Cluster	38	99	2.27	2.24	1703	1927
Large Cluster	27	86	2.27	2.26	1807	1945
Medium Cluster	52	133	2.26	2.23	1747	2114
Small Cluster	39	85	2.25	2.24	1739	1822

clusters. As an indication of the nature of the atoms in a cluster or crystal the Mulliken charges [20] on the atoms of the acidic site in the four clusters, and the crystal, as given in Table IV, are very illustrative. We see that the charges on the hydrogen and oxygen atoms in all the clusters and the crystal are relatively similar. The charges on the silicon and aluminum atoms show the effect of the saturation with hydrogen atoms. For the three largest clusters and the crystal the charges are very similar but in the Small Cluster the charges deviate by half a unit. Thus, these atoms will behave differently from the corresponding atoms in the crystal, and may, via covalent bond, alter the nature of the adsorption site. The adsorption on the Small Cluster should not be compared with the periodic calculation since the $HOSiAl$ group is too different. The adsorption energies on the Small Cluster and the crystal may seem similar, but from the previous discussion we see that this is based on an accidental cancellation of errors.

Both the Large Cluster and the Giant Cluster describe the interaction of the adsorbate

Table IV. Net charges resulting from a Mulliken population analysis on the atoms of the acidic SiOHAl-group for the crystal and the different clusters. The charges for a cluster are given in the rows, the type of atom and the geometry are given in columns. The shell model and the Wyckoff geometry are abbreviated as SH and WY.

Atom	H		O		Si		Al	
	WY	SH	WY	SH	WY	SH	WY	SH
crystal	0.269	0.213	-0.590	-0.534	1.398	1.443	1.213	1.212
Giant Cluster	0.274	0.211	-0.588	-0.528	1.435	1.456	1.251	1.228
Large Cluster	0.276	0.224	-0.591	-0.526	1.392	1.446	1.245	1.240
Medium Cluster	0.266	0.220	-0.586	-0.531	1.407	1.455	1.214	1.229
Small Cluster	0.283	0.236	-0.562	-0.477	0.930	0.849	0.800	0.798

with the acidic OH-group and with the eight-ring. The difference between the Large Cluster and the Giant Cluster is an improvement of the covalent description of the T-atoms in the eight-ring. Again, this is illustrated by the Mulliken charges, now of the T-atoms in the eight-ring. These charges are given in Table V for the Large Cluster, the Giant Cluster and the crystal. We see that the charges in the crystal and in the Giant Cluster are similar. The charges of the T-atoms in the Large Cluster deviate from them between 0.1 and 0.3 unit. The deviations are not so large as for the T-atoms in the Small Cluster, because in the Small Cluster the T-atoms have three bonds saturated with hydrogen atoms, whereas in the Large Cluster the T-atoms in the eight-ring has only two bonds saturated with hydrogen atoms. Still, the covalent interaction between the adsorbate and the eight-ring will not be described correctly in the Large Cluster.

From the previous paragraphs we have seen that the covalent descriptions of the Small Cluster and the Large Cluster are not correct. This leaves us with three correct structures; the Medium Cluster, the Giant Cluster and the crystal. From the difference in adsorption energy between the Medium Cluster and the Giant Cluster we can estimate the effect of the eight-ring, from the difference between the Giant Cluster and the crystal we can estimate the effect of the Madelung potential. The eight ring stabilizes NH_3 with -10 kJ/mol and -22 kJ/mol for the Wyckoff and shell model geometry, respectively. For NH_4^+ these numbers are -14 and -34 kJ/mol respectively. In all cases the eight-ring stabilizes the adsorbate. The effect of the Madelung potential is less predictable and strongly depends on the geometry of the crystal. For NH_3 the effect of the Madelung potential is relatively small, -6 kJ/mol and + 5 kJ/mol for the two respective geometries. For NH_4^+ , with its ionic character, the effect of the Madelung potential is larger; -53 and +23 kJ/mol for the Wyckoff and shell model geometry respectively.

Although the Giant Cluster gives a correct description of the covalent part of the adsorption process, it still shows some boundary effects of electrostatic nature. In the shell model Giant Cluster the OH-bonds are directed along the corresponding O-T bonds. We also carried out some calculations on a modification of the shell model Giant Cluster. In this modified cluster the direction of the OH-bonds is different. The T-O-H angle is equal to the T-O-T angle but the torsion angles are chosen such, that the OH-dipoles repel the adsorbate. On this modified cluster the adsorption energies are -61 kJ/mol for NH_3 and

Table V. Mulliken charges on the T-atoms in the eight-ring for the Large Cluster, the Giant Cluster and the crystal. The charges for the atoms are given in the rows, the cluster and the geometry are given in columns. The shell model and the Wyckoff geometry are abbreviated as SH and WY. For the crystal the charges of all the four T-atoms in the asymmetrical unit are given. For the Large Cluster and the Giant Cluster the charges on the T-atoms that do not belong to the acidic HOSiAl group are given.

Atom	crystal		Giant Cluster		Large Cluster	
Structure	WY	SH	WY	SH	WY	SH
Al	1.213	1.212	1.261	1.260	1.141	0.771
Si	1.398	1.444	1.417	1.477	1.053	0.920
Si	1.341	1.443	1.365	1.483	1.015	1.040
Si	1.268	1.388	1.349	1.514	1.042	0.954
Si			1.346	1.522	1.057	1.058
Si			1.327	1.526	1.062	1.096

146 kJ/mol for NH_4^+ . If we compare these numbers with the original Giant Cluster (-77 and 99 kJ/mol) we see that for a neutral adsorbate like NH_3 the adsorption energy can change by 16 kJ/mol and for NH_4^+ by 47 kJ/mol due to the direction of the OH-dipoles. For a second modification of the shell model Giant Cluster the adsorption energy of NH_4^+ on this cluster is 108 kJ/mol.

The effect of the Madelung potential on the proton transfer energy, *i.e.* the difference in adsorption energy of NH_3 and NH_4^+ , is -48 and +22 kJ/mol for the Wyckoff and the shell model geometry, respectively. The method of Allavena *et al.* [3], to embed a zeolite cluster in a potential of point charges, gives -197 kJ/mol for the effect of the Madelung potential on the proton transfer energy, it does not give the effect of the Madelung potential on the individual adsorption energies of NH_3 and NH_4^+ . The method of Allavena *et al.* seems to overestimate the effect of the Madelung potential.

For all structures the adsorbate is more stable on the Wyckoff structure than on the shell model structure. The shell model crystal was optimized for the OH- form of the zeolite without adsorbate. This structure was made more stable, and thus less reactive, towards adsorbates. This effect of the optimization of the geometry on the adsorption energy was also found in previous cluster calculations [10]. Optimizing the geometry of the OH-form of the zeolite has a larger effect on the adsorption of NH_3 than on the adsorption of NH_4^+ , because a geometry that has been adjusted to an adsorbed NH_3 molecule is closer to the geometry of the OH-form than a geometry that has been adjusted to an adsorbed NH_4^+ ion [10,11].

The average heat of adsorption of NH_3 on a large number of zeolites is -150 kJ/mol when determined with micro calorimetry and -129 kJ/mol when determined with temperature programmed desorption [21]. The adsorption energies as calculated in this chapter cannot be compared directly to the experimental heats of adsorption because of the errors of the used method, namely, Restricted Hartree Fock (RHF) in a minimal STO-3G basis set. The adsorption energies of NH_3 and NH_4^+ on a HOSiAlH₆ cluster have been calculated with a number of different basis sets [10,22]. From this work we can conclude

that a STO-3G basis set overestimates the stability of NH_3 with 30 to 50 kJ/mol and underestimates the stability of NH_4^+ between 60 and 100 kJ/mol. An improvement of the method with electron correlation in the form of second order Møller-Plesset perturbation theory [23], and the counterpoise correction to correct for the basis set superposition error [24,25], has little effect on the adsorption energy of NH_3 (it weakens the bond with 2 kJ/mol), NH_4^+ is stabilized with 10 kJ/mol. Apart from the large influence of the quality of the calculation for NH_4^+ the coordination of NH_4^+ to the lattice is very important. In this work we have kept NH_4^+ bonding with one hydrogen bond towards the anionic oxygen. From cluster calculations [11] we have learned that the NH_4^+ is about 100 kJ/mol more stable if it is coordinated with two or three hydrogen atoms towards the anionic AlO_4^- tetrahedron. Although the absolute value of the adsorption energies cannot be compared with experimental results, the error due to the used basis set and the lack of correlation can be expected to be about the same in all cases. Thus, we can draw at least quantitative conclusions from the calculations carried out at the RHF/STO-3G level concerning the relative importance of boundary effects, the interaction with the zeolite wall, and the effect of the Madelung field.

Conclusions

We have compared the adsorption energies of NH_3 and NH_4^+ in a zeolite crystal and on four clusters different in size. From the comparison we can draw some conclusions concerning the boundary effects of the clusters and of the magnitude of the physical effects, like the interaction with the channel wall of the zeolite and the Madelung potential, playing a role in the adsorption of NH_3 and NH_4^+ in the zeolite.

The first conclusion we can draw concerns the boundary effects affecting the covalent description of the cluster. We found that the T-atoms in the clusters, saturated with hydrogen atoms are different from their counterparts in the crystal, as is shown by their charge. Good agreement for the charge with respect to the crystal calculations are found for the Medium Cluster and the Giant Cluster where the dangling bonds are relatively far from the adsorption site.

The error, due to the boundary effects, can contribute up to 30 kJ/mol for NH_3 and up to 60 kJ/mol for NH_4^+ . Another shortcoming of the cluster model is also linked to the boundary effects but is of electrostatic origin. Different directions of the OH-bonds in the Giant Cluster can give rise to a difference in adsorption energy of almost 50 kJ/mol, about the same magnitude as the covalent boundary effect.

From the clusters that give a correct covalent description of the adsorption process we can estimate the effect of the opposite wall of the zeolite channel and the Madelung potential on the adsorption energy. From the difference between the Medium and the Giant Cluster we see that for NH_3 the effect of the channel wall is -10 and -22 kJ/mol for the Wyckoff and the shell model geometries, respectively. The effect of the Madelung potential, estimated from the difference between the Giant Cluster and the crystal, is -6 and +5 kJ/mol for the two geometries. For NH_4^+ the effect of the channel wall is -14 kJ/mol and -34 kJ/mol. These values are sensitive to electrostatic boundary effects. The effect of the Madelung potential on the adsorption of NH_4^+ is -53 kJ/mol and +23 kJ/mol for the Wyckoff and shell model geometry. The Madelung potential gives a relatively small

contribution to the adsorption energy of NH_3 , as it is a local process. For NH_4^+ the effect of the eight-ring is only a little larger than for NH_3 , the effect of the Madelung potential is much larger and strongly dependent on the geometry of the crystal. This means that the adsorption of NH_4^+ is less local than the adsorption of NH_3 . In the Wyckoff geometry the Madelung potential stabilizes the adsorbates whereas in the shell model the Madelung potential destabilizes the adsorbate. The dependency of the effect of the Madelung potential on the geometry of the crystal may be caused by the different positions of the atoms or by the different charges on the atoms (see Table IV and V), or a combination of these two.

The effect of the geometry on the adsorption energies is very large; the effect is the largest for the crystal. For NH_3 the difference in adsorption energy between the two geometries is 29 kJ/mol, for NH_4^+ it is 135 kJ/mol. This means that the choice of the geometry is crucial for calculating adsorption energies. The Wyckoff structure is not an equilibrium structure. To obtain a better structure we optimized the geometry of the proton form of the chabazite using the shell model. By optimizing this structure we stabilized it with respect to the zeolite containing NH_3 and NH_4^+ . Consequently, the adsorbates were adsorbed less strong. The best solution for the choice of the geometry would be to optimize the geometry of each state quantum chemically. This however, is not feasible at the moment.

In this chapter we studied the effect of the geometry and the role of the long range effects in the calculation of adsorption energies in zeolites. In previous studies we have studied the effect of the geometries, the basis set and electron correlation. We conclude that in the calculation of adsorption energies the effect of the geometry is the most important. The effects of the basis set, the Madelung potential and electron correlation are smaller, although the magnitude of the effects is strongly dependent on the nature and coordination of the adsorbate.

References

- [1] J. Sauer, H. Horn, M. Häser and R. Ahlrichs, *Chem. Phys. Lett.* **173**, 26 (1990).
- [2] H. V. Brand, L. A. Curtiss and L. E. Etou, *J. Phys. Chem.* **96**, 7725 (1992).
- [3] M. Allavena, K. Seiti, E. Kassab, Gy. Ferenczy and J. G. Ángyán, *Chem. Phys. Lett.* **168**, 461 (1990).
- [4] R. Vetrivel, C. R. A. Catlow and E. A. Colbourn, *Stud. Surf. Sci. Catal.* **37**, 309 (1988).
- [5] C. Pisani, R. Dovesi and C. Roetti, *Hartree Fock Ab-initio Treatment of Crystalline Systems, Lecture Notes in Chemistry* **48** (Springer Verlag, Berlin, 1988).
- [6] C. Pisani and R. Dovesi, *Int. J. Quantum Chem.* **17**, 501 (1980).
- [7] R. Dovesi, C. Pisani, C. Roetti and V. R. Saunders, *Phys. Rev. B* **28**, 5781 (1983).
- [8] R. Dovesi, *Int. J. Quantum Chem.* **29**, 1755 (1986).
- [9] R. Dovesi, V. R. Saunders and C. Roetti, *Crystal 92 Users's Manual, Gruppo di Chimica Teorica* (Università di Torino and SERC Laboratory 1992).
- [10] E. H. Teunissen, F. B. van Duijneveldt, and R. A. van Santen, *J. Phys. Chem.* **96**, 366 (1992), *Chapter 2 of this thesis*.

Chapter 4 : A comparison between cluster and crystal calculations

- [11] E. H. Teunissen, A. P. J. Jansen, R. A. van Santen and F. B. van Duijneveldt, *J. Phys. Chem.* **97**, 203 (1993), *Chapter 3 of this thesis*.
- [12] E. Aprá, R. Dovesi, C. Freyria-Fava, C. Roetti and V. R. Saunders, *Model. Simul. Mater. Sci. Eng.* **1**, 297 (1993).
- [13] B. G. Dick and A. W. Overhauser, *Phys. Rev.* **112**, 91 (1958).
- [14] C. R. A. Catlow, M. Dixon and W. C. Mackrodt, *Computer simulation of solids, Lecture Notes in Physics* **166**, (Springer Verlag, Berlin, 1982).
- [15] R. W. G. Wyckoff, *'Crystal Structures'*, 2nd. ed. Vol 4. (Interscience, New York, 1968)
- [16] K.-P. Schröder, J. Sauer, M. Leslie and C. R. A. Catlow, *Zeolites* **12**, 20 (1992), K.-P. Schröder, J. Sauer, M. Leslie, C. R. A. Catlow, and J. M. Thomas, *Chem. Phys. Lett.* **188**, 320 (1992).
- [17] G. Herzberg, *Molecular Spectra and Molecular Structure* Vol. 2, (van Nostrand, Princeton 1945).
- [18] J. A. Ibers and D. P. Stevenson, *J. Chem. Phys.* **28**, 929 (1958).
- [19] W. J. Hehre, R. F. Stewart and J. A. Pople, *J. Chem. Phys.* **51**, 2657 (1969).
- [20] R. S. Mulliken, *J. Chem. Phys.* **23**, 1833 (1955).
- [21] *Chapter 1 of this thesis*.
- [22] E. Kassab, K. Seiti and M. Allavena *J. Phys. Chem.* **95**, 9425 (1991).
- [23] C. Møller and M.S. Plesset, *Phys. Rev.* **46** 618 (1934).
- [24] S. F. Boys and F. B. Bernardi, *Mol. Phys.* **19**, 553 (1970).
- [25] J. H. van Lenthe, J. G. C. M. van Duijneveldt-van de Rijdt, and F. B. van Duijneveldt, *Adv. in Chem. Phys.* **79**, 521 (1978).

5

The embedded cluster model

Introduction

The cluster approximation is widely used to describe a zeolite in quantum chemical calculations. In this approximation, a group of atoms is cut from the zeolite crystal and the dangling bonds are saturated, usually with hydrogen atoms. The advantage of the cluster approximation is that adsorption processes can be described as a molecule-molecule interaction, with its computational advantages. The disadvantages of the cluster approximation are the absence of the long-range electrostatic forces of the crystal and the boundary effects of the cluster. Due to the saturation of dangling bonds with hydrogen atoms, the chemical environment of the atoms in the cluster is different from the chemical environment of the corresponding atoms in the crystal. Because of these boundary effects, the atoms in the cluster behave differently towards an adsorbate than the corresponding atoms in the crystal [1].

A perfect zeolite crystal can also be used as a model. So far, one study has been reported in which adsorption energies are calculated in a zeolite crystal [1]. For the calculation of the electronic structure and the energy of the periodically repeating structure the CRYSTAL program was used [2-7]. Such calculations have the advantage that the crystal model is more realistic than the cluster model because boundary effects are absent and the long-range electrostatic forces of the crystal are included. However, the computational effort that comes with a crystal calculation is much larger.

In order to combine the computational advantages of the cluster approximation with the better model for the zeolite provided by the crystal, we developed a method in which a zeolite cluster is embedded in a zeolite crystal by imposing an electrostatic potential onto the cluster. This electrostatic potential adds the long-range electrostatic forces of a crystal (the Madelung potential) and subtracts the electrostatic part of the boundary effects of the cluster. There is no correction for the covalent part of the boundary errors. With this embedding scheme we keep the computational advantage of the cluster approximation but we remove, at least a part of, its disadvantages.

There are two main differences in the present work with respect to other schemes in which a cluster is embedded in a potential representing in some way the long-range electrostatic potential [8-13]. The first difference is that the potential in this scheme is obtained from a periodic calculation performed with the same Hamiltonian, basis set and numerical accuracy as the (embedded) cluster calculations. In other schemes the long-range electrostatic potential is calculated from a lattice of point charges. These point charges are the full, half or three quarter formal charges [9-11] of the atoms in the lattices, or are obtained with Mortiers electronegativity equalization method [8-15]. The second difference is that in this scheme the potential is not imposed on the complete cluster, but only on the central part of it. Embedding of the boundary of the cluster prevents a proper correction for the boundary errors.

As a test for our embedding scheme we calculated the adsorption energies of NH_3 and NH_4^+ in a zeolite crystal and on three clusters embedded in the potential of the zeolite crystal. From the comparison between the adsorption energies on the embedded clusters and the crystal we can judge the value of the embedding scheme and we can give some comments on the choice of the cluster.

Methods and Computational Details

Our aim is to study adsorption and proton transfer processes on a zeolite cluster embedded in a zeolite crystal. The cluster is embedded by adding the long-range electrostatic potential of the zeolite crystal and subtracting the electrostatic potential of the boundary of the cluster. The starting point for our embedding scheme is a perfect zeolite crystal. This crystal is called the host crystal (fig. 5.1a). The second step in the embedding scheme is the creation of a cluster from the host crystal by cutting out a group of atoms around the adsorption site, in the present case the acidic HOSiAl -group, and saturating the dangling bonds with hydrogen atoms. This cluster is called the host cluster (fig. 5.1b) and it is used for the correction of the electrostatic part of the boundary errors. Apart from the dangling-bond hydrogen atoms, the host cluster must have the same chemical composition and the same geometry as the host crystal. From the host cluster we derive a second cluster: the adsorption cluster (fig. 5.1c). The adsorption cluster is the cluster on which we study the adsorption and proton transfer processes. The adsorption cluster may be equal to the host cluster, but in some cases it is desirable to make some changes in the adsorption cluster with respect to the host crystal and host cluster; atoms can be replaced by others and the geometry can be modified. However, the boundary of the adsorption cluster must remain equal to the boundary of the host cluster since the host cluster is used to correct for the boundary errors of the adsorption cluster.

The interaction between the adsorption cluster and the adsorbate can be calculated in the case the cluster is embedded, but also in the case it is not. In the latter case the cluster-adsorbate interaction is equal to a normal cluster-adsorbate interaction.

The electrostatic potential that is imposed on the adsorption cluster, the correction potential (V^{corr}), adds the Madelung potential of the crystal to the Fock matrix of the adsorption cluster and subtracts the electrostatic potential of the boundary of the cluster. For the calculation of the V^{corr} we have divided the host cluster and the host crystal into two complementary parts, the inner zone and the outer zone. The charge distribution in

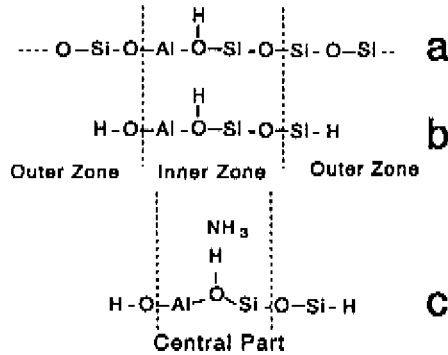


Figure 5.1. The host crystal (a), the host cluster (b) and the adsorption cluster (c). The host cluster is made by cutting a group of atoms out of the host crystal and saturating the dangling bonds. The adsorption cluster is derived from the host cluster by making some changes, leaving the outer zone unmodified. The host crystal and the host cluster are divided into a inner zone and a outer zone. The charge distribution of the outer zones are used for the calculation of the correction potential. The central part of the adsorption cluster is the part that is corrected for the long-range electrostatic effects. It is not necessarily equal to the inner zone.

the inner zones in the host cluster and the host crystal are very similar if the boundaries of the host cluster are sufficiently far from the inner zone. The correction potential is the electrostatic potential of the outer zone of the host crystal minus the electrostatic potential of the outer zone of the host cluster. It is calculated as follows. The charge distributions of the host crystal and the host cluster, obtained with a RHF-calculation, are partitioned through a Mulliken scheme [16]. From the resulting atomic charge distributions the atomic multipoles are calculated, up to the hexadecapoles [2].

$$V^{corr}(\mathbf{r}) = V_{outer\ zone}^{host\ crys}(\mathbf{r}) - V_{outer\ zone}^{host\ clus}(\mathbf{r}) \quad (5.1a)$$

$$= \sum_{A,L} \gamma_L^{host\ crys}(A) \sum_{\mathbf{h}} \Phi_L(\mathbf{r} - \mathbf{s}_a - \mathbf{h}) - \sum_{A,L} \gamma_L^{host\ clus}(A) \Phi_L(\mathbf{r} - \mathbf{r}_a) \quad (5.1b)$$

$$\Phi_L(\mathbf{r}) = X_L^m(\mathbf{r})/(|\mathbf{r}|)^{2l+1}. \quad (5.1c)$$

The A summation extends to the atoms of each unit cell of the host crystal in the first summation and to the atoms of the outer zone of the host cluster in the second. The \mathbf{h} summation extends over all unit cells in the infinite crystal, excluded those identifying the atoms of the inner zone of the host crystal. $L \equiv (l,m)$ are (spherical harmonic) quantum numbers; $\gamma_L^{host\ crys}(A)$ and $\gamma_L^{host\ clus}(A)$ are the (l,m) multipole moments of

atom A calculated according to a Mulliken partitioning from the host cluster and host crystal charge distribution (see Appendix A in Ref. [2]). X_l^m are real solid spherical harmonics (see Appendix A in Ref. [2]). The position of atom A in the reference cell is given by \mathbf{s}_a , the position in the cluster by \mathbf{r}_a . The question can be raised why in Eq. (5.1) only the outer zone is considered; in fact, if the multipoles in the inner zone of the host crystal and the host cluster coincide, V^{corr} would be exactly the same as resulting from Eq. (5.1). As we need a correction for the long-range effects, the differences in the charge distributions and thus in the multipoles of the inner zone should be negligible. However, the risk exists of magnification of minor differences by the multipole approximation or by numerical errors caused for example by small differences between the geometries of the host cluster and the host crystal. Therefore, the inner zones are ignored in the calculation of the correction potential. The correction potential is thus smooth in the inner zone of the adsorption cluster. We would like to repeat that since the host cluster is used to correct for the electrostatic boundary errors of the adsorption cluster the outer zones of the two clusters should be equal. Modification of the adsorption cluster with respect to the host cluster may only be made in the inner zone of the host cluster.

Only the part of the adsorption cluster that is of interest for the adsorption process is embedded *i.e.* corrected with the V^{corr} . The rest of the cluster remains unmodified. We will define the part of the adsorption cluster that is embedded as the central part. In the limiting case only the adsorbate molecule belongs to the central part. The correction potential must behave properly in the central part, therefore the central part must be completely inside the inner zone. The central part is defined by assigning a group of atoms around the adsorption site to the central part. An overlap distribution $\mu\nu$ is said to belong to the central part if both atomic orbitals μ and ν are centered on nuclei belonging to the inner part.

$$\mathbf{F}_{\mu\nu} = \mathbf{F}_{\mu\nu}^0 + \langle \mu | V^{corr} | \nu \rangle + V_0 S_{\mu\nu} \quad (5.2)$$

\mathbf{F} is the modified Fock matrix, \mathbf{F}^0 is the Fock matrix of the non-embedded adsorption cluster. The adsorption cluster is embedded by adding the integrals $\langle \mu | V^{corr} | \nu \rangle$ to the Fock matrix of the adsorption cluster (2). This integral is set to zero if μ or ν do not belong to the inner zone. A second term is added to all matrix elements: $V_0 S_{\mu\nu}$. $S_{\mu\nu}$ is the overlap element and V_0 a constant selected such that the host cluster and host crystal potential coincide. This term is necessary in order to fix the arbitrary zero of the potential in the periodic calculation [2,17]. This arbitrary zero is caused by the expansion of the charge distribution into multipoles. It is to be noticed that the $V_0 S_{\mu\nu}$ term has no influence on the energy of a neutral inner zone, if both electronic and nuclear terms are corrected. In our calculations we did not calculate the V_0 explicitly but it was set to zero for convenience.

From the previous discussion, and from general considerations, our model supposes that the long-range electrostatic potential has a minor influence on the wavefunction of the cluster, but a non-negligible effect on the adsorption energy. On the basis of this assumption the correction can be applied *a posteriori*, once the convergence of the self-consistent cycle in the calculation of the wavefunction has been reached. This is the first order embedding scheme since the effect of the correction is calculated as a first order

perturbation. If the correction, on the contrary, is applied to the Fock-matrix at each cycle, the full embedding scheme is obtained. In the latter the wavefunction of the adsorption cluster can adjust itself to the correction potential. In the following these two corrections are compared.

The embedding of the central part of the adsorption cluster in the correction potential changes its total energy. The effect of the embedding on the adsorption energy or on a geometry optimization is simply the difference between the change in total energy by the embedding for two different modifications of the cluster. For example, the effect of the embedding on the adsorption energy is the change in total energy of the adsorption cluster with the adsorbate minus the change in total energy of the adsorption cluster without the adsorbate. For the first order embedding scheme the effect of the embedding on the adsorption energy is given in the following equation:

$$\begin{aligned} \Delta E^{Ads}_{Embed} &= \left[\sum_{\mu,\nu} P'_{\mu\nu} \langle \mu | V^{corr} + V_0 | \nu \rangle - \sum_{\substack{Z \notin \\ \text{innerzone}}} Z'_I(\mathbf{r}_Z') (V^{corr}(\mathbf{r}'_Z) + V_0) \right] \\ &- \left[\sum_{\mu,\nu} P_{\mu\nu} \langle \mu | V^{corr} + V_0 | \nu \rangle - \sum_{\substack{Z \notin \\ \text{innerzone}}} Z_I(\mathbf{r}_Z) (V^{corr}(\mathbf{r}_Z) + V_0) \right] \quad (5.3.a) \\ &= \int_{\text{central part}} (\rho(\mathbf{r}) - \rho'(\mathbf{r})) V^{corr}(\mathbf{r}) + V_0 \int_{\text{central part}} (\rho(\mathbf{r}) - \rho'(\mathbf{r})). \quad (5.3.b) \end{aligned}$$

In Eq. (5.3.a) the atomic positions, the nuclear charges and the density matrix of the adsorption cluster with the adsorbate are indicated with \mathbf{r}'_Z , Z'_I and $P'_{\mu\nu}$. For the adsorption cluster without the adsorbate the symbols are \mathbf{r}_Z , Z_I and $P_{\mu\nu}$ respectively. In other words, in the first order embedding, the effect of the embedding on the adsorption energy is the integral over the central part of the product of the correction potential and the change in the charge distribution due to the adsorption. This is the first term in Eq. (5.3b). The charge distributions $\rho(\mathbf{r})$ and $\rho'(\mathbf{r})$ also contain the nuclear charges. Although Eq. (5.3) is only correct for the first order embedding scheme we also used it in the interpretation of the results of the full embedding scheme since, for the cluster we will discuss more extensively, there appears to be only a minor difference between the first and full embedding scheme. The second term in Eq. (5.3b) is the error made by ignoring the V_0 , as we do in this work. This error is equal to the constant V_0 multiplied by the change in the charge of the central zone by the adsorption process, i.e. the flow of charge in or out the central part as a result of the interaction with the adsorbate. Although we did not calculate the V_0 explicitly we made an estimate for it from the correction potential. Since for the zeolite system studied here the absolute value of the V^{corr} is below 10^{-3} and since the charge flow of the adsorption is at maximum a few tenths of an electron charge, the error maximally made by ignoring the V_0 is 1 kJ/mol. For other systems, in which either the charge flow or the V_0 is larger the V_0 should be calculated explicitly.

We would like to make some comments on the choice of the inner zone in the hosts and the central part in the adsorption cluster. As the correction potential should correct for

the electrostatic boundary errors the inner zone should be as small as possible because the correction potential only corrects for boundary errors outside the inner zone. On the other hand, a large inner zone has the advantage that more modifications can be made in the adsorption cluster and that the central part can be larger. In the latter case a larger part of the cluster is embedded and more changes in the electronic structure due to adsorption or changes in the geometry are embedded. We studied the effect of the size of the inner zone and the central part by varying their size in the calculation of the adsorption energies.

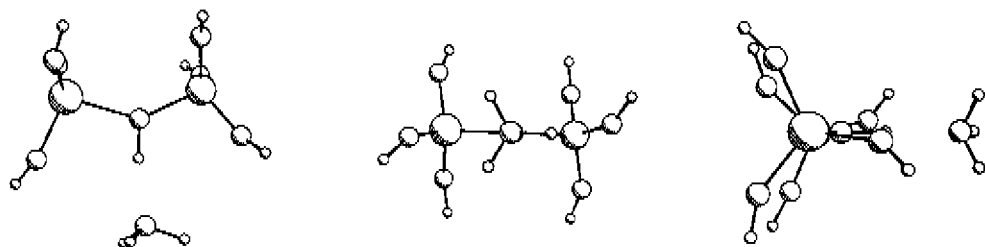


Figure 5.2. The Intermediate Cluster. The structure is shown as seen from three mutually perpendicular directions.

We calculated the adsorption energies of NH_3 and NH_4^+ on three zeolite clusters, both embedded and non-embedded, and we compared them with the adsorption energies as calculated in the host crystal. The host crystal is the shell-model optimized chabazite crystal as described in Chapter 4 of this thesis, fig. 4.1a. Three clusters were cut from the crystal. The first cluster is the Medium Cluster as described in Chapter 4, fig 4.3. The second cluster is the Intermediate Cluster, shown in fig. 5.2. the Intermediate Cluster, SiAlO_7H_7 , is smaller than the Medium Cluster; only the acidic HOSiAl -group and the oxygen atoms bonded to them are included in the cluster. The saturating hydrogen bonds are put in the direction of the bond they are saturating. The OH-bond lengths are 0.95 Å. The third cluster is the Giant Cluster as described in Chapter 4, fig. 4.5. For NH_3 and NH_4^+ experimental geometries were used [18,19]. NH_3 and NH_4^+ were adsorbed in such a way that their symmetry axes coincided with the OH-axis. All calculations are carried out at the RHF-level with a STO-3G basis set[20]. This basis set is used to enable the comparison between the embedded cluster and the crystal calculations. It is too much computer time consuming to carry out CRYSTAL calculations on the chabazite crystal with a larger basis set. The adsorption clusters were chosen equal to the host clusters.

Results and Discussion

The comparison between the adsorption energies on the three embedded clusters and the adsorption energies in the crystal allows us to draw conclusions about the role of the cluster size in the embedding scheme. The clusters differ in two ways. First, they differ in

the number of atoms directly interacting with the adsorbate and second, they differ in the quality of the covalent description. In both the Medium Cluster and the Intermediate Cluster the main interaction is the interaction between the adsorbate and the acidic OH-group. The Giant Cluster also describes the interaction between the adsorbate and the atoms in the eight-ring. In the Medium Cluster and the Intermediate Cluster this interaction is described purely electrostatically.

Apart from the number of atoms interacting with the adsorbate the clusters also differ in the quality of the covalent description. Previously, we found that the quality of the covalent description can be estimated from the Mulliken charges of the atoms [1]; if the atoms in the cluster have a charge that is close to the charge of the corresponding atom in the crystal the environment in the cluster and the crystal is very similar and the quality of the covalent description is good. Before we calculated the adsorption energies on the three clusters, we performed a RHF-calculation on the host clusters, here equal to the adsorption cluster. From the resulting Mulliken charges on the atoms interacting with the adsorbate we made an estimate of the quality of the covalent description. In Table I the Mulliken charges of the atoms of the acidic group are given for the crystal and the three clusters. The charges of the atoms of the acidic site of the Medium Cluster and the Giant Cluster deviate less than 0.01 unit from the charges in the crystal, whereas the deviation for the Intermediate Cluster is larger. The Medium Cluster and the Giant Cluster give a correct covalent description of the zeolite OH-group, whereas the Intermediate Cluster does not. Table II shows that in the Giant Cluster the atoms in the eight-ring are not described well.

We calculated the potential energy curves of NH_3 and NH_4^+ , on the embedded and non-embedded Medium Cluster. They are shown in fig. 5.3. The embedding of the cluster shifts the potential energy curves of NH_3 and NH_4^+ towards the potential energy curves as calculated in the crystal. However, the shape of the potential energy curve remains more or less the shape of the cluster curve. The reason for this is that, since the embedding is purely electrostatic, the embedded cluster describes the interaction between the adsorbate and the opposite wall of the zeolite channel purely electrostatically. The potential energy curve of the cluster is shifted the least if the central part and the inner zone are equal to HOSiAlO_6 . This combination of central part and inner zone also results in the smallest perturbation of the wavefunction of the cluster (see Table I). In the minimum the embedded cluster describes the crystal potential energy curve quite well; the crystal adsorption energies are reproduced within 6 kJ/mol for all combinations of central part and inner zone. The corresponding adsorption energies are given in Table III and IV.

The error made by the cluster approximation is reduced largely by embedding the cluster. For the non-embedded cluster the errors with respect to the crystal calculations were 16 and 23 kJ/mol for NH_3 and NH_4^+ , respectively. By embedding the cluster the errors are 1-4 and 1-6 kJ/mol. The embedding scheme produces the crystal adsorption energies with a relatively small error for a smaller part of the computer time. On a Cray Y-MP4/464 the acidic form of the chabazite crystal costed 408 seconds. The non-embedded and embedded cluster costed 194 and 220 seconds, respectively. Although the savings in time are not spectacular we should keep in mind that for basis set containing more diffuse functions the increase in required computer time will be larger for the periodic structure

Table I. The net charges resulting from a Mulliken population analysis on the atoms of the acidic SiOHAl-group and the oxygen atoms bonded to this group. The charges are given for the crystal and the three clusters. The charges for the embedded clusters are marked with an asterisk. In parenthesis the central part and the inner zone that were used in the embedding scheme are indicated.

Atom:	H	O	Si	Al
Crystal	0.213	-0.534	1.443	1.212
Medium Cluster	0.215	-0.532	1.449	1.224
Medium Cluster* (HOSiAlO ₆ /HOSiAlO ₆)	0.219	-0.533	1.473	1.203
Medium Cluster* (HOSiAl/HOSiAlO ₆)	0.220	-0.535	1.535	1.198
Medium Cluster* (HOSiAl/HOSiAl)	0.220	-0.537	1.565	1.243
Intermediate Cluster	0.222	-0.522	1.612	1.275
Intermediate Cluster* (HOSiAl/HOSiAl)	0.226	-0.527	1.586	1.123
Giant Cluster	0.219	-0.533	1.452	1.230

Table II. The charges of the atoms in the eight-ring, resulting from a Mulliken population analysis, for the Giant Cluster and the crystal. The numbering of the atoms starts with the silicon atom that is the closest to the aluminum atom of the HOSiAl-group.

Atom	Crystal	Giant Cluster	Atom	Crystal	Giant Cluster
Si1	1.443	1.477	O1	-0.728	-0.726
Si2	1.443	1.526	O2	-0.723	-0.708
Si3	1.388	1.522	O3	-0.721	-0.709
Si4	1.443	1.514	O4	-0.723	-0.712
Si5	1.388	1.483	O5	-0.745	-0.729
Al6	1.213	1.260			

than for the cluster [2]. We also note that the embedding costs only a small fraction of the total time.

The difference in adsorption energy between the full embedding and the first order embedding energy is about 1 kJ/mol in all cases. Also the effect of the embedding on the wavefunction of the cluster is small, see Table I. The effect of the choice of the inner zone and the central part on the adsorption energy has been investigated. For the case the inner zone consisted of the group of atoms described as HOSiAlO₆, we used two different central parts: the HOSiAlO₆ group itself and the HOSiAl group. The difference in adsorption energy for the two central parts is caused by the six oxygen atoms bonded to the HOSiAl-group. In the former case a change in electronic structure, caused by the adsorption, on these atoms is included in the embedding, see Eq. (5.3), in the latter case it is not. The change in electronic structure on these oxygen atoms as a result of the adsorption is larger for the adsorbate NH₄⁺ than for the adsorbate NH₃. Consequently, the dependence of the adsorption energy on the size of the central part will be larger as well; 5 kJ/mol for NH₄⁺ and 3 kJ/mol for NH₃. For a charged adsorbate a large central part should be used. The

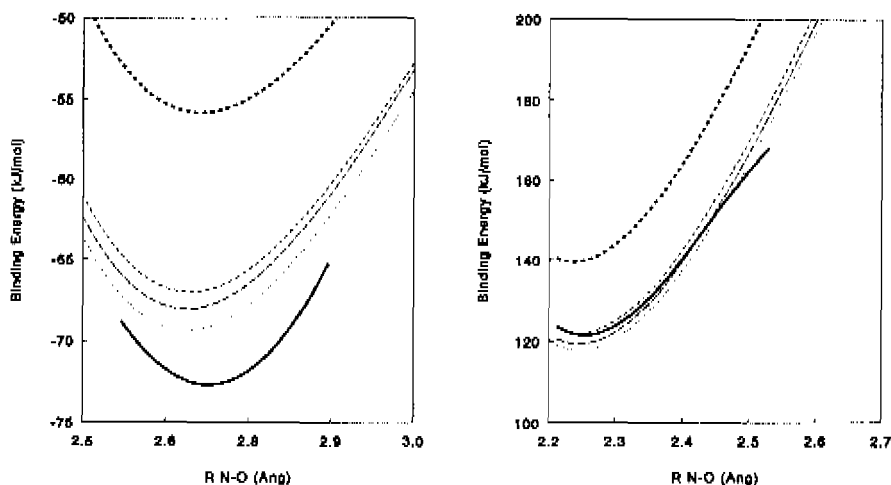


Figure 5.3. The potential energy curves of NH_3 (fig. a.) and NH_4^+ (fig. b) adsorbed on the acidic site of the Medium Cluster. The potential energy curves of the cluster and the crystal are shown in bold lines. The crystal curve is uninterrupted, the cluster curve is dotted. The curves of the embedded clusters are also given in thin lines. The lowest curve is calculated with the central part equal to HOSiAl and the inner zone equal to HOSiAlO_6 . The middle curve is calculated with the central part and the inner zone equal to HOSiAl . The upper curve is calculated with the central part and the inner zone equal to HOSiAlO_6 .

effect of the size of the inner zone is investigated by keeping the central part constant at HOSiAl and changing the size of the inner zone. In the first case there is a correction for the boundary effects of the six oxygen atoms, in the second there is no such correction. The difference in adsorption energy, as calculated with the two inner zones, HOSiAl and HOSiAlO_6 is small: 2 kJ/mol. This implies that the charge of the oxygen atoms bonded to the acidic site in the host crystal and the host cluster differ little; they are described well in the host cluster.

In Table I we showed that only the OH-group itself is described well in the Intermediate Cluster. All other atoms have relatively large boundary effects, i.e. they have a charge deviating more than 0.1 unit from the charge of the corresponding atoms in the zeolite crystal. This means that the Intermediate Cluster does not give a good covalent description of the acidic site. Since the embedding scheme only gives an electrostatic correction the Intermediate Cluster will not produce good results. A correction potential not affected by boundary effects can only be obtained if the inner zone, and the corresponding central part, consist of just the OH-group. This central part however is too small to give proper results in the embedding scheme. This becomes clear if we compare the adsorption energies calculated with the inner zone equal to the HOSiAl -group. There is a large difference in adsorption energy for the central part equal to the HOSiAl group and just the OH group. As a consequence the embedded Medium Cluster does not reproduce the adsorption energies of the crystal (Table V). Also there is a large difference in adsorption

Table III. The adsorption energies and O-N equilibrium distances of NH_3 on the Medium Cluster. The adsorption energies obtained with the first order embedding scheme are indicated with $\Delta E^{ads}(1)$, the adsorption energies obtained with the full embedding scheme are indicated with ΔE^{ads} . The adsorption energies are given in kJ/mol, the equilibrium distances in Å. The adsorption energy of NH_3 in the crystal is -72 kJ/mol, the corresponding equilibrium distance is 2.72 Å[1]. The calculated adsorption energies of the first line are the adsorption energies of the non-embedded cluster.

Central part	Inner zone	$\Delta E^{ads}(1)$	R_{N-O}	ΔE^{ads}	R_{N-O}
-	-	-56	2.67	-56	2.67
$\text{NH}_3 + \text{HOSiAl}$	HOSiAlO_6	-71	2.66	-70	2.65
$\text{NH}_3 + \text{HOSiAlO}_6$	HOSiAlO_6	-68	2.66	-67	2.66
$\text{NH}_3 + \text{HOSiAl}$	HOSiAl	-69	2.66	-68	2.65

Table IV. The adsorption energies, and O-N equilibrium distances of NH_4^+ on the Medium Cluster. The first order embedded adsorption energies are indicated with $\Delta E^{ads}(1)$, the full embedded adsorption energies by ΔE^{ads} . The adsorption energies are given in kJ/mol, the equilibrium distances in Å. The adsorption energy of the crystal is 117 kJ/mol, the corresponding O-N distance 2.21 Å[1]. The calculated adsorption energies on the first line are the adsorption energies of the non-embedded cluster.

Central part	Inner zone	$\Delta E^{ads}(1)$	R_{N-O}	ΔE^{ads}	R_{N-O}
-	-	140	2.23	140	2.23
$\text{NH}_4^+ + \text{OSiAl}^-$	HOSiAlO_6	118	2.23	117	2.25
$\text{NH}_4^+ + \text{OSiAlO}_6^-$	HOSiAlO_6	123	2.24	122	2.24
$\text{NH}_4^+ + \text{OSiAl}^-$	HOSiAl	120	2.24	119	2.24

energy for the full and the first order embedding energy.

The adsorption energies of NH_3 and NH_4^+ on the Giant Cluster are given in Table VI. The Giant Cluster is an extension of the Medium Cluster; it includes the atoms of the eight-ring, their charges however, differ from those they have in the zeolite crystal (see Table II). As in the case of the Intermediate Cluster the poor covalent description of the atoms in the eight-ring will prevent proper adsorption energies in the embedding scheme. For the 'small' inner zone and central part (the HOSiAlO_6 group) the error in the adsorption energy is a result of the poor description of the eight-ring. Because the inner zone is very large for the 'large' inner zone and central part (the HOSiAlO_6 group and the atoms in the eight-ring) there is only a small correction to the adsorption energy.

Although the Giant Cluster is an extension of the Medium Cluster, the latter yields better adsorption energies. Apparently, the error made by the purely electrostatic description of the interaction between the adsorbate and the eight-ring, as in the Medium Cluster, is smaller than the error caused by boundary errors in the eight-ring, even if there is a correction for the electrostatic part of them. By comparing the three clusters it results that the embedding scheme only produces reasonable results if atoms with boundary effects are

three or four bonds away from the adsorbate. In this embedding scheme the cluster must be relatively large because the embedding is purely electrostatic.

Even if the cluster is chosen well, some numerical errors will remain in the embedding scheme. For the systems studied in this paper a numerical error of a few kJ/mol is made by the truncation errors in the calculation of the matrix elements $\langle \mu | V^{corr} | \nu \rangle$ (see the Appendix). Another error is introduced by comparing the adsorption energies on the embedded cluster with adsorption energies in the host crystal. In the crystal calculations the adsorbate is adsorbed periodically and there is an interaction between the adsorption sites and the adsorbates. In the embedded cluster there is only one adsorbate. The error introduced by this comparison is about 2 kJ/mol for NH_4^+ and smaller for NH_3 (the crystal adsorption energies were calculated with 3 NH_3 molecules per unit cell and one NH_4^+ cation per unit cell [1]). Neglecting the V_0 causes an error of less than 1 kJ/mol.

It is useful to make a comparison between our embedding scheme and other schemes in which a zeolite cluster is embedded in a potential representing in some way the long-range electrostatic effects. Allavena and coworkers [8,9] developed a method in which the potential is calculated from a lattice of point charges whose value is obtained with Mortiers electronegativity equalization method [14,15]. From this potential a correction for the potential of the dangling-bond hydrogens is subtracted. The latter is calculated in the Mulliken point-charge approximation. The cluster is embedded completely, not just a central zone. Allavena *et al.* [8,9] did not calculate the effect of the embedding on the adsorption energy of NH_3 or NH_4^+ but they calculated the effect of the Madlung potential on the proton transfer energy; i.e., the difference in adsorption energy between the adsorbed NH_3 and NH_4^+ . They estimated the effect of the Madlung potential on the proton transfer energy to be -197 kJ/mol. We calculated this effect to be -6 or -8 kJ/mol for the Medium Cluster, depending on the size of the inner zone and the central part. The value produced by Allavena *et al.* seems a large overestimation of the effect of the long-range electrostatic potential since our values are consistent with the crystal calculations. Also the effect of the embedding on the Mulliken charges of the atoms of the acidic site is overestimated. The charges of the atoms of the acidic site changed by 0.2 unit. Cook *et al.* [13] used the embedding scheme developed by Allavena *et al.* [8,9]. They found that, as a result of the embedding, of a zeolite cluster the Mulliken charge of the acidic proton changed from 0.33 to 0.55. In our work, for the Medium Cluster, this change is 0.005 at maximum (Table I).

The overestimation of the effect of the embedding in the scheme of Allavena *et al.* and Cook *et al.* can have two causes: the size of the cluster and the embedding scheme itself. Both groups of authors used a cluster in which the silicon atom of the HOSiAl group was saturated with hydrogen atoms. These cluster are too small to be embedded in an electrostatic potential representing the crystal. Already in the Intermediate Cluster, having the dangling-bond hydrogens even further away from the adsorbate than the clusters used by Allavena *et al.* and Cook *et al.* the effect of the embedding is overestimated. Another reason for the errors made may be in the embedding scheme itself. There can be two sources of errors in the method. The first is the error in the potential. Although some error will be made by using the electronegativity equalization method to calculate the potential instead of taking the potential from the crystal, this error will not cause a large

Table V. The adsorption energies and O-N equilibrium distances of NH_3 and NH_4^+ calculated for the Intermediate Cluster. The adsorption energies marked with an asterisk are obtained with the full embedding scheme, all others are first order embedded energies. Energies are in kJ/mol, bond lengths in Å. The adsorption energy of NH_3 in the crystal is ~ 72 kJ/mol, the adsorption energy of NH_4^+ is 117 kJ/mol. The respective equilibrium distances are 2.72 and 2.21 Å[1]. The calculated adsorption energies on the first line are the adsorption energies of the non-embedded cluster.

Adsorbate		NH_3		NH_4^+	
Central part	Inner zone	ΔE^{ads}	R_{N-O}	ΔE^{ads}	R_{N-O}
-	-	-57	2.75	129	2.23
$\text{NH}_3 + \text{HO}$	HO	-82	2.63	89	2.23
$\text{NH}_3 + \text{HO}$	HOSiAl	-76	2.57	116	2.25
$\text{NH}_3 + \text{HOSiAl}$	HOSiAl	-95	2.66	92	2.26
$\text{NH}_3 + \text{HOSiAl}^*$	HOSiAl [*]	-85*	2.63*	92*	2.26*
$\text{NH}_3 + \text{HOSiAlO}_6$	HOSiAlO ₆	-118	2.59	25	2.26

Table VI. The adsorption energies and O-N equilibrium distances of NH_3 and NH_4^+ on the Giant Cluster. The embedded adsorption energies are first order embedded energies. Energies are in kJ/mol, bond lengths in Å. The adsorption energies denoted with 'small' are calculated with the central part and the inner zone equal to the HOSiAlO₆-group. The adsorption energies denoted with 'large' were obtained with the central part and the inner zone equal to HOSiAlO₆-group plus the silicon and oxygen atoms in the eight-ring. The adsorption energy of NH_3 and NH_4^+ in the crystal are -72 and 117 kJ/mol respectively, with equilibrium distances of 2.21 and 2.72 Å[1]. The calculated adsorption energies on the first line are the adsorption energies of the non-embedded cluster.

Adsorbate	NH_3		NH_4^+	
	ΔE^{ads}	R_{N-O}	ΔE^{ads}	R_{N-O}
Central Part/Inner zone				
-	-77	2.66	99	2.24
small	-65	2.69	124	2.22
large	-78	2.66	95	2.24

overestimation. The charges obtained with this scheme do not deviate more than 35 % from the Mulliken charges [21]. Probably more important errors in the scheme are the correction for the dangling-bond hydrogen atoms and the fact that the complete cluster, including the dangling bond hydrogen atoms is embedded. In the potential there is a correction for the dangling bond hydrogen atoms, i.e. the electrostatic potential of the hydrogen atoms is subtracted from the correction potential. Thus, at the position of the dangling bond hydrogen atoms, the potential will have very large values, possibly close to infinity. As such values for the potential strongly perturb the wavefunction the embedding of the complete cluster, including the hydrogen atoms, causes problems. In the work of

Allavena *et al.* another error may be caused by the fact that for the geometry of the acidic site the geometry of the isolated HOSiAlH_6 and OSiAlH_6^- clusters was used. In this way the link between the lattice of point charges and the orientation of the zeolite acidic site is not well defined.

The scheme used by Vetrivel *et al.* does not allow an estimation of the effect of the embedding since their cluster is charged [10–12]. However, some comments can still be made on the method. Probably as a result of the charge of the cluster, the effect of the embedding can be largely overestimated. For example, the Mulliken charges found in the clusters are strongly deviating from other cluster calculations, oxygen charges of -1.5 , or in another case aluminum charges of $+0.8$. Also a deprotonation energy of more than 2600 kJ/mol was calculated. On non-embedded small clusters this was calculated to be about half this value [22]. An overestimation of the effect of the long-range electrostatic potential will also be caused by the fact that the charges in this scheme are the full formal charges (Si^{4+} , O^{2-}), half the formal charge or three quarters the formal charge. A general comment on the methods used by Allavena *et al.*, Cook *et al.* and Vetrivel *et al.*, to embed a cluster in a array of point charges [8–13], is that point charges are used to describe the ions in the zeolite lattice. By ignoring the higher electrical moments of the ions a relatively large error, about 20 to 30 %, is introduced in the calculation of the potential (see the Appendix).

Conclusions

We have calculated adsorption energies on three embedded clusters. The Medium Cluster gives the best results, because the atoms close to the adsorbing molecule are properly described and their charges are very close those of the perfect zeolite crystal. On this cluster the error in adsorption energy with respect to the adsorption energy in the perfect crystal is very small; 1 to 6 kJ/mol. Roughly speaking, it results that in the present, simplified embedding scheme in which there is only a electrostatic correction, only reasonable results are obtained if the boundary of the cluster is three or four bonds away from the adsorbate. On clusters having the dangling bonds close to the adsorbate, such as the Intermediate Cluster and the Giant Cluster, erroneous results are obtained.

The effect of the additional electrostatic field on the wavefunction of the cluster is negligible, as shown by the very small difference resulting from the *a posteriori* and self-consistent correction of the Fock operator. However, the corrective contribution is important in the calculation of the adsorption energy, in particular if charged species are considered.

The present scheme contains numerical approximation in the calculation of the corrective term to the Fock matrix; the numerical error as a result of the Taylor expansion (A.1), although not negligible, is small enough to calculate precise adsorption energies.

By comparing the results of this work with other schemes in which there is a correction for the long-range electrostatic effects of the crystal we see that most of these methods tend to overestimate the effect of the long-range electrostatic potential [8–13]. The reasons for this overestimation are several: the choice of the charges used to calculate the potential, the choice of the cluster and the method to correct for the dangling bond hydrogens. Probably also an error is caused by embedding the complete cluster instead of just a part.

References

- [1] E.H. Teunissen, C. Roetti, C. Pisani, A. J. M. de Man, A. P. J. Jansen, R. Orlando, R. A. van Santen and R. Dovesi, *Mod. Simul. Mater. Sci. Eng.* **2**, 921 (1994), *Chapter 4 of this thesis*.
- [2] C. Pisani, R. Dovesi and C. Roetti, *Hartree-Fock Ab-initio Treatment of Crystalline Systems, Lecture Notes in Chemistry* **48** (Springer Verlag, Berlin, 1988).
- [3] C. Pisani and R. Dovesi, *Int. J. Quantum Chem.* **17**, 501 (1980).
- [4] R. Dovesi, C. Pisani, C. Roetti and V. R. Saunders, *Phys. Rev. B* **28**, 5781 (1983).
- [5] R. Dovesi, *Int. J. Quantum Chem.* **29**, 1755 (1986).
- [6] R. Dovesi, V. R. Saunders and C. Roetti, *Crystal 92 Users's Manual, Gruppo di Chimica Teorica, Università di Torino, and SERC Laboratory* (1992).
- [7] *Chapter 1 of this thesis*
- [8] M. Allavena, K. Seiti, E. Kassab, Gy. Ferenczy and J. G. Ángyán, *Chem. Phys. Lett.* **168**, 461 (1990).
- [9] E. Kassab, K. Seiti and M. Allavena, *J. Phys. Chem.* **95**, 9425 (1991).
- [10] R. Vetrivel, C. R. A. Catlow and E. A. Colbourn, *Proc. R. Soc. Lond. A* **417**, 81 (1988).
- [11] R. Vetrivel, C. R. A. Catlow and E. A. Colbourn, *Stud. Surf. Sci. Catal.*, **37**, 309 (1988).
- [12] R. Vetrivel, C. R. A. Catlow and E. A. Colbourn, *J. Phys. Chem.* **93** 4594 (1989).
- [13] S. J. Cook, A. K. Chakraborty, A. T. Bell and D. N. Theodorou, *J. Phys. Chem.* **97**, 6679 (1993).
- [14] W. J. Mortier, K. van Genechten and J. Gasteiger, *J. Am. Chem. Soc.* **107**, 829 (1985).
- [15] W. J. Mortier, S. K. Ghosh, S. Shankar, *J. Am. Chem. Soc.* **108**, 4315 (1986).
- [16] R. S. Mulliken, *J. Chem. Phys.* **23**, 1833 (1955).
- [17] V. R. Saunders, C. Freyeria-Fava, R. Dovesi, L. Salasco and C. Roetti, *Mol. Phys.* **77**, 629 (1992).
- [18] G. Herzberg, *Molecular Spectra and Molecular Structure* Vol. 2 (van Nostrand, Princeton, 1945)
- [19] J. A. Ibers and D. P. Stevenson, *J. Chem. Phys.* **28**, 929 (1958).
- [20] W. J. Hehre, R. F. Stewart and J. A. Pople, *J. Chem. Phys.* **51**, 2657 (1969).
- [21] K. A. van Genechten, W. J. Mortier and P. Geerlings, *J. Phys. Chem.* **86**, 5063 (1987).
- [22] E. H. Teunissen, R. A. van Santen, A. P. J. Jansen and F. B. van Duijneveldt, *J. Phys. Chem.* **97**, 203 (1993), *Chapter 3 of this thesis*
- [23] V. R. Saunders, in *Computational Techniques in Quantum Chemistry and Molecular Physics*, edited by G. H. F. Diercksen, B. T. Sutcliffe and A. Veillard, NATO ASI series C 15 (Reidel, Dordrecht, 1975)

Appendix: The calculation of the matrix elements

The integrals $\langle \mu | V^{corr} | \nu \rangle$ added to the Fock matrix of the non-embedded cluster, Eq. (5.2), are calculated with a Taylor series truncated after the second step (A.1).

$$\langle \mu | V | \nu \rangle = V \cdot S_{\mu\nu} + \frac{\delta V^{corr}}{\delta x} |C \cdot \gamma_x^{\mu\nu} + \frac{\delta V^{corr}}{\delta y} |C \cdot \gamma_y^{\mu\nu} + \frac{\delta V^{corr}}{\delta z} |C \cdot \gamma_z^{\mu\nu} \quad (5.A.1).$$

$S_{\mu\nu}$ is the overlap between the atomic orbitals μ and ν , $\gamma_i^{\mu\nu}$ are the transition dipole moments. $\frac{\delta V^{corr}}{\delta i} |C$ is the gradient of V^{corr} in the center C from which the potential is expanded. The AO's are linear combinations of gaussians. The potential is expanded from the center C of the product of the atomic orbitals μ and ν . This center is determined with the gaussian product theorem [23]. The exponents used in this theorem are the most diffuse exponents of the atomic orbitals. Using only the most diffuse exponents of the contracted gaussians gives a considerable saving in computer time but does not introduce a large error since the largest overlap between two AO's comes from the most diffuse gaussians. The potential and its derivatives are calculated from atomic multipoles, Eq. (5.1). The correction to the Fock matrix which is approximated in two ways, the truncation of the multipoles series in the calculation of the potential and the truncation of the Taylor series, Eq. (5.A.1). Both approximations are acceptable if the central part and the outer zone are not only not overlapping but also relatively apart from each other.

We studied the convergence of the potential as a function of the order of the multipole, Eq. (5.1). We calculated the interaction of NH_3 with the Madelung potential of the chabazite crystal, without an inner zone created in it, for three O-N distances: 2.77 Å, 3.19 Å and 3.62 Å. The first O-N distances are close to the O-N equilibrium distances, for the last one the NH_3 is in the middle of the cage. The order of the multipole is varied from the charge only up to the hexadecapole moment. The results of these calculations are shown in fig. 5.A.1. For the shortest distance, as expected, the convergence is slow. For an O-N distance of 3.62 Å the multipole expansion convergence is more satisfactory.

We have also studied the convergence of the Taylor series in Eq. (5.A.1). We calculated the interaction energy between a NH_3 molecule and the potential of the Medium Cluster in two ways. First the integral $\langle \mu | V | \nu \rangle$ is calculated according to Eq. (5.A.1), second the Taylor series is truncated after the first step, e.g. the integral is approximated as the product of the charge and the potential. The comparison is made for three O-N distances: 2.97 Å, 3.97 Å and 4.97 Å. The first distance is a little bit larger than the equilibrium O-N distance, in the last one NH_3 is relatively far from the cluster. The interaction energies with the electrostatic potential of the cluster are given in Table A.I. The Table shows that if the adsorbate and the part of the zeolite that is described electrostatically, e.g. the atoms outside the inner zone are separated from the adsorbate by 4 Å as is the case in the Medium Cluster and the Giant Cluster, the error we will make in the matrix elements will be at maximum 10 percent. For the calculation of the effect of the correction potential, in which the potential of the boundary effects is subtracted from the potential of the crystal, the error will be less since it can be expected that the errors made in the calculation of the host potential and the host crystal will be relatively similar. Although the integrals are approximated, they are sufficiently precise for our purposes.

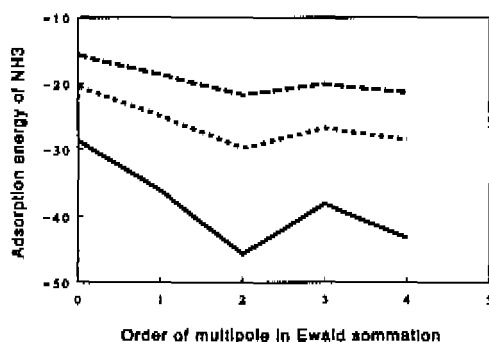


Figure 5.A.1. Convergence of the multipole series. The interaction energy of NH_3 with the Madelung potential of the chabazite crystal is shown as a function of the order of multipole used to calculate the potential. This calculation has been carried out for three O-N distances: 2.67 Å (—), 3.19 Å (.....) and 3.62 Å (-----).

Table A.I. The effect of the truncation of the Taylor series on the interaction energy of NH_3 with the electrostatic potential of the Medium Cluster (kJ/mol). The interaction energies are calculated in two ways. In the first the integral is approximated as the product of the overlap integral and the potential at the centroid of the overlap integral. In the second also the dipole contribution is included.

O-N distance (Å)	2.97	3.97	4.97
$V \cdot S + \sum \frac{\delta V}{\delta i} \cdot \gamma_i$	-28.17	-8.62	-1.83
$V \cdot S$	-25.85	-8.27	-1.93

6

Large basis sets and geometry optimizations in the embedded cluster scheme

Introduction

In this thesis we study the adsorption of NH_3 onto the acidic HOSiAl -group in zeolites and the proton transfer from the zeolite forming NH_4^+ . It appears that, for an accurate description of adsorption and proton transfer processes, it is necessary to use a relatively large basis set, to optimize the geometry and to include the long-range electrostatic forces of the crystal [1-6].

Usually, the zeolite adsorbate interaction is studied in the cluster approximation. In this approximation, a group of atoms is cut from the zeolite crystal and the dangling bonds are saturated with hydrogen atoms. The advantage of the cluster approximation is that large basis sets can be used. Furthermore, the geometry can be optimized relatively easy as a cluster can be handled with standard molecular packages such as GAMESS and Gaussian [7,8], having implemented automatic geometry optimizations using analytical gradients. The disadvantages of the cluster approximation are the absence of the long-range electrostatic forces of the crystal and the boundary errors of the cluster [5]. As a result of the saturation of the dangling bonds with hydrogen atoms the atoms at the boundary of the cluster are in a different chemical environment than in the crystal. Consequently, they behave differently towards adsorbates. Both disadvantages of the cluster calculations have a non-negligible effect on the calculation of adsorption energies [5].

In crystal calculations the model representing the zeolite is better; there are no boundary effects and the long-range electrostatic forces of the crystal are present. So far, only one study has been reported in which the adsorption and proton transfer processes were studied in a zeolite crystal [5]. The disadvantage of the crystal calculations is that for silicon-aluminum zeolites, because of the size and the symmetry of the system, the calculations are restricted to a minimal basis set. Furthermore, geometry optimizations in CRYSTAL are elaborate.

Another alternative for the calculation in zeolites is the embedded cluster method described in Chapter 5. An embedded cluster calculation has the computational advantages of a cluster, *i.e.* relatively large basis sets can be used, and a much better model for the zeolite is provided because the long-range electrostatic forces are included and a part of the boundary effects is removed [6]. The long-range electrostatic forces are calculated from the wavefunction of the zeolite crystal. This wavefunction is calculated at the RHF (Restricted Hartree Fock) level using the CRYSTAL program [9–13]. An embedded cluster reproduces the adsorption energies of the crystal within a few kJ/mol, requiring less computer time. Until now, the embedded cluster method has only been used with clusters having the same basis set and geometry as used to calculate the long-range electrostatic potential of the crystal [6].

We used the embedded cluster scheme to study the adsorption of NH_3 and NH_4^+ in a zeolite crystal. NH_3 is adsorbed hydrogen bonded onto the zeolite OH-group, in the case of the adsorption of NH_4^+ the proton has been transferred and NH_4^+ is interacting with a zeolite anion. We compared the adsorption energies for three different basis sets on the embedded cluster and we optimized the geometry of the zeolite acidic site.

On a small cluster, keeping the geometry fixed, we calculated the adsorption energies of NH_3 and NH_4^+ with a minimal, a large and a mixed basis set. The latter has a large basis set on the atoms around the adsorption site and a minimal basis set on the atoms at the boundary of the cluster. We used a mixed basis set for two reasons. First, to embed the cluster properly, the atoms in the boundary of the cluster must have the same basis set as the corresponding atoms in the crystal [6]. As we can only use a minimal basis set in the crystal calculations, the atoms in the boundary of the cluster should have a minimal basis set as well. Second, a large basis set on all atoms of a relatively large cluster would increase the number of basis functions, such that the calculations are not feasible any more. The accuracy of the mixed basis set was estimated by comparing its results with those calculated with the large basis set. As an application of the mixed basis set the adsorption energies of NH_3 and NH_4^+ were calculated on an embedded and a non-embedded larger cluster, using the minimal and the mixed basis set.

Using a minimal STO-3G basis set, we optimized the geometry of a part of the cluster relatively far from the boundary effects, namely the acidic OH-group. It was optimized in the non-embedded cluster, the embedded cluster and the crystal. We also calculated the changes in energy, with respect to a reference structure, as a result of the optimizations of the various structures. Finally, we calculated the adsorption energy of NH_3 and NH_4^+ using a mixed basis set and partially optimizing the geometry.

Methods and Computational Details

We studied the adsorption of NH_3 and NH_4^+ on two clusters, one of them embedded in a zeolite crystal. The zeolite is the shell-model optimized acidic chabazite as described in Chapter 4, fig. 4.1a. We calculated the adsorption energies of NH_3 and NH_4^+ on two clusters cut from the chabazite. One is the Medium Cluster as described in Chapter 4, fig. 4.4. The other one is the Intermediate Cluster as described in Chapter 5, fig. 5.2. For NH_3 and NH_4^+ the experimental geometries were used [14,15]. They were adsorbed

onto the acidic OH-group with their symmetry axes coinciding with the OH-axis. The ON-distance is the only parameter optimized in the calculation of adsorption energies.

On the Intermediate Cluster, we compared the results of three different basis sets. The first basis set was the standard minimal STO-3G basis set. The second basis set is referred to as the large basis set. In this basis set, the silicon and aluminum atoms of the acidic HOSiAl-group had a 6-31G(d) basis set [16,17], the oxygen atom of the acidic group had a 6-311G(d) basis set [18]. All other atoms had a 6-31G basis set [19,20]. The third basis set is the mixed basis set. In this basis set the adsorbate and the HOSiAl-group had the same basis set as in the large basis set. All other atoms had the minimal STO-3G basis set. The minimal basis set has two advantages: it requires little computer time and it is the same basis set used to calculate the charge distribution of the zeolite crystal. However, it does not yield precise adsorption energies. The large basis set, requiring more computer time, produces the adsorption energies of NH_3 with an error of 10 kJ/mol and underestimates the adsorption energy of NH_4^+ by about 50 kJ/mol [1,21,22].

The mixed basis set has a part of the advantages of both basis sets: it requires less computer time than the large basis set and it is less probable to cause problems in the embedding scheme as the boundary of the cluster has the same basis set as the crystal. Also it can be expected to give a acceptable description of the acidic site of the zeolite cluster. The disadvantage of the mixed basis set is that it is unbalanced; one part of the cluster is described well whereas another part is not. This imbalance may cause a flow of electronic charge to the part that is described better, thus perturbing the calculation of adsorption energies.

The Medium Cluster was embedded in the chabazite crystal with the method described in Chapter 5. The host cluster is equal to the Medium Cluster. The charge distributions of the host cluster and host crystal are calculated at the RHF-level, using a minimal STO-3G basis set [23]. The atomic multipoles of the HOSiAlO₆ group, both in the crystal and the cluster, are ignored in the calculation of the correction potential. It is not added to the complete cluster but only to the atoms of the HOSiAlO₆ group and the adsorbate.

We optimized the geometry of the zeolite OH-group on the non-embedded Medium Cluster, the embedded cluster and the crystal. These optimizations were carried out with a minimal STO-3G basis set. The *x*, *y* and *z*-coordinates of the oxygen and the hydrogen atom were optimized. This means that the O-H, Si-O, Al-O distances, the Si-O-H-angle and the H-O-Si-Al and H-O-Si-O dihedral angles were optimized. In all cases the start for the optimization was the shell-model geometry. The OH-groups of the crystal, the embedded cluster and the non-embedded cluster were optimized with the CRYSTAL program [9-13]. A parabolic interpolation algorithm [24] was used as analytical derivatives are not implemented in CRYSTAL.

In CRYSTAL, the Coulomb and exchange integrals are calculated exactly if some of the overlaps between the atomic orbitals for which the integral is calculated are above a certain threshold. If the overlaps are below this threshold the integral is approximated with multipolar expansions [9,13]. For the cluster, the crystal and the embedded cluster we used the same value for the thresholds: 10^{-5} for Coulomb integrals and 10^{-6} for exchange integrals. The convergence criteria are affected by the approximations in the calculation of the integrals; the potential energy surface is slightly discontinuous. Although it is possible

to avoid these discontinuities [13], we decided to stop the optimizations when the changes in energy became of the order of magnitude of the numerical noise due to the approximation of the integrals. In practice, this means that the energy was converged below 10^{-6} H ($2.5 \cdot 10^{-3}$ kJ/mol) in all cases. This change in energy corresponds to a step size of about $5 \cdot 10^{-4}$ Å.

The OH-group in the non-embedded cluster was also optimized with the Berny algorithm [25], an algorithm using analytical derivatives and implemented in the Gaussian 92 program package [8]. Here, all Coulomb and exchange integrals are calculated exactly. There are two criteria for the convergence of the optimization; one for the step size, 10^{-3} a.u., and one for the forces on the atoms, $2 \cdot 10^{-4}$ a.u.. As a result of the latter, the energy converges below 10^{-8} H ($2.5 \cdot 10^{-5}$ kJ/mol). By comparing the geometry of the OH-group in the non-embedded cluster optimized with the parabolic interpolation the accuracy of the latter can be estimated since the optimization with the Berny algorithm is more accurate.

We calculated the adsorption energies of NH_3 and NH_4^+ on the embedded and non-embedded Medium Cluster using the mixed basis set and optimizing the geometry of the OH-group and the adsorbate. The optimizations were carried out with the Gaussian program package. During the optimizations the O-H-N-angle was kept fixed at 180° . For NH_4^+ there was an additional restriction; the N-H distance of the proton bonding to the anionic oxygen atom was kept fixed at the experimental value of 1.03 Å [15]. The adsorption energy was calculated from a potential energy curve consisting of three O-N distances; the equilibrium distance found with the optimization and two distances 0.1 Å longer and shorter, keeping all other parameters fixed.

Results and Discussion

The comparison of the three basis sets

The adsorption energies of NH_3 and NH_4^+ on the Intermediate Cluster calculated with three basis sets are given in Table I. As found earlier, the adsorption energy of the hydrogen bonding NH_3 is relatively independent of the basis set [1]. The adsorption energy of NH_4^+ depends more strongly on the basis set as a result of the diffuse nature of the anionic oxygen atom in the zeolite cluster [1]. If the large basis set is taken as a reference, the minimal basis set underestimates the stability of the ionic structure by more than 120 kJ/mol.

With respect to the large basis set, the mixed basis set slightly overestimates the adsorption energies of NH_3 and NH_4^+ . Probably, this overestimation is caused by the imbalance in the Intermediate Cluster as a result of the mixed basis set. Because of the better description of the acidic site its electronic population is increased. In this way, it stabilizes the adsorbate and causes an overestimation of the adsorption energies by about 5 to 10 kJ/mol on the Intermediate Cluster. In the Medium Cluster this overestimation is smaller. Probably, the imbalance in the Medium Cluster is smaller as it is buffered by a larger cluster. Thus, with the mixed basis set adsorption energies on the large cluster can be calculated well.

Table I The adsorption energies (in kJ/mol) of NH_3 and NH_4^+ on the Intermediate Cluster, calculated with three different basis sets: a minimal STO-3G basis set, the mixed basis set and the large basis set.

Adsorbate	Large	Mixed	STO-3G
NH_3	-58	-62	-57
NH_4^+	6	-4	129

Table II The adsorption energies (in kJ/mol) of NH_3 and NH_4^+ calculated on the Medium Cluster [6], calculated with the STO-3G basis set on the non-embedded and the embedded cluster.

Adsorbate	Non-embedded	First Order Embed	Full Embed
NH_3	-56	-67	-68
NH_4^+	140	123	122

Table III The adsorption energies (in kJ/mol) of NH_3 and NH_4^+ calculated on the Medium Cluster, calculated with the mixed basis set on the non-embedded and the embedded cluster.

Adsorbate	Non-embedded	First Order Embedded	Full Embed
NH_3	-60	-80	-80
NH_4^+	-8	-27	-29

The adsorption energies of NH_3 and NH_4^+ for the non-embedded, the first order embedded and the full embedded Medium Cluster are given in Table II for the minimal STO-3G basis set and in Table III for the mixed basis set. On the Medium Cluster, the difference between the adsorption energies calculated with the STO-3G and the mixed basis set are larger than for the Intermediate Cluster. This larger difference is probably not the result of the imbalance in the basis set, but most probably the result of the larger Basis Set Superposition Error (BSSE) [26,27]. Because there are more atoms in the Medium Cluster the adsorbate and the cluster have more possibilities to use each others orbitals to lower their own energy; as a consequence the BSSE is larger.

Although the mixed basis set gives much better adsorption energies than the minimal basis set the charge distribution is not strongly affected [6]. This is illustrated by the fact that the difference between the effect of the embedding for the minimal and the mixed basis set is at most 3 kJ/mol. Also, there is a very small difference between the full and the first order embedding scheme. This was seen before for the STO-3G basis (Table II).

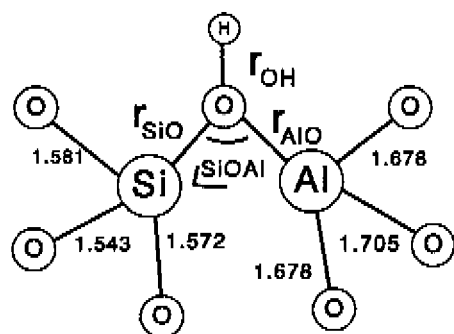


Figure 6.1. The results of the geometry optimizations of the OH-groups of the non-embedded Medium Cluster, the embedded Medium Cluster and the crystal. The calculations were carried out with a minimal STO-3G basis set. On the left, the geometry of the acidic site. In the table the results of the optimizations obtained with the various techniques are given.

parameter	shell model geometry	geometry optimized with gaussian	geometry optimized on non-embedded cluster	geometry optimized on embedded cluster	geometry optimized in the crystal
r_{O-H}	0.999	0.975	0.975	0.976	0.976
r_{O-Si}	1.712	1.738	1.742	1.742	1.748
r_{O-Al}	1.884	1.829	1.825	1.825	1.820
$\angle_{Si-O-Al}$	138.1	140.7	140.7	140.7	140.5

The geometry optimizations

The results of the geometry optimizations of the OH-group of the non-embedded and embedded Medium Cluster and the crystal, all with a minimal basis set, are shown in fig. 6.1. The shell model structure is different from the structures in which the OH-group is optimized quantum-chemically. Especially the O-H bond is predicted too long. For a purely siliceous system a better agreement was found between the shell model geometry and the *ab-initio* geometry [28]. Apparently, the parametrization of the shell model for the atoms of the acidic site [29] is less accurate than the parametrization for the purely siliceous system [30]. The quantum-chemical optimized structures are similar to each other, bond-lengths for the various structures are equal within 0.01 Å and the Si-O-Al angles within 0.2°. The geometries of the acidic group of the non-embedded cluster as optimized with Gaussian and CRYSTAL differ only slightly. This difference can be caused by the approximation of the integrals in CRYSTAL, but is more likely that it is caused by the less strict convergence criteria used in the CRYSTAL optimizations.

The optimizations of the various structures i.e., the non-embedded cluster, the embedded cluster and the crystal, with CRYSTAL show a large resemblance to each other. We concluded before that in the Medium Cluster the atoms of the acidic HOSiAl-group are in the same chemical environment as in the crystal [5,6]. Here, this is illustrated by the very similar bond lengths. Although the long-range effects of the crystal affect the

relative weak interaction with adsorbates, they hardly affect the covalent binding between the atoms in the acidic site of the cluster.

Table IV The gain in energy, ΔE^{opt} , due to the optimization, given with respect to the shell model geometry. The ΔE^{opt} has been calculated for four geometries of the OH-group. In column **A**, the ΔE^{opt} is calculated for the geometry obtained with the geometry optimization on the non-embedded cluster using the Berny algorithm. In the columns **B**, **C** and **D** the ΔE^{opt} is calculated for the geometries as obtained with the parabolic interpolation geometry optimization of the non-embedded cluster, the embedded cluster and the crystal, respectively. In row **I** the ΔE^{opt} is calculated for the non-embedded cluster, using Gaussian. In rows **I**, **II** and **III** ΔE^{opt} is calculated with CRYSTAL on the non-embedded cluster, the embedded cluster and the crystal respectively.

geometry: ΔE^{opt} calculated on:	A	B	C	D
I	-8.771	-8.714	-8.708	-8.476
II	-8.868	-9.052	-9.046	-8.809
III	-9.193	-9.434	-9.434	-9.269
IV	-10.797	-11.179	-11.183	-11.277

In Table IV, the ΔE^{opt} , the lowerings in energy of the cluster as a result of the optimization with respect to the shell-model geometry, are given. We calculated the ΔE^{opt} for geometries obtained from optimizations of the non-embedded cluster, optimized with both Gaussian and CRYSTAL, and geometries obtained from the optimization, using CRYSTAL, of the embedded cluster and the crystal. The ΔE^{opt} is relatively independent of the method used to optimize the geometry. The differences are never larger than 0.5 kJ/mol. The differences between the optimizations on the cluster with the Berny algorithm with Gaussian and the parabolic interpolation with CRYSTAL are not negligible but rather constant. They seem to be caused more by the approximations in CRYSTAL than by the difference in the accuracy of the parabolic interpolation algorithm. Probably, the ΔE^{opt} for the CRYSTAL-calculation on the cluster are about 0.3 kJ/mol larger because the energy of the shell model geometry cluster was calculated 0.3 kJ/mol higher in energy as a result of the approximations used in CRYSTAL.

For each structure, the ΔE^{opt} as a result of the various optimizations is similar. This means that, for the geometries investigated here, the potential energy surfaces seem parallel. On the other hand, the ΔE^{opt} of a geometry differs for each structure. The ΔE^{opt} in the embedded cluster are 0.3 to 0.4 kJ/mol lower than the ΔE^{opt} in the non-embedded cluster. Although the geometries found with the optimization in the embedded and non-embedded cluster are similar, the ΔE^{opt} in the former is larger. Apparently, the potential energy surfaces are similar in the sense that the minima are in the same position but the depths of the potential energy well are different. The same is true for the crystal, in which the ΔE^{opt} are even larger. The covalent binding and the long-range electrostatic effects of the crystal seem to enforce the bonds in the acidic site.

So far, we have seen that the optimized geometries are the same in the cluster, the embedded cluster and the crystal. Also the ΔE^{opt} for the geometries are the same in a

Table V The results of the geometry optimization of the Medium Cluster without the adsorbate (the OH-form), and the cluster with NH_3 and NH_4^+ adsorbed on it. The geometries have been optimized with the mixed basis set.

	OH	NH_3	NH_4^+
R_{OH}	0.953	0.996	1.468
$R_{\text{O-Si}}$	1.713	1.700	1.670
$R_{\text{O-Al}}$	1.894	1.900	1.886
$\angle_{\text{Si-O-Al}}$	137.2	137.7	141.7

Table VI The adsorption of NH_3 and NH_4^+ on the partially geometry optimized Medium Cluster. The adsorption energies have been calculated on the non-embedded and the embedded cluster with the mixed basis set.

	non-embedded		full-embedded	
	R_{NO}	ΔE	R_{NO}	ΔE
NH_3	2.76	-79	2.75	-89
NH_4^+	2.48	-14	2.52	-35

structure. However, we should keep in mind that the geometry optimization was limited; only the positions of the atoms of the OH-group were optimized. For more extensive geometry optimizations one could expect larger deviations, since in the cluster the boundary effects are getting more important. However, more extended geometry optimization are not feasible for the crystal at this moment.

The adsorption of NH_3 and NH_4^+ with the mixed basis set and optimized geometry

The geometry and adsorption energies of NH_3 and NH_4^+ on the embedded and non-embedded Medium Cluster augmented with the mixed basis set are given in Tables V and VI. With this basis set, the OH-distance is shorter than in the shell model geometry and the STO-3G geometry. For the OH-form of the cluster the Al-O and Si-O distances are relatively close to those of the shell model geometry.

The adsorbates are more stable on the geometry optimized cluster than on the shell model geometry cluster (Tables III and VI). Previously, we saw that NH_3 is adsorbed less strongly if the geometry is optimized: the zeolite is more stable and less-reactive [1,5]. Apparently, the effect of the optimization on the adsorption is dependent on the starting geometry. In this case the shell model geometry provided a good model for the OH-form of the cluster; the Al-O and Si-O bond lengths are very similar. With respect to the shell model geometry the cluster with NH_3 adsorbed on it could, during the optimization, stabilize itself by elongating the Al-O bond length and shortening the Si-O bond length. NH_4^+ is stabilized by the geometry optimization by shortening the Si-O and Al-O distances after proton transfer. The stabilization of NH_4^+ is larger than for NH_3 because its adsorption energy is more sensitive to the geometry than that of NH_3 [1,4-6]. Moreover, the optimized geometry of NH_4^+ adsorbed on the zeolite differs more from the shell-model optimized structure than that of NH_3 (compare fig. 6.1). With respect to the minimal basis

set, the mixed basis set stabilizes the anionic oxygen. This is illustrated in the elongation of the O-N bond with respect to the minimal basis set calculations [5]. The enlargement of the cluster, with respect to the calculations in which a small cluster and a larger basis set was used, also seems to stabilize the anion as the O-N bond is elongating [1,4]. As the charge separation is larger, the large O-N distance is enlarging the effect of the embedding [5].

Conclusion

We calculated the adsorption energies of NH_4^+ and NH_3 on a zeolite cluster with three different basis sets: a minimal basis set, a large basis set and a mixed basis set. The mixed basis set has a large basis set on the atoms around the adsorption site and a minimal basis set on the rest of the cluster. We deduced that there was an imbalance in the Intermediate Cluster as a result of the use of the mixed basis set, as it showed a slight overestimation of the adsorption energies with respect to the large basis set. This error is 4 kJ/mol for the adsorption of NH_3 and 10 kJ/mol for the adsorption energy of NH_4^+ . The minimal basis set underestimates the stability of NH_4^+ by more than 120 kJ/mol. The imbalance, and thus the overestimation of adsorption energies, is smaller for the Medium Cluster.

We optimized the position of the atoms of the OH-group in the non-embedded cluster, the embedded zeolite cluster and in the crystal. In all these structures the geometry has been optimized with the CRYSTAL program, using parabolic interpolation. The OH-group has also been optimized on the non-embedded cluster with the Gaussian program package, using the Berny algorithm. The convergence criteria in CRYSTAL were not as strict as in Gaussian because of the numerical noise in the latter as a result of the approximation of some integrals. The resulting geometries were very similar in all cases. The ΔE^{opt} , the change in energy with respect to the reference geometry, was almost the same for all optimized geometries. The potential energy surfaces for the OH-group, a group relatively far from the boundary, are parallel for the non-embedded cluster, the embedded cluster and the crystal.

We calculated the adsorption energies of NH_3 and NH_4^+ with a partial optimization of the cluster and the mixed basis set. With respect to the fixed geometry calculations the adsorbates are stabilized.

The calculations presented here, namely those of the embedded cluster scheme using a mixed basis set and partial optimization of the geometry offer an improved method for the calculation of the adsorption energies of NH_3 and NH_4^+ . We have shown that the use of the mixed basis set does not cause problems due to the imbalance in the basis set. As we can use the cluster optimized geometries for the embedded cluster, we can remove some arbitrariness in the adsorption energies caused by the choice of the geometry. This arbitrariness can be introduced if a geometry is used that resembles the OH-form of the zeolite, in this case the stability of the adsorbates is underestimated, or if a geometry is used that resembles that of the cluster-adsorbate complex, in this case the stability of the adsorbate is overestimated.

The calculations presented here are an important step towards the calculation of accurate adsorption energies as they showed that we can use large basis sets and geometry optimizations from clusters in the embedded cluster method. The deficiencies in this

calculations, such as the limited optimization, the low coordination of NH_4^+ towards the zeolite lattice, and the absence of electron correlation and a correction for the BSSE are not likely to cause problems in the embedded cluster scheme.

References

- [1] E. H. Teunissen, F. B. van Duijneveldt and R. A. van Santen, *J. Phys. Chem.* **96**, 366 (1992), *Chapter 2 of this thesis*.
- [2] P. Ugliengo, V. Saunders and E. Garrone, *Surf. Sci.* **224**, 498 (1989).
- [3] P. Ugliengo, V. Saunders and E. Garrone, *J. Phys. Chem.* **94**, 2260 (1990).
- [4] E. H. Teunissen, R. A. van Santen, A. P. J. Jansen and F. B. van Duijneveldt, *J. Phys. Chem.* **97**, 203 (1993), *Chapter 3 of this thesis*.
- [5] E. H. Teunissen, C. Roetti, C. Pisani, A. J. M. de Man, A. P. J. Jansen, R. Orlando, R. A. van Santen and R. Dovesi, *Mod. Simul. Mater. Sci. Eng.* **2**, 921 (1994), *Chapter 4 of this thesis*.
- [6] E. H. Teunissen, A. P. J. Jansen, R. A. van Santen, R. Orlando and R. Dovesi, *J. Chem. Phys.*, in press, *Chapter 5 of this thesis*.
- [7] M. F. Guest and J. Kendrick, *GAMESS Users Manual*, (SERC Daresbury Laboratory, CCP1/86/1, 1986), M. Dupuis, D. Spangler and J. Wendoloski, *GAMESS (NRCC Software Catalog, Vol. 1, Program No. QG01, 1980)*, M. F. Guest, R. J. Harrison, J. H. van Lenthe and L. C. H. van Corler, *Theor. Chim. Acta.* **71**, 117 (1987).
- [8] M. J. Frisch, G. W. Trucks, M. Head-Gordon, P. M. W. Gill, M. W. Wong, J. B. Foresman, B. G. Johnson, H. B. Schlegel, M. A. Robb, E. S. Replogle, R. Gomperts, J. L. Andres, K. Raghavachari, J. S. Binkley, C. Gonzalez, R. L. Martin, D. J. Fox, D. J. DeFrees, J. Baker, J. J. P. Stewart, and J. A. Pople, *Gaussian 92 Revision D.3*, (Gaussian Inc., Pittsburgh PA, 1992).
- [9] C. Pisani, R. Dovesi and C. Roetti, *Hartree-Fock Ab-initio Treatment of Crystalline Systems*, Lecture Notes in Chemistry **48** (Springer Verlag, Berlin, 1988).
- [10] C. Pisani and R. Dovesi, *Int. J. Quantum Chem.* **17**, 501 (1980).
- [11] R. Dovesi, C. Pisani, C. Roetti and V. R. Saunders, *Phys. Rev. B* **28**, 5781 (1983).
- [12] R. Dovesi, *Int. J. Quantum Chem.* **29**, 1755 (1986).
- [13] R. Dovesi, V. R. Saunders and C. Roetti, *Crystal 92 Users's Manual* (Gruppo di Chimica Teorica, Università di Torino and SERC Laboratory, 1992)
- [14] G. Herzberg, *Molecular Spectra and Molecular Structure*, Vol. 2 (van Nostrand, Princeton, 1945)
- [15] J. A. Ibers and D. P. Stevenson, *J. Chem. Phys.* **28**, 929 (1958).
- [23] W. J. Hehre, R. F. Stewart and J. A. Pople, *J. Chem. Phys.* **51**, 2657 (1969).
- [16] M. M. Franci, W. J. Pietro, W. J. Hehre, J. S. Binkley, M. S. Gordon, D. J. DeFrees and J. A. Pople, *J. Chem. Phys.* **77**, 3654 (1982).
- [17] M. S. Gordon, J. S. Binkley, J. A. Pople, W. J. Pietro and W. J. Hehre, *J. Am. Chem. Soc.* **104**, 2797 (1982).
- [18] R. Krishnan, J. S. Binkley, R. Seeger and J. A. Pople, *J. Chem. Phys.* **72**, 650 (1980).
- [19] R. Ditchfield, W. J. Hehre and J. A. Pople, *J. Chem. Phys.* **54**, 724 (1971).
- [20] W. J. Hehre, R. Ditchfield and J. A. Pople, *J. Chem. Phys.* **56**, 2257 (1972).
- [21] D. J. DeFrees and A. D. McLean, *J. Comput. Chem.* **7**, 321 (1986).

- [22] K. Szalewicz, S. J. Cole, W. Kolos and R. J. Bartlett, *J. Phys. Chem.* **89**, 3662 (1988).
- [24] W. H. Press, B. P. Flannery, S. A. Teukolsky, and W. T. Vetterling, *Numerical Recipes C*, (Cambridge University Press, Cambridge 1988).
- [25] M. Frisch, J. Foresman and A. Frisch, *Gaussian 92 User's Guide*, (Gaussian Inc., Pittsburgh 1990).
- [26] S. F. Boys and F. B. Bernardi, *Mol. Phys.* **19**, 553 (1970).
- [27] J. H. van Lenthe, J. G. C. M. van Duijneveldt-van de Rijdt and F. B. van Duijneveldt, *Adv. in Chem. Phys.* **79**, 521 (1987).
- [28] E. Aprà, R. Dovesi, C. Freyria-Fava, C. Pisani, C. Roetti and V. R. Saunders, *Mod. Sim. Mater. Sci. Eng.* **1**, 297 (1993).
- [29] K.-P. Schröder, J. Sauer, M. Leslie and C. R. A. Catlow, *Zeolites* **12**, 20 (1990), K.-P. Schröder, J. Sauer, M. Leslie, C. R. A. Catlow and J. M. Thomas, *Chem. Phys. Lett.* **188**, 320 (1990).
- [30] R. A. Jackson and C. R. A. Catlow, *Mol. Sim.* **1**, 207 (1988).

7

The adsorption energy of NH_3 and NH_4^+ in chabazite

Introduction

So far in this thesis, as an example of an adsorption and proton transfer reaction on the zeolite acidic site, we studied the adsorption of NH_3 and the proton transfer forming NH_4^+ . We concluded that an accurate description of the adsorption and proton transfer in zeolites requires a correct model for the zeolite and a quantum chemical method yielding adsorption and proton transfer energies as accurate as the size of the system allows. The accuracy of various quantum chemical methods were tested in the calculation of the adsorption energies of NH_3 and NH_4^+ on small zeolite clusters [1–4]. A relatively large basis set should be used, as especially the heat of adsorption of NH_4^+ is strongly dependent on the size of the basis set. It is also important to apply the counterpoise correction (CPC) to correct for the basis set superposition error (BSSE) [5,6]. Without this correction the adsorption energy can be largely overestimated. Furthermore, it is important to include electron correlation. A factor as important as the choice of the basis set is the choice of the geometry. After proton transfer the zeolite lattice can stabilize itself by adjusting its geometry. NH_4^+ is stabilized to a large extent by a high coordination to the zeolite lattice. This also requires relaxation of the lattice.

Although small clusters enable the use of accurate quantum-chemical methods they are not satisfactory because they do not provide a proper model for the zeolite acidic site [7]. A comparison between cluster and crystal calculations, using the CRYSTAL program [8–12], shows that, first, the long-range electrostatic forces of the crystal are non-negligible [7]. Second, the clusters have boundary errors. Because of the saturation of the dangling bonds with hydrogen atoms the atoms of the acidic site are in a different chemical environment in the cluster than in the crystal and thus behave differently towards the adsorbate. These are the boundary effects. To avoid the boundary effects having a large influence on the adsorption process the dangling bond hydrogens should be at least four bonds away from the adsorbate [7].

The crystal seems to be a more attractive alternative for the zeolite than a cluster; in the crystal all atoms interacting with the adsorbate are present and boundary effects are absent. Also, the long-range electrostatic forces of the crystal are included. However, the crystal model does not yield accurate adsorption energies because the crystal calculations on silicon aluminum zeolites are restricted to a minimal basis set, for the electron correlation only density functional estimates are available [12] and, in the absence of the implementation of analytical gradients geometry optimizations are elaborate.

With the embedded cluster method the advantage of the crystal model can be combined with the computational advantages of the cluster approximation. In this model, the zeolite crystal is represented by a zeolite cluster embedded in a correction potential. This potential is the long-range electrostatic potential of the crystal minus the electrostatic potential of the boundary of the cluster [3]. For a cluster having the boundary errors relatively far from the adsorption site the adsorption energies from the crystal are reproduced within a few kJ/mol with the embedded cluster method.

Although the adsorption energies of NH_3 and NH_4^+ in acidic chabazite have been calculated with the embedded cluster method with a mixed basis set, a basis set having a good basis set on the atoms of the acidic site and a minimal basis set on the boundary of the cluster, and a limited geometry optimization they have not yet been calculated satisfactory because in these calculations the BSSE was ignored and electron correlation was absent [4]. At least of the same importance is that in these calculations NH_4^+ was not optimally coordinated to the lattice.

Here, we present calculations of the adsorption energies of NH_3 and NH_4^+ meeting all the requirements. We used a mixed basis set on an embedded cluster. The CPC is applied and electron correlation is included through second order Møller Plesset perturbation theory [13]. The geometry of the cluster and the adsorbate is optimized partially and different orientation of NH_4^+ towards the lattice have been studied. We studied the effect of the deficiencies in the calculation, for example the basis set and the limited geometry optimization, on small clusters. From these comparisons we corrected the calculated heats of adsorption. After correction the heats of adsorption were accurate enough to be compared to the experimental value. Our calculations allowed us to obtain detailed information on the proton transfer and the interaction of NH_4^+ with the zeolite wall.

Methods and Computational details

We studied the adsorption of NH_3 and NH_4^+ in the shell-model optimized acidic chabazite (Chapter 4, fig. 4.1a). The chabazite is described with the embedded cluster method, as introduced in Chapter 5. The embedded and non-embedded Medium Cluster, as described in Chapter 4, fig. 4.4, is used to adsorb NH_3 and NH_4^+ . The charge distributions of the host cluster and host crystal are calculated at the RHF-level, using a minimal STO-3G basis set [14]. The atomic multipoles of the HOSiAlO_6 -group, both in the crystal and the cluster, are ignored in the calculation of the correction potential. It is not added to the complete cluster but only to the atoms of the HOSiAlO_6 group and the adsorbate. With this cluster, the embedded cluster method reproduces the adsorption energies of the corresponding zeolite crystal within a few kJ/mol [3].

The geometry of a part of the cluster, as well as of the adsorbate, is optimized

quantum-chemically at the RHF-level to allow for the relaxation of the lattice. We did not optimize the cluster completely for several reasons. Since we used the embedded cluster method to describe the chabazite, the cluster must fit into the chabazite. Therefore, the boundary must be left unmodified in a geometry optimization. In this way, structural information of the chabazite is passed onto the acidic site and the adsorbate. Thus, the acidic site is not an arbitrary acidic site but the acidic site in a chabazite. An additional advantage of a partial optimization is that the geometry optimization converges more rapidly; in some cases already a partial optimization took several months of computing time on an Alliant FX/2816.

The result of a partial optimization depends on the group of atoms being optimized. To estimate this dependence we compared the results of the optimization of two different groups of atoms. In group A, we optimized the positions of the atoms of the adsorbate, of the acidic OH-group, of the aluminum atom bonded to it and of the oxygen atoms bonded to the aluminum atom. In group B, the position of the atoms of the adsorbate, and of the atoms of the acidic HOSiAl-group were optimized. As another estimate for the effect of the partial optimization we compared the adsorption energies on a completely optimized $\text{Al}(\text{OH})_3\text{H}$ cluster, a cluster used in Ref. [2], and the same cluster in which the geometry is kept fixed in the geometry found with the partial optimization of the chabazite cluster.

The adsorption energy is calculated in two steps. First, the geometry of the cluster-adsorbate complex and of the cluster is optimized at the RHF-level. With this optimization the zeolite can adjust itself to the adsorbate. For group A, the geometry optimization started with NH_4^+ bonding with three hydrogen bonds towards the oxygen atoms of the AlO_4^- tetrahedron, a structure found favorable in small cluster calculations [2]. To keep NH_4^+ coordinated with three hydrogen bonds, the N-H bond lengths were kept fixed at the experimental bond length of 1.03 Å [15] and three dihedral angles H-N-Al-O, determining the coordination of NH_4^+ towards the zeolite lattice were kept fixed at zero. Starting from this optimized structure a second one was generated by reoptimizing it with the dihedral angles no longer fixed, and fixing only one N-H distance at 1.03 Å. Finally, a third structure was generated from the second one without any constraints on the adsorbate. For group B only one optimization, without any constraint on the adsorbate, was carried out.

From the structures optimized at the RHF-level four extra points for a intermolecular potential energy curve were generated by taking two distances longer and two distance shorter than the equilibrium intermolecular distance at the RHF-level. This energy curve is calculated at the MP2-level, applying the CPC and embedding the cluster. The distance selected as an appropriate intermolecular distance depends on the coordination of the adsorbate. As in small cluster calculations we choose the Al...N distance for the triply bonding NH_4^+ [2], and the O-N distance in the singly bonding and hydrogen bonding structures [1].

In the Results and Discussion section we will discuss both the adsorption energy of NH_4^+ and the interaction energy of NH_4^+ . These terms have the same meaning as in Chapter 2 of this thesis. The interaction energy of NH_4^+ is the interaction energy between NH_4^+ and the zeolite anion i.e. the energy of the NH_4^+ -cluster complex with respect to the energy of NH_4^+ and the zeolite anion in the geometry they have in the complex. The adsorption energy of NH_4^+ is the energy of the NH_4^+ -cluster complex with respect to the

energy of NH_3 and the energy of the OH-form of the cluster.

For the geometry optimization as well as for the calculation of the interaction energies we used a mixed basis set. In this basis set the silicon and aluminum atoms have a 6-31G(d) basis set [16,17]. The oxygen atom of the acidic group has a 6-311G(d) basis set [18], all other oxygen atoms have a 6-31G basis set [19]. The acidic proton and the protons of the adsorbate have a 3-1G basis set [20]. The nitrogen atom in the adsorbate has a 6-31G(d) basis set [19,21]. All other atoms have a standard minimal STO-3G basis set [14]. This mixed basis set produces the adsorption energy of NH_3 with an error of 10 kJ/mol and underestimates the adsorption energy of NH_4^+ with 40 to 50 kJ/mol [1,4,22,23].

Results and Discussion

The results of the partial geometry optimizations for group A are shown in the figs. 7.1 to 7.4. Some of the geometrical parameters of the optimized structures are given in Table I. In the first optimization of group A NH_4^+ was kept triply bonding. Therefore, we refer to it as the triply bonding or the triple structure. In the chabazite calculations presented here, the coordination between the NH_4^+ and the AlO_4^- tetrahedron of the lattice is not as regular and well defined as the coordination between NH_4^+ and the $\text{Al}(\text{OH})_3\text{H}^-$ cluster [2]. On the small cluster all OH-distances, i.e. the distances between the oxygen atoms of the lattice and the proton of the adsorbate, were 1.85 Å. Here, the NH_4^+ -ion has one short O-H distance, comparable to an O-H bond of a NH_4^+ bonding with one hydrogen towards a OSiAlH_6^- cluster [1]. The other O-H bonds are much longer.

The result of the further optimization of the triple structure without constraints on the dihedral angles determining the coordination, is called the singly bonded or single structure because it shows some similarities with NH_4^+ singly bonded on a small cluster; also here, the N-H-O angle is close to 180° [1]. During the optimization of the triple structure, resulting in the single structure, NH_4^+ is rotated around the NO-axis, the oxygen atom on this axis being the bridging oxygen atom, the atom on which the acidic proton was bonded originally. Doing so, it increases its interaction with oxygen atoms of the eight ring other than those of the AlO_4^- tetrahedron, keeping constrained the distance with the bridging oxygen atom. Although this structure is called the single structure there is a relatively small difference in coordination with this lattice between this structure and the triple structure. The coordination is not changing as dramatically as in the small cluster calculations where the clusters and their symmetry were chosen to describe a certain coordination. The names of the structures are a bit misleading, because, in the zeolite, the differences between the singly and triply coordinated NH_4^+ are not as large as in the cluster calculations. As we have seen in the previous paragraph, the lattice does not deform to such an extent that NH_4^+ can be perfectly doubly or triply bonding as in the small cluster and, on the other hand, in the singly bonded structure NH_4^+ is interacting with other oxygen atoms in the zeolite channel.

The result of reoptimization of the singly bonded structure, without any constraints on the adsorbate, is a structure in which the proton has been transferred to the zeolite and NH_3 is hydrogen bonding to the zeolite OH group. Also the optimization of group B, in which the atoms of the HOSiAl -group are optimized without any constraint on the adsorbate resulted in a hydrogen bonding NH_3 . Apparently, at the RHF-level NH_4^+ is not

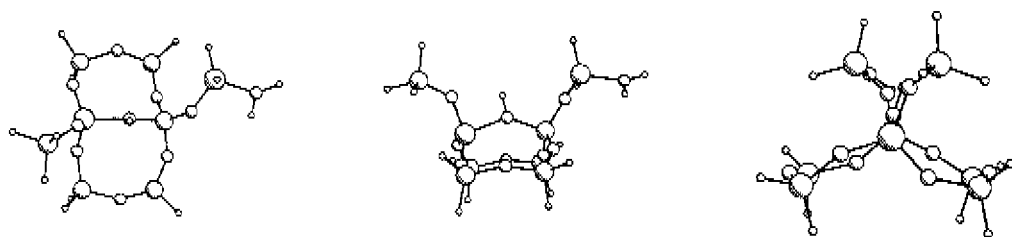


Figure 7.1. The OH-form of the cluster. The structure is shown from three mutually perpendicular directions.

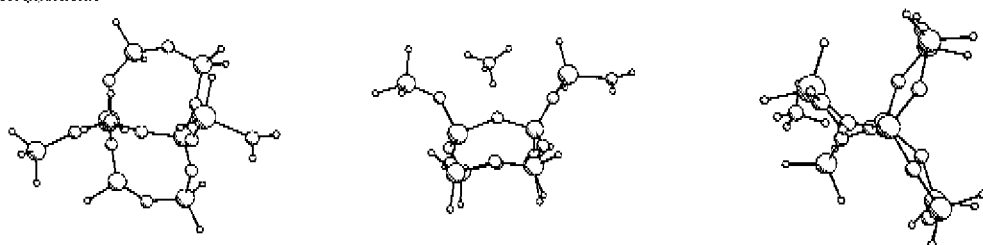


Figure 7.2. The triple structure. The dihedral angles H-N-Al-O, determining the coordination of NH_4^+ , and the N-H distances were kept fixed during the optimization. The structure is shown from three mutually perpendicular directions.

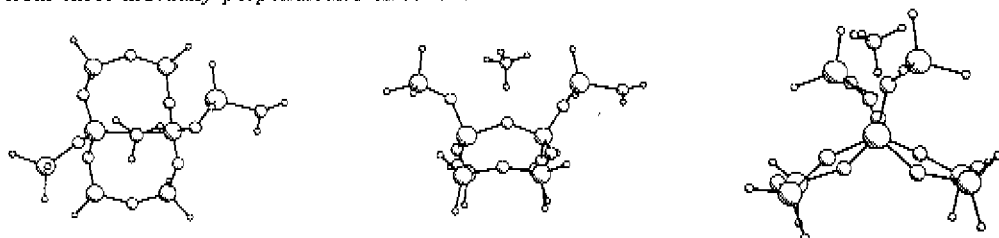


Figure 7.3. The singly bonded structure, the result of further optimization of the triply bonded structure. The N-H distance of the proton bonding to the bridging oxygen atom was kept fixed. The structure is shown from three mutually perpendicular directions.

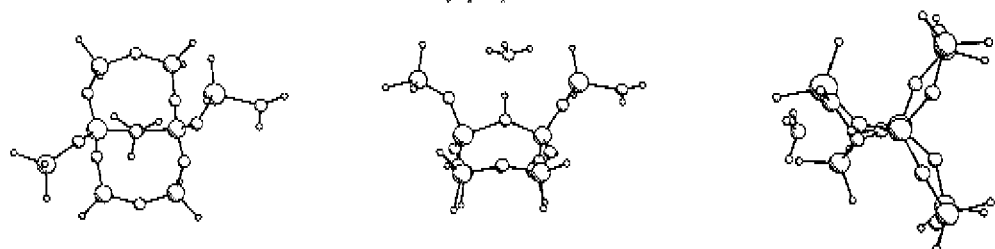


Figure 7.4. The hydrogen bonding structure. This structure is the result of further optimization of the singly bonded structure without any constraints. The structure is shown from three mutually perpendicular directions.

Table I The geometrical parameters of the OH-form of the cluster (fig. 7.1), for the single and triple bonded structure (figs. 7.2 and 7.3, respectively) and for the hydrogen bonding structure (fig. 7.4). The three shortest O-H distances are tabulated. They are those between the oxygen atoms of the cluster and the protons of the adsorbate. For the hydrogen bonded forms, indicated with an asterisk, the torsion angle H-N-O-Al instead of the torsion angle N-H-Al-O is tabulated. The N-H distances and H-N-H angles in the column of the OH form of group A refer to the parameters of the free NH₃ molecule.

parameter	group A OH-form	group A H-bond	group A triple	group A single	group B OH-form	group B H bond
r_{O-H}	0.96	1.00	1.49	1.50	0.95	1.00
r_{O-H}	-	2.74	2.24	2.45	-	2.76
r_{O-H}	-	3.18	3.77	2.62	-	3.35
r_{N-H}	1.00	1.01	1.03	1.03	-	1.01
r_{N-H}	1.00	1.01	1.03	1.02	-	1.00
r_{N-H}	1.00	1.01	1.03	1.01	-	1.00
r_{N-H}	-	-	1.03	1.01	-	-
r_{O-Al}	1.87	1.84	1.77	1.77	1.91	1.88
r_{O-Si}	1.68	1.67	1.62	1.61	1.70	1.67
$\angle Al-O-N$	-	112	102	107	-	112
$\angle H-N-H$	114	111	112	110	-	112
$\angle H-N-H$	114	113	105	108	-	110
$\angle H-N-H$	114	114	105	104	-	112
$\angle Si-O-Al$	139	137	141	140	136	136
$\angle N-H-Al-O$	-	34*	0	34	-	20*
$\angle N-H-Al-O$	-	82*	0	47	-	40*
$\angle N-H-Al-O$	-	155*	0	8	-	80*

stable. This is in contrast to our earlier findings, that, if NH₄⁺ can coordinate to more oxygen atoms in the zeolite, it is favorable over hydrogen bonding NH₃ [2]. This may be the result of the absence of diffuse functions on the oxygen atoms in the large cluster calculation presented here, or of the decreased interaction between the zeolite and NH₄⁺ in the chabazite cluster with respect to the small zeolite clusters.

Earlier, the adsorption energies of NH₃ and singly bonded NH₄⁺ were calculated at the SCF and SCF/CPC-level, just optimizing the adsorbate and the OH-group. With this more extended geometry optimization the adsorbates are less stable [4].

The adsorption energies of NH₃ and NH₄⁺ for the various structures are tabulated in Table II. The most accurate adsorption energies are those including electron correlation, the CPC and the long-range electrostatic forces of the crystal. Some important differences between the SCF/CPC/MP2/EMB level and the SCF-level are that, at this level, the adsorption energies of NH₃ and the triple bonding NH₄⁺ are almost equal in energy and that the relative stability of the single and triple structure is reversed. The various quantum chemical methods have a relatively similar effect on the adsorption energies as in the small cluster calculations. However, there are some differences. In the chabazite cluster

Table II The adsorption energies of NH_3 and NH_4^+ , for the single structure (fig. 7.3), the triple structure (fig. 7.2) and the hydrogen bonded structure (fig. 7.4), the latter for the optimization of group A and group B. The adsorption energies are calculated at the RHF-level and at the MP2-level with and without the CPC and for the embedded cluster (EMB) and for the non-embedded cluster. The adsorption energies are in kJ/mol, intermolecular distances in Å.

Structure	NH_3 (A)		NH_4^+ single (A)		NH_4^+ triple (A)		NH_3 (B)	
	ΔE	R_{NO}	ΔE	R_{NO}	ΔE	R_{AIN}	ΔE	R_{NO}
SCF	-77	2.72	-38	2.52	-31	3.31	-87	2.68
SCF/CPC	-31	2.80	6	2.55	-5	3.52	-41	2.76
SCF/MP2	-98	2.68	-69	2.52	-67	3.32		
SCF/CPC/MP2	-36	2.80	-9	2.56	-26	3.53		
SCF/EMB	-92	2.71	-64	2.55	-48	3.31	-99	2.67
SCF/CPC/EMB	-45	2.77	-21	2.59	-28	3.55	-52	2.74
SCF/MP2/EMB	-113	2.66	-94	2.55	-84	3.32		
SCF/CPC/MP2/EMB	-51	2.78	-36	2.60	-50	3.55		

calculations the effect of the CPC is much larger [1,2]. Already at the RHF-level it is very large and at the MP2-level the largest part of the interaction energy appears to be BSSE. The effect of the electron correlation, if the CPC is applied, is comparable to that of the small clusters [1,2]. It stabilizes NH_4^+ because it stabilizes the anionic lattice, thus decreasing the proton affinity. It stabilizes both NH_3 and NH_4^+ because a part of the Van der Waals energy is included. The effect of the embedding is almost the same as found in earlier calculations, in which the geometry of the cluster and the adsorbate were not optimized [3,4].

There are two reasons for the BSSE being larger than in the small cluster calculations. First, the basis set is smaller than in the small cluster calculations. On comparing different basis sets on the small clusters we saw that a smaller basis set increases the BSSE [1]. Second, the cluster is much larger, this implies that there are more atoms providing orbitals that can be used by the interacting particles, the adsorbate and the zeolite cluster, to lower their energy, thus increasing the BSSE [5,6]. Therefore, adsorption energies for systems as described here must be calculated with the use of the CPC.

The adsorption energy of NH_3 is 10 kJ/mol less than on the small cluster, the adsorption energies of NH_4^+ shows much larger deviations. We will discuss two causes for the differences in adsorption energy between the calculations described here and the small cluster calculations: the smaller basis set and the difference in coordination. Here, we will not discuss the differences in adsorption energy caused by the poor covalent description by the small cluster as found in Ref. [7]. To study the effect of the basis set we repeated the calculations of NH_4^+ triply coordinated on a $\text{Al}(\text{OH})_3\text{H}^-$ cluster as in Ref. [2] with the basis set used in this paper. The geometry of the $\text{NH}_4^+ \cdots \text{Al}(\text{OH})_3\text{H}^-$ complex and the $\text{Al}(\text{OH})_3\text{H}_2$ cluster were fully geometry optimized. The N-H distances and the dihedral angles H-N-Al-O, determining the coordination were kept fixed as in the chabazite cluster calculation. The first restriction was also imposed in the previous cluster calculations.

The result of this optimization is shown in fig. 7.5. The geometry is similar to that found with the larger basis set although slightly less regular because of the different basis sets on the oxygen atoms in the basis set used in this paper. With the basis set used in Ref. [2] the O-Al-O angles were 101° , here they were 100° and two times 101° . The OH-distances were 1.79 \AA with the large basis set and were 1.78 \AA and two times 1.73 \AA with the mixed basis set used here. The longer distance corresponds to the oxygen with the larger basis set. The adsorption energies at the SCF/MP2/CPC level with the mixed basis set was -85 kJ/mol , about 30 kJ/mol less than with the large basis set [2]. Thus, one of the reasons for the decreased stability of the NH_4^+ is the lower quality of the basis set.

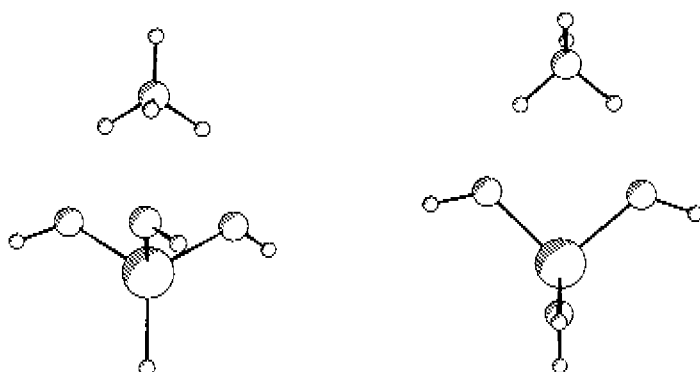


Figure 7.5. The difference in coordination between the fully optimized $\text{NH}_4^+ \cdots \text{Al}(\text{OH})_3\text{H}^-$ complex and the same complex with the AlO_3 part kept fixed to the geometry found with the optimization of the triple structure. As in the optimization of the triple structure the N-H distances and the dihedral H-N-Al-O determining the coordination were kept fixed. On the left Figure 7.5a) the fully optimized structure and on the right Figure 7.5b) the structure in which the AlO_3 part is kept fixed.

Another reason for the decreased stability of NH_4^+ is the decreased interaction between NH_4^+ and the zeolite lattice, caused by the less optimal and less regular coordination. In the small cluster the interaction between the cluster and NH_4^+ is enlarged by directing the oxygen atoms towards NH_4^+ . The O-Al-O angles of the oxygen atom directing towards the NH_4^+ are equal to 101° , and 95° in the $\text{Al}(\text{OH})_3\text{H}^-$ and $\text{Al}(\text{OH})_2\text{H}_2^-$ cluster respectively. In the chabazite cluster the O-Al-O angles of the AlO_4 -tetrahedron are 94° , 113° and 114° . The O-Al-O angle of the two oxygen atoms with the shortest O-H distance is 94° . The Al-O distances in the chabazite cluster are a little bit shorter than in the small cluster; 1.76 , 1.72 , 1.70 and 1.69 \AA in the chabazite cluster and 1.78 , 1.73 , 1.73 \AA in the fully optimized $\text{Al}(\text{OH})_2\text{H}_2^-$ cluster.

It is an important question whether the partial optimization makes the zeolite appear to be too rigid, or whether the coordination is described well in the chabazite and the flexibility of the zeolite, and thus the coordination, is overestimated in the completely geometry optimized small clusters. In order to answer this important question we compared

the loss in interaction energy by comparing the interaction energy of a fully geometry optimized $\text{Al}(\text{OH})_3\text{H}$ cluster and the same cluster in which the AlO_3 part is kept fixed in that of the triple structure. Furthermore, we estimated the interaction energy that could be gained by a more complete geometry optimization of the chabazite cluster.

We made an estimate of the loss of the interaction energy as a result of the decreased coordination by repeating the optimization of NH_4^+ on the $\text{Al}(\text{OH})_3\text{H}^-$ cluster keeping the AlO_3 part fixed in the geometry found with the optimization of the triple structure, fig. 7.5b, and comparing the interaction energy to that of the fully optimized $\text{Al}(\text{OH})_3\text{H}^-$ cluster, fig. 7.5a. Because of the less optimal coordination for the structure in which the AlO_3 part is kept fixed the interaction energy between NH_4^+ and the zeolite cluster is 36 kJ/mol less at the RHF-level. The decreased interaction energy is a result of the less optimal coordination.

The decreased coordination may be caused by the partial optimization of the chabazite cluster, making the zeolite appear to rigid. In a more extended optimization the coordination may be improved because the silicon atoms can also be displaced. The extra interaction that can be gained maximally by the displacement of the silicon atoms in a more extended geometry optimization is 36 kJ/mol, the difference in interaction energy of the NH_4^+ between the fully optimized $\text{Al}(\text{OH})_3\text{H}^-$ cluster and the same cluster in which the AlO_3 part is kept fixed in the triple geometry. This 36 kJ/mol is an upper bound because first, by increasing the interaction with the aluminum tetrahedron the interaction with the other parts of the zeolite is decreased, and second, and probably more important, is that to increase the interaction, the zeolite lattice has to be deformed. The deformation energy has to be subtracted from the interaction energy that is gained.

We made a rough estimate of the deformation energy required to obtain the optimal coordination between the NH_4^+ and the zeolite lattice. The deformation energy can be split into two parts. The first is the extra deformation of the AlO_4 tetrahedron, the second is the displacement of the silicon atoms bonded to this tetrahedron to accommodate the deformed tetrahedron. After all, the extra interaction energy should come from the displacements of these silicon atoms because in the partial optimization the atoms in the AlO_4 tetrahedron were already free to move. The deformation energy of the AlO_3 part is easy to estimate as the difference between the energy of the $\text{Al}(\text{OH})_3\text{H}^-$ clusters in fig. 7.5a and 7.5b; this is 7 kJ/mol. The deformation energy needed for the displacement of the silicon atoms is roughly estimated from the deformation of small clusters. We estimated the deformation of the Al-O and Si-O stretching and for the Al-O-Si bending on a OSiAlH_6^- cluster and the Si-O-Si bending on a OSi_2H_6 cluster. The stretching of the Al-O and Si-O bonds by 0.05 Å, necessary for the optimal configuration, costed 2.1 and 5.7 kJ/mol respectively. The bending of the angles by 10° costed 1.7 and 0.8 kJ/mol respectively. Thus, it seems more favorable to displace the silicon atoms by the bending of the Si-O-Al and Si-O-Si angles, although some stretching will also appear. For each displaced silicon atom two Si-O-Si angles and one Si-O-Al angle must be bended. The displacement of one silicon atom costs 4 kJ/mol, and thus, the displacement of three silicon atoms will cost 12 kJ/mol. Thus, in this simple model, not including the stretching of bonds, apart from those in the AlO_3 part, the deformation energy is 19 kJ/mol (7 + 12).

The adsorption energy that can maximally be gained by a more extended geometry

optimization is 17 kJ/mol. From this number we should also subtract the decrease in interaction between NH_4^+ and the other atoms in the eight-ring as a result of the higher coordination to the aluminum tetrahedron and the deformation energy as a result of the stretching of the bonds not taken into account in the simple model to calculate adsorption energies. This means the adsorption energy that can be gained maximally by a more extended optimization is about 10 kJ/mol.

Another estimate for the effect of the partial instead of a full optimization can be made from the differences in adsorption energy of NH_3 for group A and B since the adsorption energy was calculated for two different partial optimizations. In group A the HOAlO_3 group was optimized and in group B the HOSiAl -group. The difference in adsorption energy of NH_3 is 10 kJ/mol at the SCF-level. This is a relatively large difference and the partial optimization does not seem valid but, we should keep in mind that one of the differences between group A and group B is the optimization of the position of the silicon atom, an atom close to the adsorbate in the hydrogen bonded structure. The effect of further enlargement of the group of atoms to be optimized will be smaller than 10 kJ/mol. Although, for the triple structure, the interaction energy, is more dependent on the geometry an enlargement of the group of atoms to be optimized will not have a larger effect on the interaction energy than for NH_3 . Already all the atoms close to the NH_4^+ , i.e. the AlO_4 group are optimized. The estimation of the effect of a more extended optimization of is 10 kJ/mol.

In our cluster calculation, where the geometry is partially optimized, the zeolite does not seem to be too rigid. For example, the difference in cell constants and average T-O bond lengths is 1 or 2 % for the H-form and the NH_4^+ -form of Zeolite Rho [24,25]. These numbers do not deviate significantly from the deformations we found. Thus, the partial optimization seems to be valid and we can conclude that the coordination of NH_4^+ is lower in the zeolite lattice because the atoms are less free to move than in a cluster since they are bonded in a zeolite lattice. In a cluster in which the geometry is completely optimized without passing any information from the lattice to the cluster, the interaction energy is overestimated. Cluster calculations in which the cluster is completely optimized and in which the coordination between the adsorbate and the cluster is important and strongly dependent on the deformation of the zeolite cluster, as in Refs. [2,26-34] overestimate the stability of the adsorbate by about 20 kJ/mol.

From the comparison of the various quantum chemical methods, we can question the value of the geometry optimizations at the SCF-level. First, the geometry is optimized at a level that, because of the absence of electron correlation, underestimates the stability of NH_4^+ . Therefore, constraints must be used in the optimization of the NH_4^+ . The effect of the constraints on the geometry and the interaction energy is relatively small, because the main part of the effect of the optimization on the interaction energy lies in the relaxation of the lattice and not in the deformation of NH_4^+ . The absence of the effect of the embedding on the geometry is negligible, the internal geometry of the lattice and the adsorbate cluster distances are almost independent of the embedding [3,4]. A larger problem is that for a cluster like the chabazite cluster, the potential energy surface is quite complicated and the difference between the RHF and the MP2 potential energy surfaces will be larger than in the case of the small clusters. The largest problem of the optimization at the SCF-level are

the BSSE-effects. We tried to avoid the shortcomings of the optimization at the RHF-level by calculating the interaction from an appropriate potential energy curve, and calculating the adsorption energy at the SCF/CPC/MP2/EMB level. Even so, the optimization of the geometry at the SCF-level will certainly cause some errors in the geometry and the adsorption energy. It is difficult to give an estimate for the error in the adsorption energies caused by the optimization of the geometry at the RHF-level; it will however not be much larger than 10 kJ/mol.

By making an estimate of the deficiencies and the errors in the calculation we can produce a value for the adsorption energies that can be compared to the experimental heat of adsorption. The largest deficiency is the limited size of the basis set, it does not have a large effect on the adsorption energy of NH_3 [1], but the adsorption energy of NH_4^+ is strongly affected by the deficiencies of the basis set. The adsorption energy of NH_4^+ is underestimated by 40 to 50 kJ/mol [1,4,22,23]. Other errors are caused by the limited geometry optimization and the optimization at the RHF-level. Together, they will give an error in the adsorption energy between 10 and 20 kJ/mol. Also we should add some extra Van der Waals energy. With the cluster and this basis set not all the Van der Waals energy between the zeolite and the adsorbate is obtained. From the adsorption energy of CH_4 , having the same number of electrons as NH_3 and NH_4^+ in zeolite X [35], the missing Van der Waals energy is estimated to be 10 kJ/mol. This Van der Waals energy stabilizes both NH_3 and NH_4^+ . If we take into account the errors and the deficiencies of the calculation for the adsorption energy of NH_3 will be about -70 ± 10 kJ/mol. The adsorption energy of NH_4^+ , in the favorable triple structure, will be about -120 ± 15 kJ/mol. The latter compares quite well with the experimental heat of adsorption of -130 kJ/mol [36].

Conclusion

We studied the adsorption of NH_3 and NH_4^+ in zeolites using an accurate quantum chemical method. The calculations were performed with the embedded cluster method using a mixed basis set, including electron correlation and applying the counterpoise procedure. The geometry of the adsorbate, and the part of the cluster that is interacting with it, was optimized. We only optimized a part of the cluster since, by keeping the boundary of the cluster fixed, the cluster can be embedded and structural information is passed from the zeolite to the cluster.

The adsorption energy of NH_3 and NH_4^+ , in a conformation with a high coordination towards the zeolite lattice, are almost equivalent: -51 and -50 kJ/mol, respectively. If the calculated adsorption energies are corrected for their errors, as estimated from small cluster calculations, such as the deficiencies in the basis set, the incomplete Van der Waals energy, the only partial optimization and the errors made with the optimization at the RHF-level, the adsorption energies become -70 ± 10 kJ/mol and 120 ± 15 kJ/mol respectively. The latter compares quite well with the experimental heat of adsorption.

The comparison between these embedded cluster calculations, in which the geometry is only partially optimized such that the cluster still fits into a real zeolite, and cluster calculations in which the geometry is completely optimized, shows that in the latter the effect of the optimization of the geometry is overestimated. Therefore, in adsorption processes in which the coordination between the adsorbate and the lattice is crucial and the

geometry is completely optimized, the stability of the adsorbate is overestimated by about 20 kJ/mol. Because of this, the cluster should contain structural information from the zeolite and should not be an arbitrary zeolitic cluster.

The counterpoise correction to correct for the BSSE is very important in the calculation of the adsorption energies, because of the basis set that was used and the size of the zeolite clusters, the BSSE can be more than 40 kJ/mol at the SCF-level and more than 60 kJ/mol at the MP2-level. Electron correlation stabilizes both NH_3 and NH_4^+ because it includes the Van der Waals energy, it decreases the difference in adsorption energy between NH_3 and NH_4^+ because it stabilizes the zeolite anion. The embedding of the cluster stabilizes both adsorbates by 10 to 20 kJ/mol.

References

- [1] E. H. Teunissen, F. B. van Duijneveldt and R. A. van Santen, *J. Phys. Chem.* **96**, 366 (1992), *Chapter 2 of this thesis*.
- [2] E. H. Teunissen, R. A. van Santen, A. P. J. Jansen and F. B. van Duijneveldt, *J. Phys. Chem.* **97**, 203 (1993), *Chapter 3 of this thesis*.
- [3] E. H. Teunissen, A. P. J. Jansen, R. A. van Santen, R. Orlando and R. Dovesi *submitted to J. Chem. Phys.*, *Chapter 5 of this thesis*.
- [4] E. H. Teunissen and A. P. J. Jansen *submitted to the Intern. J. Quantum Chem.*, *Chapter 6 of this thesis*.
- [5] S. F. Boys and F. B. Bernardi, *Mol. Phys.* **19**, 553 (1970).
- [6] J. H. van Lenthe, J. G. C. M. van Duijneveldt-van de Rijdt and F. B. van Duijneveldt, *Adv. in Chem. Phys.* **79**, 521 (1987).
- [7] E. H. Teunissen, C. Roetti, C. Pisani, A. J. M. de Man, A. J. P. Jansen, R. Orlando, R. A. van Santen and R. Dovesi, *Mod. Simul. Mater. Sci. Eng.* **2**, 921 (1994), *Chapter 4 of this thesis*.
- [8] C. Pisani, R. Dovesi and C. Roetti, *Hartree-Fock Ab-initio Treatment of Crystalline Systems*, *Lecture Notes in Chemistry* **48** (Springer Verlag, Berlin, 1988)
- [9] C. Pisani and R. Dovesi, *Int. J. Quantum Chem.* **17**, 501 (1980).
- [10] R. Dovesi, C. Pisani, C. Roetti and V. R. Saunders, *Phys. Rev. B* **28**, 5781 (1983).
- [11] R. Dovesi, *Int. J. Quantum Chem.* **29**, 1755 (1986).
- [12] R. Dovesi, V. R. Saunders and C. Roetti, *Crystal 92 Users's Manual*, (Gruppo di Chimica Teorica, Università di Torino and SERC Laboratory, 1992).
- [13] C. Møller and M. S. Plesset, *Phys. Rev.* **46**, 618 (1934).
- [14] W. J. Hehre, R. F. Stewart and J. A. Pople, *J. Chem. Phys.* **51**, 2657 (1969).
- [15] J. A. Ibers and D. P. Stevenson, *J. Chem. Phys.* **28**, 929 (1958).
- [16] M. M. Franci, W. J. Pietro, W. J. Hehre, J. J. Binkley, M. S. Gordon, D. J. DeFrees and J. A. Pople, *J. Chem. Phys.* **77**, 3654 (1982).
- [17] M. S. Gordon, J. S. Binkley, J. A. Pople, W. J. Pietro and W. J. Hehre, *J. Am. Chem. Soc.* **104**, 2797 (1982).
- [18] R. Krishnan, J. S. Binkley, R. Seeger and J. A. Pople, *J. Chem. Phys.* **72**, 650 (1980).
- [19] W. J. Hehre, R. Ditchfield and J. A. Pople, *J. Chem. Phys.* **56**, 2257 (1972).
- [20] R. Ditchfield, W. J. Hehre and J. A. Pople, *J. Chem. Phys.* **54**, 724 (1971).
- [21] P. C. Hariharan and J. A. Pople, *Theor. Chim. Acta.* **28**, 213 (1973).

- [22] D. J. DeFrees and A. D. McLean, *J. Comput. Chem.* **7**, 321 (1986).
- [23] K. Szalawich, S. J. Cole, W. Kolos and R. J. Bartlett, *J. Phys. Chem.* **89**, 3662 (1988).
- [24] L. B. McCusker, *Zeolites* **4**, 51 (1984).
- [25] D. R. Corbin, L. Abrams, G. A. Jones, M. M. Eddy, W. T. A. Harrison, G. D. Stucky and D. E. Cox, *J. Am. Chem. Soc.* **112**, 4821 (1990).
- [26] E. Kassab, J. Fouquet, M. Allavena and E. M. Evleth, *J. Phys. Chem* **97**, 9034 (1993).
- [27] A. S. Medin, V. Yu. Borovkov, V. B. Kazansky, A. G. Pelmenschikov and G. M. Zhidomirov, *Zeolites* **10**, 668 (1990).
- [28] A. G. Pelmenschikov, G. Morosi and A. Gamba, *J. Phys. Chem* **96**, 2241 (1992).
- [29] A. G. Pelmenschikov and R. A. van Santen, *J. Phys. Chem.* **97**, 10678 (1993).
- [30] A. G. Pelmenschikov, R. A. van Santen, J. Jänchen and E. L. Meijer, *J. Phys. Chem.* **97**, 11071 (1993).
- [31] J. Sauer, H. Horn, M. Häser and R. Ahlrichs, *Chem. Phys. Lett.* **173**, 26 (1990).
- [32] L. R. Sierra, E. Kassab and E. M. Evleth, *J. Phys. Chem.* **97**, 641 (1993).
- [33] I. N. Senchenya and V. B. Kazansky, *Catal. Lett.* **8**, 317 (1991).
- [34] J. Sauer, C. M. Kölmel, J.-R. Hill and R. Ahlrichs, *Chem. Phys. Lett.* **164**, 193 (1989).
- [35] S.-Y. Zhang, O. Talu and D. T. Hayhurst, *J. Phys. Chem.* **95**, 1722 (1991).
- [36] *Chapter1 of this thesis*

Summary and General Conclusions

In this thesis we studied the adsorption of NH_3 in acidic zeolites, the proton transfer from the zeolite to form NH_4^+ and the interaction of NH_4^+ with the zeolite lattice by means of quantum chemical calculations. The aim of the research was twofold. One aim of the study was to obtain detailed information on the adsorption and proton transfer processes. The second aim was to develop a quantum chemical method able to produce accurate adsorption and interaction energies.

The reliability of the quantum chemical model used for the description of the adsorption processes depends on three factors. The first is the quantum chemical method itself, i.e. the way in which the electronic structure is calculated. The second is the geometry of the zeolite and the coordination of the adsorbate. The third is the model used to describe the zeolite, e.g. a crystal or a clusters with a certain shape.

In the first part of the thesis we studied the accuracy of various quantum chemical methods. We described the zeolite with a small cluster, allowing us to use high-quality but computer time consuming methods. We studied the effects of the basis set, the basis set superposition error and electron correlation on the adsorption energy. We compared three different basis sets, a small one, comparable to a split valence basis set with polarization functions, a large one, containing diffuse function on the anionic oxygen atom, and a basis set expected to give adsorption and proton transfer energies within a few kJ/mol of the Hartree-Fock limit. For further calculations we decided to use the large basis set. Although it underestimates the stability of NH_4^+ by about 10 kJ/mol it is still small enough to be used more or less routinely. The adsorption energy of NH_3 is relatively independent of the basis set.

Electron correlation cannot be neglected in the calculation of adsorption energies, it adds about 10 kJ/mol of Van der Waals energy to the adsorption energy of both NH_3 and NH_4^+ and it stabilizes the anionic oxygen atoms formed by the proton transfer also by about 10 kJ/mol. The calculated adsorption energies must be corrected for the basis set superposition error. Without this correction, adsorption energies can be overestimated by 10 kJ/mol at the SCF-level and 20 kJ/mol at the MP2-level if the large basis set is used. For smaller basis sets this error is larger.

The geometry of the zeolite and the coordination between NH_4^+ and the zeolite are important factors in the calculation of adsorption energies. The coordination of NH_3 usually does not cause problems because it is adsorbed linearly onto the acidic OH-group with an adsorption energy of -60 kJ/mol. The coordination of NH_4^+ with the zeolite lattice however, is very important. NH_4^+ bonded to a zeolite cluster with a single hydrogen bond has an adsorption energy of only -15 kJ/mol. NH_4^+ bonded to a zeolite cluster with a high coordination, i.e. with two or three hydrogen bonds, has an adsorption energy of -110 kJ/mol. The high coordination of NH_4^+ with the zeolite lattice stabilizes NH_4^+ and enables proton transfer.

The geometry of the zeolite has a large influence on the adsorption energy. For NH_3 the influence is relatively limited. Optimization of the zeolite cluster, making it more stable and less reactive, decreases the adsorption energy by about 10 kJ/mol. For NH_4^+ the effect is much larger. For the high coordination between NH_4^+ and the zeolite lattice the latter has to deform. On a zeolite of which the geometry is not optimized the adsorption energy

Summary and general conclusions

of a triply bonding NH_4^+ is only -10 kJ/mol. After a geometry optimization, in which the cluster can adjust itself to accommodate NH_4^+ , the adsorption energy is -110 kJ/mol.

After having investigated the various quantum chemical methods we studied the validity of small clusters as a model for the zeolite lattice. We compared the adsorption energies and Mulliken charges of the atoms of the acidic site of four different clusters and a zeolite crystal. It appears that the cluster calculation have two errors. The first are the boundary effects; as a result of the saturation of the dangling bonds with hydrogen atoms the charges of the neighboring atoms are different from their counterparts in the crystal. Consequently, they behave differently towards an adsorbate. To avoid the boundary effects having a large influence on the calculated adsorption energy the saturating hydrogen atoms should be four, or more, bonds away from the adsorption site. If not, an error in the adsorption energy of about 50 kJ/mol can be made. A second disadvantage of the cluster approximation is the absence of the long-range electrostatic forces of the crystal. The effect of these forces on the adsorption energy can be as large as 50 kJ/mol.

Although the crystal offers a much better model for the zeolite, boundary errors are absent and the long-range electrostatic forces are present, crystal calculations do not enable us to calculate accurate adsorption energies because, as a result of the size of the system, we are restricted to use minimal basis sets. Furthermore, geometry optimizations are too elaborate and for the electron correlation only density functional estimates are available.

In search for a satisfactory method to calculate adsorption energies we developed a method offering a good model for the zeolite while keeping the computational advantages of the cluster approximation. We did so by embedding a zeolite cluster in a correction potential. This correction potentials adds the long-range electrostatic forces of the crystal and subtracts the electrostatic potential of the boundary of the cluster. The correction potential is only added to the atoms around the adsorption site. If an appropriate cluster is used, i.e. a cluster having the boundary effects four, or more, bonds away from the adsorption site, the adsorption energies of the crystal are reproduced within a few kJ/mol.

Within the embedded cluster method, we tested the use of mixed basis sets. Such a mixed basis set has a high quality basis set on the atoms around the adsorption site and a minimal basis set on the atoms in the boundary of the cluster. This minimal basis set on the atoms of the boundary is necessary for several reasons. First, there is the restriction that, within the embedded cluster scheme, the atoms on the boundary must have the same basis set and geometry as in the crystal. Second, by using a minimal basis set on the boundary of the cluster the required computer time is reduced. The mixed basis set produces the adsorption energies calculated with a good basis set on all atoms within 10 kJ/mol. It underestimates the adsorption energy of NH_4^+ by about 40 to 50 kJ/mol. The adsorption energy of NH_3 is less dependent on the basis set.

We compared the results of the geometry optimizations performed with the cluster, the embedded cluster and the crystal. It appeared that, although the long-range electrostatic forces have a non-negligible effect on the adsorption energies the effect on the geometry of the acidic site is very small. This is important, because in this way, we can use the geometry of the acidic site found with an optimization of a cluster, for which automatic optimizations using gradients can be used, as a geometry for the embedded cluster for which no such techniques are available.

We calculated the adsorption energy of NH_3 and NH_4^+ on a cluster embedded in a chabazite crystal, using a mixed basis set and a limited optimization of the geometry. The limited geometry optimization stabilizes the adsorbates.

Finally, we calculated the adsorption energy of NH_3 and NH_4^+ on a cluster embedded in a chabazite crystal combining all features important for the calculation of accurate adsorption energies. We used a mixed basis set, corrected for the basis set superposition error, and calculated the contribution of the electron correlation. The geometry of the cluster was partially optimized. Some different coordinations of NH_4^+ with the zeolite lattice were studied. After correction for some of the deficiencies in the calculation, i.e. the error made with the limited size of the basis set, the limited Van der Waals energy and the limited geometry optimization, the adsorption energy of NH_3 was estimated to be -70 ± 10 kJ/mol and the adsorption energy of NH_4^+ , in a conformation having a high coordination with the zeolite lattice, was estimated to be -120 ± 15 kJ/mol. The latter value corresponds well with the experimental heat of adsorption.

From our final calculations we can draw two conclusions:

- We have developed a reliable and generally usable method to calculate adsorption energies of small molecules in zeolites.
- After adsorption of NH_3 in the zeolite proton transfer takes place and NH_4^+ is formed. It is stable because it has a high coordination with the zeolite lattice.

Samenvatting en Algemene Conclusies

In dit proefschrift hebben we de adsorptie van NH_3 in zure zeolieten, de protonoverdracht waarbij NH_4^+ gevormd wordt en de interactie tussen NH_4^+ en het zeolietrooster bestudeerd met behulp van quantumchemische methoden. Het onderzoek had twee doelen. Het eerste was gedetailleerde informatie over de adsorptie- en protonoverdrachtsprocessen te verkrijgen. Het tweede was een quantumchemische methode te ontwikkelen waarmee nauwkeurige adsorptie- en interactieënergieën berekend kunnen worden.

De betrouwbaarheid van een quantumchemisch model dat gebruikt wordt om adsorptieprocessen te beschrijven hangt af van drie factoren. De eerste is de quantumchemische methode zelf, dat wil zeggen de manier waarop de elektronenstructuur berekend wordt. De tweede is de geometrie van het zeoliet en de coördinatie van het adsorbaat. De derde is het model dat gebruikt wordt om het zeoliet te beschrijven, bijvoorbeeld een kristal of een cluster met een bepaalde vorm.

In het eerste deel van het proefschrift hebben we de nauwkeurigheid van diverse quantumchemische methoden bestudeerd. We beschreven het zeoliet met een klein cluster waardoor we tijdrovende methoden van hoge kwaliteit konden gebruiken. We bestudeerden de effecten van de basisset, de basisset-superpositiefout en elektronencorrelatie op de adsorptieënergie. We hebben drie verschillende basissets met elkaar vergeleken: een kleine, vergelijkbaar met een split-valence-basisset met polarisatiefuncties, een grote met diffuse functies op het anionische zuurstofatoom en een basisset waarvan verwacht kan worden dat ze adsorptie- en protonoverdrachtsenergieën binnen enkele kJ/mol van de Hartree-Fock-limiet levert. We besloten om voor verdere berekeningen de grote basisset te gebruiken. Hoewel ze de stabiliteit van NH_4^+ met zo'n 10 kJ/mol onderschat is ze klein genoeg om min of meer routinematig gebruikt te worden. De adsorptieënergie van NH_3 is relatief onafhankelijk van de gebruikte basisset.

Electronencorrelatie kan niet verwaarloosd worden bij de berekening van adsorptieënergieën omdat het ongeveer 10 kJ/mol Van der Waals-energie toevoegt aan de adsorptieënergieën van NH_3 en NH_4^+ . Bovendien stabiliseert het het anionische zuurstofatoom dat gevormd wordt bij de protonoverdracht met ongeveer 10 kJ/mol. De berekende adsorptieënergieën moeten gecorrigeerd worden voor de basisset-superpositiefout omdat zonder deze correctie adsorptieënergieën overschat worden met 10 kJ/mol op het SCF-niveau en met 20 kJ/mol op MP2-niveau. Bij het gebruik van kleinere basissets worden deze overschattingen groter.

De geometrie en de coördinatie tussen NH_4^+ en het zeoliet zijn belangrijke factoren bij de berekening van adsorptieënergieën. De coördinatie van NH_3 geeft meestal geen problemen omdat het lineair geadsorbeerd is op de zure OH-groep met een adsorptie-energie van -60 kJ/mol. De coördinatie van NH_4^+ met het zeolietrooster daarentegen is zeer belangrijk. NH_4^+ gebonden aan het zeolietrooster met een enkele waterstofbrug heeft een adsorptieënergie van slechts -15 kJ/mol. NH_4^+ gebonden aan het rooster met een hoge coördinatie, dat wil zeggen met twee of drie waterstofbruggen, heeft een adsorptieënergie van -110 kJ/mol. De hoge coördinatie van NH_4^+ met het zeoliet stabiliseert NH_4^+ en maakt protonoverdracht mogelijk.

De geometrie van het zeoliet heeft een grote invloed op de adsorptieënergie. Voor NH_3 is deze invloed vrij beperkt. Door optimalisatie wordt het zeolietcluster stabiel en minder

reactief, de adsorptieënergie vermindert daardoor met ongeveer 10 kJ/mol. Voor NH_4^+ is het effect veel groter. Het zeolietrooster moet zich vervormen om een hoge coördinatie met het NH_4^+ mogelijk te maken. Op een zeoliet waarvan de geometrie niet vervormd is, is de adsorptieënergie van drievoudig gebonden NH_4^+ slechts -10 kJ/mol. Als het rooster de gelegenheid krijgt om zich, door middel van een geometrieoptimalisatie, aan te passen aan het NH_4^+ dan is de adsorptieënergie -110 kJ/mol.

Nadat we de diverse quantumchemische methoden onderzocht hadden hebben we de geldigheid van kleine clusters als model voor een zeoliet bestudeerd. We hebben de adsorptieënergie en Mulliken ladingen van de atomen van de zure groep van vier verschillende clusters en een kristal onderzocht. Het blijkt dat de clusterberekeningen twee fouten hebben. De eerste zijn de randeffecten; als gevolg van de verzadiging van de verbroken bindingen met waterstofatomen zijn de ladingen van de aanliggende atomen verschillend van hun equivalenten in het kristal. Daardoor gedragen ze zich ook anders tegenover adsorbaten. Om te voorkomen dat de randeffecten een grote invloed hebben op de berekende energieën moeten de waterstofatomen minstens vier bindingen van het adsorbaat verwijderd zijn. Een tweede nadeel van de clusterbenadering is de afwezigheid van de elektrostatische lange-dracht interacties van het kristal. Het effect van deze interacties op de adsorptieënergieën kan 50 kJ/mol zijn. Hoewel het kristal een beter model voor het zeoliet is omdat de randeffecten afwezig zijn en de elektrostatische lange-dracht-interacties aanwezig zijn, leveren de kristalberekeningen geen nauwkeurige adsorptieënergieën omdat we door de grootte van het systeem alleen minimale basissets kunnen gebruiken. Verder zijn geometrie optimalisaties te bewerkelijk en zijn er alleen dichtheidsfunctionaal-schattingen voor de elektronencorrelatie beschikbaar.

Op zoek naar een bevredigende methode om adsorptieënergieën te berekenen hebben we een methode ontwikkeld die een goed model voor het zeoliet levert terwijl de rekentijd nauwelijks meer is dan die van een de clusterbenadering. Dit hebben we bereikt door een zeolietcluster in te bedden in een correctiepotentiaal. Deze correctiepotentiaal zet de elektrostatische lange-dracht-interacties van het kristal over het cluster en corrigeert voor het elektrostatische gedeelte van de randeffecten. De correctiepotentiaal wordt alleen over de atomen van de zure groep en het adsorbaat toegezet. Als een goed gekozen cluster gebruikt wordt, dat wil zeggen de met waterstof verzadigde bindingen zitten tenminste vier bindingen van de zure site af, dan reproduceert het ingebedde cluster de adsorptieënergieën van het kristal binnen enkele kJ/mol.

Binnen deze ingebedde clustermethode hebben we het gebruik van gemengde basissets getest. Zo'n gemengde basisset heeft een basisset van hoge kwaliteit op de atomen rond de zure groep en een minimale basisset op de atomen aan de rand van het cluster. Het is om verschillende redenen noodzakelijk om een minimale basisset te gebruiken aan de rand van het cluster. Ten eerste legt de ingebedde clustermethode de restrictie aan het cluster op dat de atomen aan de rand van het cluster dezelfde geometrie en basisset moeten hebben als die in het kristal. Ten tweede wordt de benodigde hoeveelheid rekentijd behoorlijk beperkt door het gebruik van een minimale basisset op de rand van het cluster. De gemengde basisset geeft de adsorptieënergieën met een afwijking van maximaal 10 kJ/mol ten opzichte van een grote basisset. Ze onderschat de adsorptieënergie van NH_4^+ met ongeveer 40 tot 50 kJ/mol. De adsorptieënergie van NH_3 is minder afhankelijk van de basisset.

Samenvatting en Algemene Conclusies

We hebben de resultaten van de geometrie-optimalisaties van het cluster, het ingebedde cluster en het kristal met elkaar vergeleken. Het blijkt dat de elektrostatische lange-dracht-interacties, hoewel ze een niet-verwaarloosbare invloed op de berekende adsorptieënergieën hebben, nauwelijks invloed hebben op de geometrie van de zure site. We kunnen dus de geometrie van een zure groep zoals we die gevonden hebben met een clusteroptimalisatie gebruiken voor een ingebed cluster. Dit is belangrijk omdat we voor een cluster automatische geometrie-optimalisaties, waarbij gradienten gebruikt worden, kunnen gebruiken. Deze technieken zijn niet beschikbaar voor een ingebed cluster.

We hebben de adsorptieënergieën van NH_3 en NH_4^+ berekend voor een cluster ingebed in een chabazietkristal, waarbij we een gemengde basisset gebruikten en de geometrie gedeeltelijk optimaliseerden. Het blijkt dat in dit geval de geometrie-optimalisatie de adsorbaten stabiliseert.

Uiteindelijk hebben we de adsorptieënergieën van NH_3 en NH_4^+ berekend op een cluster ingebed in een zeolietkristal waarbij we verder alle karakteristieken belangrijk voor een nauwkeurige berekening aanwezig waren. We gebruikten een gemengde basis set, corrigeerden voor de basisset-superpositiefout en we namen de bijdrage van de elektronencorrelatie mee. De geometrie van het cluster werd gedeeltelijk geoptimaliseerd. Er werden meerdere coordinaties van NH_4^+ met het zeolietrooster bestudeerd. Na correctie voor de tekortkomingen van de berekening zoals de fout in de basis set, de beperkte Van der Waals energie en de beperkte geometrie-optimalisatie werd de adsorptieënergie van NH_3 geschat op -70 ± 10 kJ/mol en die van NH_4^+ op -125 ± 15 kJ/mol. Deze laatste komt goed overeen met de experimenteel gemeten adsorptiewarmte.

Uit onze laatste berekeningen kunnen we de volgende conclusies trekken.

- We hebben een betrouwbare en algemeen toepasbare methode om adsorptieënergieën van kleine moleculen in zeolieten uit te rekenen ontwikkeld.
- Na adsorptie van NH_3 in het zeoliet vindt protonoverdracht plaats waarbij NH_4^+ gevormd wordt. NH_4^+ is stabiel omdat het een hoge coördinatie heeft met het zeolietrooster.

Sommario e Conclusioni Generali

Questa tesi riassume lo studio, condotto con metodi quanto-meccanici, della assorbimento di NH_3 nelle zeolite acide, il trasferimento protonico, grazie al quale si forma NH_4^+ , e, infine, l'interazione fra NH_4^+ e la rete della zeolite. La ricerca ha fondamentalmente due obiettivi. Il primo è quello di ottenere informazioni dettagliate sui processi di assorbimento e di trasferimento protonico. Il secondo obiettivo riguarda il tentativo di sviluppare un metodo quanto-meccanico con il quale sia possibile calcolare energie di assorbimento e di interazione in maniera accurata.

La solidità di un modello quanto meccanico, usato per descrivere processi di assorbimento, dipende da tre fattori. Il primo è il metodo quanto meccanico usato, cioè il modo in cui viene calcolata la struttura elettronica. Il secondo concerne la geometria e la coordinazione dell'assorbato. Il terzo riguarda il modello usato per descrivere la zeolite.

Nella prima parte di questa tesi abbiamo studiato l'accuratezza dei vari metodi quanto-meccanici. Dal momento che abbiamo considerato la zeolite come un cluster di piccole dimensioni, abbiamo usato metodi di alta qualità richiedenti molto tempo di calcolo. Abbiamo successivamente studiato gli effetti sull'energia di assorbimento indotti dal set base, dall'errore di sovrapposizione di set base (BSSE) e dalla correlazione elettronica. Abbiamo preso a confronto tre diversi set base: uno di piccole dimensioni, simile ad un set base split-valence, dotato di funzioni di polarizzazione, uno grande caratterizzato da funzioni diffuse sull'atomo di ossigeno, avente carica negativa c , infine, un set base attraverso il quale fosse possibile prevedere se le energie di assorbimento e trasferimento protonico siano realmente contenute entro il limite Hartree-Fock. Abbiamo deciso di usare il secondo set base, quello grande, per ulteriori calcoli. Anche se questo set base sottovaluta la stabilità di NH_4^+ di circa 10 kJ/mol, si dimostra sufficientemente piccolo così da essere usato più o meno abitualmente. L'energia di assorbimento di NH_3 risulta relativamente indipendente dal set base. La correlazione elettronica non può essere trascurata perché contribuisce di circa 10 kJ/mol (questo contributo è l'energia di Van der Waals) alle energie di assorbimento di NH_3 in NH_4^+ . Inoltre stabilizza di circa 10 kJ/mol l'atomo anionico di ossigeno ottenuto per mezzo del trasferimento protonico. Le energie di assorbimento devono però essere corrette al fine di evitare il BSSE. Senza questa correzione, le energie di assorbimento sarebbero infatti sopravvalutate di 10 kJ/mol e di 20 kJ/mol, rispettivamente per i livelli SCF e MP2. Se il set base usato è di minori dimensioni, le energie saranno maggiormente sopravvalutate.

La geometria e la coordinazione esistente fra NH_4^+ e la zeolite sono fattori molto importanti al fine del calcolo delle energie di assorbimento. Di solito, la coordinazione di NH_3 non crea problemi di sorta perché NH_3 viene assorbito linearmente sul gruppo acido OH con un'energia di assorbimento pari a 60 kJ/mol. D'altra parte, la coordinazione di NH_4^+ con la rete zeolitica è fonte di qualche problema. La ione NH_4^+ , infatti, legato alla rete della zeolite con un singolo legame ad idrogeno, ha un'energia di assorbimento pari a soli -15 kJ/mol. NH_4^+ , legato alla rete, avente un alto numero di coordinazione (con due o tre legami di idrogeno), ha un'energia di assorbimento di -110 kJ/mol. L'alta coordinazione di NH_4^+ con la zeolite stabilizza NH_4^+ e rende possibile il trasferimento protonico.

La geometria della zeolite influenza l'energia di assorbimento. Per NH_3 , questa influenza è di poco rilievo. L'ottimizzazione geometrica stabilizza e rende meno reattivo

Sommario e Conclusioni Generali

il cluster zeolitico; pertanto l'energia di assorbimento si riduce di circa 10 kJ/mol. Per quanto riguarda NH_4^+ , l'effetto è di maggiore intensità. La rete zeolitica, infatti, si deve deformare in modo da raggiungere un'alta coordinazione con NH_4^+ . Su una zeolite, avente geometria non deformata l'energia di assorbimento di NH_4^+ , legato mediante tre legami ad idrogeno, è di solo -10 kJ/mol. Se, in una ottimizzazione geometrica, la rete ha l'opportunità di deformarsi, l'energia di assorbimento è pari a -110 kJ/mol.

Dopo aver preso in considerazione i vari metodi quanto-meccanici, abbiamo vagliato la possibilità di adattare un cluster di piccole dimensioni ad un modello zeolitico. In questo contesto, abbiamo esaminato l'energia di assorbimento e le cariche di Mulliken per gli atomi del gruppo acido di quattro diversi cluster e di un cristallo. Due diversi tipi di errore risultano dai calcoli effettuati sui cluster. Un tipo di errore è rappresentato dai cosiddetti effetti di margine: in seguito alla saturazione, mediante atomi di idrogeno, dei legami precedentemente rotti, le cariche degli atomi in prossimità degli idrogeni, sono diverse da quelle che gli stessi atomi presentano nel cristallo. Pertanto il loro comportamento cambia a seconda del tipo di assorbito.

Per evitare che gli effetti di margine acquistino una relativa importanza nel calcolo delle energie, gli atomi di idrogeno devono essere separati di almeno quattro legami dall'assorbito. Un secondo svantaggio derivante dall'approssimazione con un cluster è l'assenza delle interazioni a lungo raggio. L'effetto di queste interazioni sull'energia di assorbimento può essere pari a 50 kJ/mol.

Sebbene il cristallo rappresenta un modello migliore per la zeolite perché gli effetti di margine sono assenti e, d'altra parte, sono presenti le interazioni a lungo raggio, i calcoli sul cristallo non forniscono accurate energie di assorbimento perché, a causa delle grandi dimensioni del sistema, si è costretti ad usare un set base minimo. Inoltre, l'ottimizzazione geometrica risulta troppo laboriosa e per quanto riguarda la correlazione elettronica, esistono solo stime in funzione della densità.

Nella ricerca di un meccanismo più soddisfacente per calcolare le energie di assorbimento, abbiamo sviluppato un metodo in grado di fornire un discreto modello per la zeolite e che, simultaneamente, richieda un tempo di calcolo di poco maggiore a quello impiegato nell'approssimazione di cluster. Mediante questo metodo, ci è stato possibile "intarsiare" un cluster in un potenziale di correlazione. Questo potenziale include il cluster nelle interazioni a lungo raggio e corregge, per quanto riguarda la parte elettrostatica, gli effetti di margine. Il potenziale di correzione è usato solo sugli atomi del gruppo acido e dell'assorbito. Se si fa uso di un cluster adeguatamente scelto (questo significa che i legami, saturati con atomi di idrogeno sono separati dal gruppo acido da almeno quattro legami), lo schema del cluster "intarsiato" riprodurrà quasi fedelmente le energie di assorbimento del cristallo, con una differenza di pochi kJ/mol.

Nell'ambito del metodo del cluster "intarsiato" abbiamo verificato l'uso di un set base misto. Un tale set base è costituito da una set base di alta qualità sugli atomi del gruppo acido e un set base minimo sugli atomi al margine del cluster. Da tutto ciò risulta che il metodo del cluster "intarsiato" richiede che gli atomi al margine del cluster debbano avere la stessa geometria e lo stesso set base del cristallo. Inoltre, il tempo di calcolo risulta ridotto nel caso in cui si faccia uso di un set base di grande dimensioni sul margine del cluster. Il set base misto conduce ad una energia di assorbimento avente un deviazione di

10 kJ/mol rispetto a quella derivante da un set base più grande. L'energia di assorbimento di NH_4^+ è sottovalutata di circa 40–50 kJ/mol. L'energia di assorbimento di NH_3 risulta invece meno dipendente dal set base usato.

Abbiamo successivamente confrontato i risultati ottenuti dall'ottimizzazione geometrica del cluster, del cluster "intarsiato" e del cristallo. Sebbene le interazioni a lungo raggio abbiano un'influenza non trascurabile sulle energie di assorbimento, l'influenza sulla geometria del gruppo acido non è di grande rilievo. Pertanto è possibile usare la geometria del gruppo acido, precedentemente ottenuto per il cluster, per il cluster "intarsiato". Tutto ciò è di grande importanza perché, per il cluster, è possibile usare l'ottimizzazione automatica basata sull'uso dei gradienti. Queste tecniche non sono disponibili per il cluster "intarsiato". Abbiamo quindi calcolato le energie di assorbimento di NH_3 e NH_4^+ su un cluster "intarsiato" in un cristallo di cabazite. In questo contesto abbiamo usato un set base di tipo misto, effettuando una parziale ottimizzazione di geometria. In questo caso, l'ottimizzazione di geometria stabilizza i sorbati.

Per ultimo, abbiamo calcolato l'energia di assorbimento di NH_3 e NH_4^+ su un cluster "intarsiato" in un cristallo di cabazite, in presenza di condizioni favorevoli per un calcolo accurato. In questo caso, è stato usato un set base di tipo misto; il BSSE è stato corretto ed è stato calcolato il contributo derivante dalla correlazione elettronica. In questo contesto, sono state studiati diversi tipi di coordinazione di NH_4^+ con la rete zeolitica. Dopo aver eseguito le necessarie correzioni (per esempio quelle sull'energia di Van der Waals e quella sull'ottimizzazione di geometria incompleta), l'energia di assorbimento di NH_3 fu stimata pari a -70 ± 10 kJ/mol e quella di NH_4^+ pari a -125 ± 15 kJ/mol. L'ultima risulta in un buon accordo con le misure sperimentali. Dagli ultimi calcoli è possibile concludere quanto segue:

- È stato possibile sviluppare un metodo attendibile e applicabile al calcolo dell'energie di assorbimento di piccole molecole nella zeolite.
- Dopo l'assorbimento di NH_3 ha luogo il trasferimento del protone; in seguito a ciò, si forma NH_4^+ . NH_4^+ è stabile perché presenta un'alta coordinazione con la rete della zeolite.

Dankwoord

In dit dankwoord wil ik degenen bedanken die hebben bijgedragen aan de totstandkoming van dit proefschrift. Allereerst wil ik natuurlijk mijn promotor Rutger van Santen bedanken. Je hebt dit onderzoek geïnitieerd en je hebt tijdens de gehele promotieperiode ideeën aangedragen. Wij waren het niet altijd met elkaar eens maar ik denk dat onze (vaak felle) discussies, en het feit dat je me altijd voldoende vrijheid hebt gegeven, hebben bijgedragen aan de kwaliteit van dit proefschrift.

Ik wil bij deze gelegenheid ook mijn copromotor Tonek Jansen bedanken die voor mij, vooral in de belangrijke fases van het onderzoek, en zeker bij het schrijven, van grote waarde is geweest. Ik mag niet vergeten Frans van Duijneveldt te bedanken. Niet alleen heb ik bij hem, tijdens mijn afstuderen, het vak quantumchemie geleerd, maar ik van hem heb ik ook veel steun buiten het werk om gehad. Verder wil ik nog mijn afstudeerders Eric Meijer bedanken, ik heb het idee dat ik door jouw afstudeerwerk wat valkuilen heb kunnen ontlopen in mijn verdere onderzoek.

Vorrei inoltre ringraziare il mio secondo promotore Roberto Dovesi per avermi suggerito una nuova 'direzione' della mia ricerca e per avermi aiutato a scrivere questa tesi. A Roberto Orlando va il mio grazie per essere sempre stato d' aiuto, soprattutto durante la fase di programmazione. Vorrei comunque ringraziare tutti gli altri membri del gruppo teorico per aver reso piacevole il soggiorno in Torino, fra gite attraverso la città, escursioni in montagna e giri in bicicletta.

Verder wil ik iedereen in de vakgroep bedanken die mijn vier jaren in Eindhoven door de koffie, de borrel en de gezamenlijke fietstochten en vakanties, tot een aangename bezigheid hebben weten te maken.

En, *last but certainly not least*, wil ik Sonia bedanken, voor alles.

Curriculum Vitae

Erik Teunissen werd geboren op 7 juli 1967. Na in 1985 het atheneum afgerond te hebben aan het *Christelijk College Groevenbeek* te Ermelo, begon hij aan een studie scheikunde aan de toenmalige Rijksuniversiteit Utrecht. Na de keuzevakken thermodynamica en chemische informatica afgerond te hebben deed hij extra bijvak katalyse. Tijdens dit bijvak werkte hij enkele maanden voor het ingenieursbureau 'COMPRIMO' te Amsterdam. Hij studeerde, met genoegen, af in de theoretische chemie bij prof.dr. F.B. van Duijneveldt.

In september 1990 begon hij zijn promotieonderzoek, dat uitmondde in dit proefschrift, aan de Technische Universiteit Eindhoven, onder leiding van prof.dr. R.A. van Santen. Tijdens zijn promotieonderzoek verbleef hij zeven maanden als gast in de vakgroep theoretische chemie van de Universiteit van Turijn (Italië).

Op 28 augustus 1993 trad hij, in Turijn, in het huwelijk met Sonia Colletto.

List of Publications

- [1] H. A. J. Oonk, M. T. Calvet, M. A. Cuevas-Diarte, Y. Haget, J. C. van Miltenburg and E. H. Teunissen, *The system p-dibromobenzene + p-chloroiodobenzene + p-bromoiodobenzene – a methodological study on thermal analysis and thermodynamic phase analysis*, *Thermochim. Acta* **146**, 297 (1989).
- [2] R. A. van Santen, A. J. M. de Man, W. P. J. H. Jacobs, E. H. Teunissen and G. J. Kramer, *Lattice relaxation of zeolites*, *Catal. Lett.* **9**, 273 (1991).
- [3] E. H. Teunissen, F. B. van Duijneveldt and R. A. van Santen, *Interaction of NH₃ with a zeolitic proton: Ab initio Quantum-Chemical Cluster Calculations*, *J. Phys. Chem.* **96**, 366 (1992).
- [4] E. H. Teunissen, A. P. J. Jansen, R. A. van Santen and F. B. van Duijneveldt, *NH₄⁺ in zeolites: coordination and solvation effects*, *J. Phys. Chem.* **97**, 203 (1993).
- [5] E. H. Teunissen, W. P. J. H. Jacobs, A. P. J. Jansen and R. A. van Santen, *Spectroscopy, Energetics and Siting of NH₄⁺ in zeolites; Theory and Experiment*, in *Proceedings of the ninth International Zeolite Conference, Montreal 1992*, edited by R. von Ballmoos, J. B. Higgins and M. M. J. Treacy, (Butterworth-Heinemann, Boston, 1993).
- [6] E. H. Teunissen, C. Roetti, C. Pisani, A. J. M. de Man, A. P. J. Jansen, R. Orlando, R. A. van Santen and R. Dovesi, *Proton Transfer in zeolites: a comparison between cluster and periodic calculations*, *Mod. Sim. Mat. Sci. and Eng.* **2**, 921 (1994).
- [7] E. H. Teunissen, A. P. J. Jansen, R. A. van Santen, R. Orlando and R. Dovesi, *The adsorption energies of NH₃ and NH₄⁺ in zeolites corrected for the long-range electrostatic potential of the crystal*, *J. Chem. Phys.*, in press.
- [8] E. H. Teunissen and A. P. J. Jansen, *Large basis sets and geometry optimizations in embedded zeolite cluster calculations*, submitted to *Int. J. Quantum Chem.*.
- [9] E. H. Teunissen, A. P. J. Jansen, R. A. van Santen, and R. Orlando, *An accurate ab-initio study of the adsorption of NH₃ and NH₄⁺ in chabazite*, submitted to *J. Phys. Chem.*.

Stellingen

behorende bij het proefschrift

'A quantum chemical description of proton transfer in zeolites'

E. H. Teunissen

- 1 Vergelijkingen tussen experiment en quantum-chemische berekeningen geven vaak een verschillende uitkomst, niet omdat de quantum-chemische methode niet goed genoeg zou zijn, maar omdat deze van goed gedefinieerde systemen uitgaat, iets wat experimenteel niet altijd het geval is.
- 2 Het "ongebruikelijke mechanisme" zoals voorgesteld door Medin *et. al* is niet alleen ongebruikelijk maar ook hoogst onwaarschijnlijk.
A. S. Medin, V. Yu Borovkov, V. B. Kazansky, A. G. Pelenschikov and G. M. Zhidomirov, *On the unusual mechanism of Lewis acidity manifestation in HZSM-5 zeolites*, *Zeolites* 10, 668 (1990).
- 3 The methode, gebruikt door Derouane en Fripiat, om Al-substitutie energieën uit te rekenen mag hoogst onbetrouwbaar genoemd worden.
E. G. Derouane and J. G. Fripiat, *Non-empirical quantum chemical study of the siting and pairing of aluminium in the MFI framework*, *Zeolites* 5, 165 (1985).
- 4 Aangezien er zoiets als een acceptabele wachttijd bestaat, neemt het aantal quantum-chemische berekeningen dat uitgevoerd wordt niet toe bij vergroting van de rekencapaciteit, de kwaliteit ervan echter wel.
- 5 Editors van tijdschriften zouden erop toe moeten zien dat artikelen waar naar verwezen wordt als 'in preparation', 'to be published' en 'to be submitted' na enige tijd ook daadwerkelijk verschijnen.
- 6 Blijkbaar is de hoeveelheid literatuur zo toegenomen dat er in het werk waarin de Al-H afstand gemeten wordt, er niet meer gerefereerd wordt naar metingen van Al-H afstanden van minder recente datum.
N. P. Kenaston, A. T. Bell and J.A. Reimer, *Determination of the Al-H Internuclear Distances in ZSM-5 using NMR spectroscopy*, *J. Phys. Chem.* 98, 894 (1994).
R. L. Stevenson, *The location of proton in dehydrated Y-Faujasite*, *J. Catal.* 21, 113 (1971).

7 De conclusie van Sauer *et al.* betreffende de protonoverdrachtsenergie van water in zeolieten zou waarschijnlijk anders zijn geweest als zij de Basis Superpositie Fout uitgerekend zouden hebben.

J. Sauer, J. Horn, M. Häser and R. Ahlrichs, *Formation of hydronium ions on Brønsted sites in zeolite catalysts: a quantum-chemical ab initio study*, Chem. Phys. Lett. **173**, 26 (1990).

8 Aangezien men absoluut niet geïnteresseerd is in de conformatie van een zeolietcluster die correspondeert met het absolute minimum, en de waterstofatomen die de verbroken verbindingen verzadigen geen invloed horen te hebben, is het werk van O'Malley *et al.* weinig zinvol te noemen. Bovendien is het verschil in adsorptieënergie van NH_3 voor beide conformeren, slechts 0.4 kJ/mol, te verwaarlozen.

P. J. O'Malley, H. Sosun and S. J. Collins, *The "true" minimum energy structure of $\text{H}_3\text{SiOHAlH}_3$. Implications for conformational preferences of bridged hydroxyl groups in zeolites*, Chem. Phys. Lett. **217**, 29 (1994).

9 In het algemeen is het zo dat als de kwaliteit van een berekening toeneemt degene die ze uitvoert minder aan de analyse van het resultaat doet en minder aandacht besteedt aan het mogelijke belang van deze berekening.

10 Het zou opportuun genoemd mogen worden dat er een grote hoeveelheid clusterberekeningen gedaan is voordat de waarde van de clusterbenadering bepaald was.

11 Zeebakjes zouden van onbreekbaar plastic moeten zijn, en gesloten moeten blijven tijdens de reis.

12 Pannclappen zouden van onbrandbaar materiaal moeten zijn.